FINAL SCIENTIFIC REPORT
RESEARCH ENTITLED:

PSYCHOPHYSIOLOGICAL ASPECTS OF
HUMAN PERFORMANCE CAPABILITIES
IN AEROSPACE SYSTEMS

AF [illegible]-75-C-0036

LABORATORY OF ENVIRONMENTAL NEUROBIOLOGY

UNIVERSITY OF CALIFORNIA

LOS ANGELES, CALIFORNIA 90024

FINAL SCIENTIFIC REPORT ON RESEARCH ENTITLED:

"NEUROPHYSIOLOGICAL ESTIMATES OF HUMAN PERFORMANCE CAPABILITIES IN AEROSPACE SYSTEMS"

RESEARCH CONTRACT AF-44620-75-C-0039 WITH THE

AIR FORCE OFFICE OF SCIENTIFIC RESEARCH

1 OCTOBER 1974 - 30 SEPTEMBER 1976

NOVEMBER 30, 1976

W.R. Adey, M.D.

PRINCIPAL INVESTIGATOR

AIR FORCE OFFICE OF SCIENTIFIC RESEARCH (AFSC)
NOTICE OF TRANSMITTAL TO DDC
This technical report has been reviewed and is approved for public release IAW AFR 190-12 (7b).
Distribution is unlimited.
A. D. BLOSE
Technical Information Officer

INTRODUCTION

This Final Report on AFOSR Contract No. AF44620-70-C00017 covers the period October 1, 1974 through September 30, 1976.

Our research has covered a wide range, including human performance measures and physiological mechanisms underlying these measures.

The Report is presented in seven sections:

1. Visual and auditory task performance following perturbed sleep in man.
2. Behavioral neurophysiology in subhuman primates.
3. Neurocr ry.
4. Effects of weak environmental electromagnetic fields on calcium ion binding in cerebral tissue.
5. Bioengineering developments.
6. Evaluation of operational potential of remote medical monitoring by cryomagnetometry and other techniques.
7. Bibliography.

SECTION I

VISUAL AND AUDITORY TASK PERFORMANCE FOLLOWING PERTURBED SLEEP IN MAN

TABLE OF CONTENTS

APPENDIX

Pages 51, 52, 53, 54, 94, 95, 96, 97 + 98 - Best Available pages

Abstract 1: Task Performance after Interrupted Sleep: A Study of the Human EEG

(John Hanley, M.D.)

There are many operational situations of interest to the Air Force in which personnel are aroused from sleep in order to perform tasks, some of which are emergency in nature. Though there are many articles on the consequences of sleep deprivation, the literature is sparse on sleep interruption, particularly with respect to electroencephalographic correlates.

In this study, 4 subjects were aroused from different stages of sleep according to EEG criteria. Two subjects were awakened during Stage II sleep, one was awakened during Stage III and REM (rapid eye movement sleep which is highly correlated with the dream state); and a fourth participant was awakened during Stages III, IV and REM. Awakenings took place all on different nights. These stages correspond descriptively to light, medium, deep, sleep and the dream state.

Upon awakening, the subjects performed a series of tasks under computer control which involved a variety of visual interactions. One set of tasks were statistically equivalent; the second set had no learning curve effects.

In general, subjects performed worse after sleep and took longer to execute the tasks. Good pre-sleep performance was consistently correlated with a high degree of shared electrical activity in the 1-5 Hz band from frontal and temporal electrode derivations. Performance after sleep was correlated with an increase in shared electrical activity from bi-occipital (posterior) and parietal locations. There were other changes in the spectral content of the EEG, but the above were consistent and virtually impossible to identify by visual inspection of the raw data ink trace.

Thus, the effects of sleep interruption parallel the consequence of sleep deprivation in that reactions to novel situations calling for sustained attention and judgement are not trustworthy. It is therefore recommended

that the Air Force actively seek those individuals who are the reverse of usual in terms of the nervous systems response to the light-dark cycle and who are alert at night for those operations which require skill and judgement during the nocturnal cycle.

The study also tends to show that performance is worse after Stage III and IV as compared to Stage II and REM. Therefore, when shift work is required, it should be possible to schedule the work so that the nocturnal 70-90 minute sleep and dream cycle can be exploited so that planned arousal could take place during Stage II or REM.

"Neurophysiological Estimates of Human Performance"

1. Task performance after interrupted sleep: An EEG study.
2. Task performance during different degrees of supine reclination: couch tilt: An EEG study.

1. Introduction:

This study investigates the EEG correlates of task performance after interrupted sleep. The circadian rhythms of the sleep-wake cycle have interested researchers around the world and the literature in the field is now voluminous, including several books as well as papers (1) (2) (3) (4). With some striking exceptions, mankind is tied to the light-dark cycle - rising with the onset of light and retiring for nocturnal sleep in the hours of darkness. The activity of man's brain is also tied to light and dark: with the discovery by Berger (5) of the electromagnetic waves generated by human brain tissue, it has been possible to quantify the electrical activity and to demonstrate its cyclical nature during the total day-night experience and the repetitive nature of the activity during the subset of cycles which constitute normal nocturnal sleep (6) (7) (8).

Though no uniform method of scoring sleep and wake stages is accepted throughout the world, sleep investigators generally know what the other investigators are talking about whether the terminology is alphabetical or numerical. In this report we will use the arbitrarily accepted numerical Stages II, III and IV and REM for the rapid eye movement stage that highly correlates with the dream experience. Descriptively, these stages are identified in the literature as light, intermediate, deep, and paradoxical sleep respectively.

Rationale:

The above mentioned literature contains a subset of data on sleep deprivation (9) (10) including marathon wakefulness (11) (12). There are also a number of papers on performance after sleep deprivation (13) (14) including selective sleep deprivation (15). These studies, however, do not address the question of EEG correlate of performance, particularly in the context of sleep interruption. There are a number of operational situations in which personnel are awakened and must act in the on-call situation, and the problem of shift-scheduling frequently occurrs. There is, therefore, a clear need for detailed investigations into performance after sleep interruption. This pilot investigation initiates study of the problem.

Summary of task performance and correlation of task results and spectral energy changes in the EEG:

Below, we summarize the pertinent data extracted from extensive scrutiny of the computer analyses of the multichannel EEG data. The evidence for the consistent findings thus summarized is examined on a case-by-case basis in the Appendix labelled Results of Tasks Scores and Spectral Analysis of EEG. Graphs of the spectral analyses are illustrated from one subject.

1. During wakefulness, task performance was excellent in those tasks designed for learning carry-over, in terms of score and time taken.
2. After sleep interruption, these tasks took longer to perform and were some times performed incorrectly despite learning.
3. The worst difficulty was encountered by subjects after interruption from Stage III & IV (deep sleep) and less trouble was experienced after Stage II and REM, with the trend of Stage II being the least disruptive.

4. The tasks in which a learning curve was not demonstrated provided the most difficulty, both with errors committed and time taken. Again, Stages III and IV sleep provided the most difficulty versus REM and Stage II.
5. When exactly the same task was given, subject was able to perform well even after interruption from Stage III.

Correlation of Task Results and EEG Spectral Energy Changes:

Despite the wealth of spectral data generated from multichannel recordings in the 4 situations of pre-sleep eyes closed rest; pre-sleep task performance; post sleep task performance, and post-sleep eyes closed rest, there are, with few exceptions, remarkable consistencies which will now be summarized:

1. With pre sleep task performance, coherence (shared electrical activity) in the 1-5 Hz band at the frontal/temporal pairs bilaterally has very high values: up to 0.8 (1.0 is the highest possible). This is a considerable increase over the values in the resting state. It is a consistent finding with no exceptions.

2. With post-sleep task performance, these high coherence values decrease uniformly. At the same time, coherence at the bilateral posterior occipital-parietal pairs increase over the pre-task levels. Again, this is a consistent finding.

3. In the resting state, the spectral profile is dominated by a 10 Hz peak most prominent posteriorly but also present at frontal locations. This is the well known alpha rhythm. In general, the energy on the right side is greater than the left in symmetrical locations.

4. With pre-sleep successful task performance, energy increases anteriorly and decreases posteriorly.

5. With post-sleep task performance (generally characterized by greater duration and less well performed) energy at all locations is increased over the pre-sleep tasks. In comparison with the pre-sleep resting record, the energy is greater anteriorly and less posteriorly in the post sleep task.

6. On resumption of eyes-closed rest after the post-sleep task, the alpha peak reappears, but is 1-2 Hz slower than pre-sleep resting records. The energy is also higher.

Significance of these results for Air Force goals:

1. These results indicate that sleep interruption has effects similar to longer duration sleep deprivation: tasks take longer to perform and even familiar tasks can be wrongly performed.

2. The stage of sleep disruption has an effect on the results. Therefore, when it is possible to schedule shift work, the 70-90 minute cycle should be exploited so that waking would most likely take place during Stage II or REM.

3. Success and difficulties in task performance are related to underlying brain states and not merely to psychological factors related to being abruptly awakened.

4. In view of the difficulty of performing tasks which require judgement vs. those in which there is a considerable carry-over in learning, it would be better to search out those individuals whose physiology is at odds with the rest of us in terms of the light-dark cycle for duty at night in those situations in which quick thinking and soundness of judgement is required rather than rely on awakening on-call personnel. The world might be said to have two populations: those who take all day to go to sleep - the 8 a.m. to 5 p.m. job is designed for such people - and a much smaller population who take all day to wake up. It is from this smaller population that come the individuals who function better

at night. They must be distinguished from the chronic insomniac who is chronically sleep deprived and miserable day and night. Chronic sleep deprivations can lead to errors of omission and commission - when sustained attention is required. It has been said in that case that "...they do the right thing at the wrong time; fail to do the right thing; and do the wrong thing at any time." The pseudo-insomniac - the true "night-owl" can be distinguished from the true insomniac by habit preference - they sometimes recognize their condition - they seek jobs at night - alertness and feeling of renewed energy at bed time, poor response to normal doses of sleep medication, and sleep habits on weekends and vacations. The dangers of critical task performance after sleep interruption are well highlighted by a study conducted at the Columbia P & S Hospital in which house officers after a night on-call were asked to evaluate rhythm strip (Standard lead II) EKGs. They were awarded significant cash prizes for correct interpretations - $25 - $50. Not only did they make hazardous errors, they thought they were correct, so insidious is the consequence after a night of interrupted sleep (18).

5. Routine tasks can be performed after sleep interruption as they can after sleep deprivation. It would be preferable not to have tight time constraints even on routine tasks, however.

Discussion:

There are several aspects of this research that are worthy of further consideration. The first is the highly shared electrical activity (coherence) in frontal and bitemporal areas in pre-sleep tasks. In a previous study funded in its entirety by AFOSR it was shown that intelligent adults with reading difficulties had low coherence across the hemispheres during attempted reading tasks, while matched subjects who were normal good readers had high coherences in symmetrical locations across the hemisphere (19). This is also true in children with and without the

problem (20). This present study adds to the significance of what may be thought of as electrical communication between the hemispheres as fundamental to efficient and accurate task performances. This is even further emphasized by the lowering of the coherence during the post-sleep tasks during which subjects experienced greater difficulty.

Another interesting feature is that the activity involves the lower frequency band: 1-5 Hz since classically mental activity has been thought to involve increased higher frequency activity, notably in the so-called beta bands which are 15 Hz and above. The low frequency activity deserves further study, particularly in view of the previous study performed in one laboratory that demonstrated that contrary to the classical notion that faster activity supervenes after alpha blocking with light input to the human eye, alpha was not blocked but attenuated and faster activity did not replace alpha (10 Hz) (21).

There is, however, a different finding in this present study with respect to the 10 Hz alpha peak. As we have discussed, and as is well illustrated in Figures 1 and 2, alpha "blocking" does take place. Thus, there is a fine differentiation between light input alone and light input plus task performance requiring mental effort evident in EEG activity, again underscoring the EEG as reflecting the state of the organism under these conditions of transform. While it is true that alpha peaks did emerge in some spectra, this was mainly during the post-sleep task performance and was indicative of inattention on the part of the subject as was the actual microsleep that was occasionally observed.

The observation that there was in general higher energy at all locations during the post sleep tasks when compared to the pre-sleep tasks is in keeping with this laboratory's earlier research in performance in the chimpanzee. During performance of an electronic version of the tic-tac-toe game, correct moves were associated with decreased energy in the EEG signal when compared to the EEG in incorrect moves. Moreover, this was predictive of performance before the chimpanzee actually made the choice of move (22). This data was obtained from

depth brain electrodes anchored in bone and was free from artefact, which gives encouragement that our findings from scalp electrodes represent the EEG data and are not due to visually inobvious artifact. (The raw data is visually inspected so that visually obvious movement, EMG and EOG artifact are eliminated from the data analysis).

Though the described spectral energy shifts at this present level of understanding can only be viewed as correlative data, the structures within which they are generated have been related to function by a body of neuroanatomical and neurophysiological data. While a lengthy exegesis of this material will not be presented, we will mention the changes in subtle levels of awareness and attention as well as more gross social difficulties that have been reported after frontal lobectomy and lobotomy (23) (24) (25) (26) (27). There are also short-term memory requirements in the performance of these tasks and there is certainly evidence that intactness of the temporal lobe in man and animals is necessary for memory functions (28)(29)(30)(31)(32)(33)(34)(35).

Finally, the response of the occipital lobes to light both patterned and non-patterned has fascinated electroencephalographers from Hans Berger on (36) (37) (38) (39) (40) (41) (42) (43) and our own aforementioned studies have further refined knowledge of this reaction. The present studies of interrupted sleep, though performed on a small number of subjects, have been extensive in terms of detail, and, in the investigator's opinion warrant further addition to the subject data base.

Task Design and Statistical Evaluation:

Task design and implementation were achieved with the use of a Digital Equipment Corporation (DEC) PDP-8 small general purpose digital computer interfaced with a Conrac CRT screen and a Digilog keyboard. Tasks were presented under computer control which involved recognition, location, and manipulation of alphanumeric symbols displayed in a variety of sequences; tracking a moving cursor; and several tests of mental alertness.

The statistical study was designed to determine whether or not there were significant differences between 7 different versions, including an introductory version, of the six tasks finally arrived at. The purpose was to establish:

a. Statistical equivalence between tasks

b. Which tasks did not have learning transfer effects.

This would enable us to vary the presentation of versions to avoid in some tasks the learning phenomenon and in others to be reasonably certain of the degree of difficulty. The tasks were designed and this phase of the research carried out by Dr. Barbara D.Leake who was a Post-Doctoral Fellow in this laboratory during the course of the investigation.

TASKS

1. Task 1 required the subject to correctly position alphanumeric symbols backwards from that shown on a CRT console display by manipulating keys. There are 3 minitasks in this category and they are scored for efficiency (time taken) as well as correctness. Highest possible score overall is 27, and time is tracked to the nearest $\frac{1}{10}$ of a second. They are labelled 1a, 1b, and 1c.

2. Task 2 requires the subject to accurately follow the various positions of a cursor on the CRT screen and then to correctly identify the number of those cursor locations. Time taken is also observed.

3. Task 3 consists of words appearing in different locations on the screen. Both words and locations have to be recalled to earn full score (1/2 a point is deducted for words correctly remembered but incorrectly located). Misspellings are not penalized.

4. Task 4 required the subject to manipulate the cursor in order to remove x symbols displayed on the screen. Tactics defined legal and illegal moves. Scoring was automatically computed as follows:

J score: number of x's removed

T score: number of moves to position cursor

P score: number of illegal moves

Efficiency: number of x's removed per second.

The J score is regarded as the most important parameter. Maximum possible value is 31 which is very difficult to achieve. If T score is high, or efficiency is low, the subject can be considered indecisive. A J score below 25 can indicate inattention or poor strategy.

5. Task 5 consists of a maze with multiple exit paths. There are both legal and illegal moves to negotiate the maze (which is displayed on the CRT) as well as excess moves. The task is scored with respect to the efficient legal paths through the maze with subtractions for the number of excessive moves. The time taken is also measured.

6. Task 6, x's and y's are displayed in a matrix. The subject is instructed to exchange the x's and y's according to certain permissible strategies. The task scored is as follows:

J score: letter exchanges

T score: cursor moves to effect exchanges

P score: illegal moves

Efficiency: time taken

Again, the J score is the most important and should be as low as possible with a minimum value of 46. If T score or time is high, then the subject can be indecisive and/or confused about strategy.

It should be noted here that 4 and 6 were considered to be the most difficult tasks.

Task Validation

Twenty-four subjects from a volunteer pool attempted to work through an introductory or training version of the tasks and then they did the six versions of the actual tasks. It should be noted here that this validation was done at completely no charge to the Air Force: the small budget in the contract could in no way support the many hours involved in the validation studies. After the 24 subjects attempted the total of 576 tasks, a subset of 284 completed task was used to test for differences between six versions of tasks 1-4. A smaller subset was used to test for learning curves in tasks 5 and 6.

The general assumption was made that the volunteers- undergraduate college students - constituted an homogenous population. In order to compensate for possible learning effects, the presentation of the different versions was systematically varied: e.g. 1,2,3,4,5,6; 2,3,4,5,6,1; 3,4,5,6,1,2; and so on. A second assumption was that there was no subject-version interaction. Consequently, single factor F tests were used to compare the different versions of tasks 1 through 4. The same design was also used to test for learning or frustration effects in tasks 5 and 6.

Results

Table 1 gives average scores on the six versions of tasks 1-3 and 5. At the $2\alpha = .05$ level of significance, the critical value of F for all the parameters in this table is $F_{crit}(5,66)$ 2.37. It can be seen from the table that with two exceptions all the parameters are below F_{crit} (these values are also insignificant for $2\alpha \leq 0.25$). In addition, the overall time taken for

tasks 1-3 and 5 in the different versions has an insignificant F value. The two significant F values both derive from the differences in task 5 across versions. In particular, versions 5 and 6 of task 5 differ from the other versions in that there is a somewhat inobvious way to exit the maze tasks using considerably less moves.

Table 2 gives average scores on tasks 1-3 and 5 as a function of the order of presentation. For example, trial #1 results are the average of those obtained from the subset of 12 subjects on the first presentation of a complete task version. These overall averages were compiled from all task versions for all parameters that did not exhibit significant F values when compared across versions. At the α=.05 level of significance, the critical value of F for all the parameters in this table is F_{crit} (5,66) = 2.37. Inspection of the table shows that many of the F values associated with efficiency, i.e. time taken and correct moves are significant. It can also be seen that parameter values do not differ significantly in trials 4,5, and 6. Thus for the purposes of the sleep interruption experiment, the sequence of trials in 4,5,6, would be discarded and learning effects compensated for by having subjects tackle the introductory version then work through a sequence selected from trials 1-3.

Table 3 gives average scores over 12 and 6 subjects for task 4 as a function of repetition. For example, the results listed under trial 1 are the averages of those obtained from subjects undertaking task 4 for the first time after working through the introductory practice version. At the α=.05 level of significance the critical values of F for all parameters in the first and second part of this table are respectively F_{crit} (3,44) = 2.84 and F_{crit} (5,30) = 2.53. Inspection of the table discloses that none of the F values are significant. Hence, the conclusion is that no significant learning curve is associated with this task.

Table 4 displays average scores over 3 and 5 subjects for task 6 as a function of repetition. At the .05 level of significance, the critical values of F for all parameters in both halfs are respectively F_{crit} (4,10)=3.48 and F_{crit} (2,12)=3.80. Since none of the F values in the table exceeds its respective critical value, again the conclusion is that there are no significant learning effects associated with this task.

Importance of the Validation Data:

The regular 6 versions (as opposed to the introductory practice versions) of tasks 1,2, and 3 are statistically equivalent. The six versions of task 5 are also equivalent provided they are scored for correct moves per second and illegal moves. Because of the similarities of the different versions of tasks 1,2,3, and 5, there are significant learning curves for these tasks ($2 = p < .05$). As seen, however, tasks 4 and 6 do not have any significant learning curves. Therefore, when the subject arrives for the pre-sleep tasks, the sequence of presentation is logically as follows: the subject is shown how the Digilog keyboard terminal is to be operated. After this familiarization, the introductory versions of the tasks are presented and the subject is guided through them with verbal instruction. Then the subject works tasks 4 and 6 without guidance. (The only learning possible here is if the subject has previously performed similar tasks; this can be ascertained by interview. Otherwise, it takes many hours to develop perfect strategies.)

The subject is then presented with a version of tasks 1-6 and recorded from in a manner to be discussed. After being awaken from a specific stage of sleep, other versions of tasks 1-6 are presented for execution. In this way, computer control of the presentation tasks is uniform with respect to absolute replicability from task to task in terms of equivalence and time with a minimum of learning curve influence on the performance. The controlling programs are written in machine language from the punched tape in-put for the DEC PDP-8, and can be converted to Fortran for more general use.

Subjects for Sleep Studies:

The subjects who were the paid volunteers for the sleep interruption were four males whose chronological age fell well within the age bracket of active duty Air Force personnel. All had at least the equivalent of college education. One subject was very familiar with the tasks; one was totally ignorant until the night of performance; and two subjects were taken through the tasks as finally arrived at after the validation studies were completed. Together with preparatory and adaptation studies, the four subjects spent some 80 hours or more in the sleep laboratory.

Procedure:

The subjects arrived at the laboratory at least 2 hours prior to their normal time of retiring. Following the aforementioned practice, the subjects are instrumented with the task electrode montage. Electrodes were positioned according to the International 10-20 system at F_3-T_3; F_4-T_4 frontal/temporal bipolar locations, bilateral and symmetrical; P_3-O_1, P_4-O_2; bipolar locations at the right and left parietal/occipital areas. Eye movements are monitored by electrodes placed at the outer canthus of the eye. The electrodes are attached via winchester plug to a radio biotelemeter designed and developed in this laboratory with Air Force support (16) (17). During the performance of the tasks, the EEG is telemetered according to multiplexing and modulation principles to a receiver and subcarrier discriminators and is written out by a conventional inkwriter polygraph (Beckman Dynograph Type R) and also stored on FM magnetic tape (Ampex FR 1300 recorder).

Following the tasks, the subject retires (still instrumented) to the bed adjacent to the task console. The bed and task console are remote from the dynograph and tape recorder - hence the advantage of telemetry - and the noise from these devices do not interfere with sleep. The stages of sleep were monitored continuously at the Beckman Dynograph paper write out (since no computation of the sleep state was planned, this phase of the experiment was not recorded on magnetic tape) and scored visually. Based on EEG criteria, subjects were woken up during Stage II, Stage III, Stage IV and REM sleep.

After being awakened in the given sleep stage, the subject resumes position at the Digilog console and proceeds with the other versions of tasks 1-6. Again, the multichannel telemetry system permitted rapid transition from the bed to the Digilog console virtually on arousal from the specific sleep stage.

Results: A: task scores:

The results of presleep and sleep interruption tasks are summarized next, on a subject-by-subject basis.

1. Stage II

Two subjects were compared with the awakenings effected during Stage II. One subject was experienced and one naive, pre-sleep scoring was as follows:

	Experienced	Naive	
Task 1a	9	9	(all correct)
Time taken (in $\frac{1}{10}$ secs.)	120	107	
Task 1b	7	7	
	153	129	(all correct
Task 1c	11	11	(all correct)
	229	152	
Total time in 10ths of seconds:	502	388	
Task 2	1	0	(2 total correct score)
	137	254	
Task 3	4	1	(4 possible)
	264	315	
Task 5	(correct) J score 95	121	
	(incorrect) P score 1	45	
	721	2549	

Task 6	(correct)	J score 64		2
		T score 157		48
		P score 14		65
			4150	1675

Total over all time for these tasks: 5774 5181

(Note that this task requires low J scores for best performance. However, the best strategy gives a minimum of 46. Below this indicates overwhelming difficulty with strategy).

Following arousal from Stage II the performances were as follows:

Task 1a	8	9
	151	110
1b	7	7
	324	274
1c	11	11
	276	165
Task 2	2	2
	42	112
Task 3	4	2-1/2
	269	217

Task 4 (still being developed when these early subjects were seen)

Task 5	80	80
	3	11
	756	1308
Task 6	71	2
	190	8
	29	2
	4932	314
Total time:	6649	2390

These results disclose the following:

1. The naive subject was better than the experienced one in the simpler reverse - copying tasks. This might reflect greater experience with console since naive subject was a computer programmer with familiarity with Digilog keyboards.

2. In the more difficult identification tasks, the experienced subject was better as expected, though performance after sleep interruption was poorer in tasks 1a and 6. The naive subject retained learning and improved after sleep interruption.

3. In the most difficult, final task, the naive subject essentially did not perform.

4. In general, following sleep, time taken was greater for both subjects both for task execution and total time.

Since the naive subject, despite familiarity with programming, entering data and the use of graphics computers did so poorly on the more difficult tasks, it was decided to allow future subjects the practice with introductory versions.

The next subject was awoken from Stage III. The results were as follows:

Pre:	Task 1c		11	Post	11
			278		268
	(1a and 1b did not register this evening)				
	Task 2		1		0
			198		101
Pre:	Task 3		4	post	4
			317		303
	Task 4	J score	0		0
		T score	10		3
		P score	8		2
			1351		187
	Task 5	T score	38		38
		P score	0		0
			210		218

Task 6	J score	3	
			4
	T score	14	3
	P score	33	2
		508	208

Thus, task 1 shows some evidence for learning, as anticipated, but task 2 did not. Learning was retained for task 3, the only one of the more difficult tasks in which the subject achieved a perfect score. As compared to the Stage II results, however, this subject took more time. On task 4, despite training and time taken, the subject could not invent a successful strategy during the baseline pre-sleep task and essentially found it too difficult after Stage III sleep and gives up after a brief time period for this task. The T scores (number of moves through the maze) are equal but time taken after sleep interruption is longer. Task number 6 is essentially not performed and subject, as in task 4, does not develop a strategy.

This subject was next awakened on a different night in REM sleep:

Pre:	Task 1a	9	Post	9
		466		196
	Task 1b	7		7
		179		246
	Task 1c	0		11
				253
	Task 2	2		2
		56		55
Pre:	Task 3	4	Post	3
		272		281
	Task 4			
	J score	24		27
	T score	46		58
	P score	0		4
		1936		2616
	Task 5			
	T score	80		79
	P score	0		0
		1466		1886

Task 6	J score	37	79
	T score	51	147
	P score	1	1
		2183	6434
Total time taken		6561	11967

It is evident from these results that the expected learning from those tasks so established from the statistical studies has again taken place with the errors that are committed coming after sleep interruption. Again the time taken after sleep interruption is greater, very much greater, after sleep interruption in the more difficult tasks 5, 4, & 6. This subject has now developed a more effective strategy for tasks 4 & 6 but does not carry through after sleep interruption, confirming the lack of carry over and effects of sleep interruption.

The next subject was awakened on 3 separate nights during REM, Stage III and Stage IV sleep. These results will now be detailed in that order.

REM		
Pre:	1a 9	Post 9
	263	270
	1b 7	7
	276	285
	1c 11	10
	246	331
Task 2		
Pre:	2	Post 2
	190	251
Task 3		
	4	4
	602	492
Task 4		
	J score 0	0
	T score 6	3
	P score 14	3
	205	88

Task 5		
T score	74	72
P score	2	0
	829	515
Task 6		
J score	68	86
T score	146	222
P score	4	14
	7833	7336
Total time:	10444	10088

Stage III

pre	1a	9	post	8
		138		178
		16		
		7		7
		401		163
	1c	11		11
		279		191
Task 2		1		1
		97		216
Task 3		3		4
		660		351
Task 4				
J score		30		29
T score		80		85
P score		5		5
		5250		6055
Task 5				
J score		0		0
T score		72		72
P score		0		0
		548		415

Task 6

J score	63	64
T score	200	192
P score	14	13
	4913	4738
	12278	12307

In the sub task of 1a the subject takes longer after sleep interruption and does slightly worse. Then, the learning carry-over becomes obvious as the scores become even and the subject takes less time. In the more difficult task 2, the subject only equals his pre-sleep score, even though in this case the tasks were exactly the same. After sleep, however, the time is much longer. In task 3, the subject was again presented with the same task, pre and post and this time the subject improves both the score and the time.

In the next three tasks, the subject does slightly better in terms of time in task 5 performance. Recall from the statistical study that task 5 is one which has a learning carry-over. In the most difficult tasks, 4 and 6, the performance is worse after sleep interruption both in terms of scores and time of execution in task 4; in task 6, the score is worse after interruption but execution time is faster.

It will be noted here that this was the third night that the subject had been involved in the experiment and not only was he fully familiar with the tasks, but the identical tasks were presented in two conditions.

Stage IV

pre	Task 1a	9	post	9
		566		272
	1b	7		6
		540		354
	1c	11		11
		282		292
	Task 2	2		0
		183		154

	Task 3	4	4
		339	373
pre	Task 4		post
	J score	28	28
	T score	76	72
	P score	8	2
		3702	5051
	Task 5		
	T score	70	73
	P score	2	2
		670	737
	Task 6		
	J score	60	62
	T score	194	192
	P score	4	3
		4534	3855
		10816	11088

In task 1 the subject does slightly worse on the score after sleep interruption and definitely better on the time, taking an unusually long time during pre sleep with sub tasks 1a and 1b, particularly when it is noted that this is the second night the subject has participated in the experiment.

Spectral Analysis of EEG Data:

In view of these results, we will now examine the EEG spectral analysis of the task data. In doing so, we will concentrate on the subjects who were awakened from the several sleep states. First we will consider the subject who was awakened on the 1st night during Stage III sleep. The illustrations of autospectra (labelled SUMSPEC) and coherence will aid in the description of the changes. The number after SUMSPEC = is representative of the energy in the process. It is the number of digitizer counts ^{2}/Hz (10^4 counts ^{2}Hz = 64 x 10^{-8} V^2/Hz), thus the greater the number the greater the power.

The following descriptions of EEG spectra were obtained by visually inspecting some 192 graphs of spectral estimates. Since this large number bewilders the unpracticed eye, we have chosen to include one complete set of illustrations

from one subject as examples. The rest are presented narrative form as if the reader were looking at the spectra. Referral to the examples given, because of the consistent findings in the data, will aid the reader in following the narrative. The examples are taken from the first subject in the test who was interrupted from REM sleep. The text also identifies this as the example subject. The remaining spectrographs will be furnished on request from AFOSR.

In the eyes closed rest situation before beginning the task we see the subjects alpha rhythm centered at 10 Hz posteriorly and anteriorly in a fine, narrow-band peak. This peak disappears dramatically on task performance both during the pre sleep tasks and after sleep interruption at all locations. Comparison of pre sleep task and post sleep task shows higher energy posteriorly from about 16-30 Hz bilaterally in the pre sleep task. Comparison of spectral profiles pre and post sleep in the eyes-closed rest state (ECR) shows a virtual overlapping spectrum. We will now examine the energy shifts.

EYES CLOSED REST

PRE		POST	
$F_3 - T_3$	$F_4 - T_4$	$F_3 - T_3$	$F_4 - T_4$
3312	3598	3734	4350
$P_3 - O_1$	$P_4 - O_2$	$P_3 - O_1$	$P_4 - O_2$
3742	5257	4724	6695

For convenience, we will adopt the format of simply writing the numbers of the SUMSPEC on the left then on the right for frontal leads and similarly write the posterior values under them without repeating the lead locations. Note the relationships in the pre sleep state: The frontal energy is higher on the right than the left; the posterior energy is higher than both frontal leads and is greatest on the right. This remains true for post sleep ECR but the energy here is greater at each corresponding location.

TASKS

Pre sleep		Post Stage III sleep	
5090	5749	16981	13221
1570	991	2441	1319

With pre sleep task performance, frontal energy increases, again more on the right; posterior energy decreases, again with a greater decrease on the right. Comparing the post sleep tasks to post sleep eyes-closed rest, frontal energy drops and posterior energy increases.

The other spectral feature we have examined is the coherence function. This function expresses the shared electrical activity between two given wave trains. Its value ranges between zero and one: zero indicates no sharing and one indicates perfect sharing. Coherence is analogous to the correlation coefficient of classified statistics. The eyes-closed rest pre task coherences show peaks near one in all pairs at 10 Hz with secondary peaks at 15-16 Hz. With task performance, these peaks disappear and there is a striking increase in coherence - approximately to 0.8 - at the $F_3 - T_3 \mid F_4 - T_4$ pair in the 1-5 Hz frequency band.

In comparison with the post sleep tasks, this high coherence sustains. The biggest change is in the $F_3 - T_3 \mid P_3 - O_1$ at 25-30 Hz: coherence is distinctly lower in the post sleep task. Post sleep eyes closed rest resembles the pre-sleep-ECR state. With the above exceptions, coherence overall is less during tasks than during rest.

We now examine this subject under conditions of REM interruption. This is the subject with the illustrations. Once more, the 10 Hz narrow-band alpha peak is strongly evident and is even narrower posteriorly. The peak is eliminated with both pre and post sleep task performance and restored with post sleep eyes-closed rest. Comparison of pre and post peaks show that the post sleep peak is one Hz slower in the frontal leads and almost 2 Hz slower in the parieto-occipital leads - recall that in the post Stage III case the peaks virtually overlapped.

The pre-sleep task spectrum, like the one in the Stage III night displays a large energy increase at the higher frequencies posteriorly, especially on the left. This is also true of the post sleep tasks but is not as marked.

We will now list the energy shifts:

pre ECR		post ECR	
2518	3287	3206	3809
3017	2408	4290	5097
	TASKS		
3626	6902	6260	9751
2088	768	1456	1057

So again we see that with task performance, energy in frontal leads increases and energy in posterior leads decreases, again most strikingly on right side both in pre sleep and post sleep performance with the biggest energy increase in the post sleep tasks. Though decreased energy in the post sleep tasks is obvious in posterior leads, it is not as low as in pre sleep tasks.

Coherences in REM interruption:

Coherences in all pairs in pre sleep eyes closed rest show peaks at 10-11 Hz with secondary peaks at 20-22 Hz. The 10-11 Hz peak is again almost as high as possible - nearly one.

During the pre sleep tasks, the peaks disappear except for small yet definite peaks at about 11 Hz in the $F_3 - T_3 \mid P_4 - O_2$ and $F_3 - T_3 \mid F_4 - T_4$ pairs. By far the most striking changes, however are the increases in coherence at 1 - 5 Hz in $F_3 - T_3 \mid F_4 - T_4$ pair (about .75) and 20-31 Hz (about 6.5) in the $F_3 - T_3 \mid P_3 - O_1$ pair. On resumption of post sleep eyes closed rest, the peaks reappear but they are 1-2 Hz slower.

The most striking difference between pre and post sleep task coherences is at the $F_3 - T_3 \mid P_3 - O_1$ pair where the high frequency coherences drop to about .2. In general, the 10-11 Hz peak is more evident in the post sleep task.

Comparison between post sleep coherences during task performance after REM and Stage III interruption also reveals that the 10-11 Hz peak is more prominent in post III and that coherence is slightly higher post III in virtually all pairs.

It will now be interesting to compare the task data between the two interrupted sleep states with respect to energy shifts:

Stage III		REM	
16981	13221	6260	9751
2441	1319	1456	1057

Clearly, greater energy in all symmetrical channel comparisons exists in the Stage III data.

We now compare the autospectral estimates for the subject who was awakened from REM, Stage III and Stage IV. We will examine the data in that order.

In pre sleep eyes closed rest, this subject also has a 10 Hz alpha peak anteriorly and posteriorly. It is more broad-band and shorter than that of the previous subject. With task performance, the peak disappears with just a hint of its presence anteriorly - more easily seen at $F_3 - T_3$. It is eliminated posteriorly. Comparison with post sleep task spectrum anteriorly shows increased energy in the post sleep spectrum from 17 - 21 Hz. This is also seen posteriorly, and there are also peaks seen in the lower frequencies at 5 and 10 Hz, peaks are quite low however. The larger peaks return with resumption of eyes closed rest with the alpha peaks anteriorly slower by 1-2 Hz and posteriorly definitely by 2 Hz. We will now list the energy changes.

Pre sleep ECR		Post REM	
3232	3766	4775	3528
2559	2626	3601	2710

Pre sleep task		Post REM task	
15786	11476	3110	2085
3780	3800	1742	826

We see pre sleep eyes closed rest again that energy is higher on the right. Energy increases with task performance at all linkages, unlike the previous subject. Post REM tasks show less energy at linkages - less than even at rest. On resumption of eyes closed rest, energy increases at all linkages.

Coherences:

Pre sleep eyes closed rest shows high coherence at 10 Hz in all pairs with secondary peaks at 17 and 20 Hz at $P_3 - O_1 \mid P_4 - O_2$. These peaks disappear during pre sleep task performance and in general coherences are lower with the striking exception of the $F_3 - T_3 \mid F_4 - T_4$ pair where the coherence in the 1-7 Hz band reaches as high as .8. Recall that this spectacular coherence increase was also seen with the previous subject. When compared to post-REM tasks, the coherence at this pair falls to about .58 in the 5 Hz region - still comparatively high - but at the $P_3 - O_1 \mid P_4 - O_2$ pair it reaches about .62. Otherwise, coherences are low and fairly even. Resumption of eyes closed rest results in reappearance of the previous peaks seen in pre sleep eyes closed rest - but they are about 1 Hz slower.

Stage III

The pre sleep, eyes closed rest spectrum is again characterized by alpha peaks at about 9-10 Hz both anteriorly and posteriorly. These are still evident anteriorly in the pre sleep task performance at very low amplitude, however. Posteriorly, it is evident on the right side after interruption of sleep, however sharp, narrow band peaks appear in all channels. On resumption of eyes closed rest, approximately 9-10 dominant alpha peaks reappear slightly slower posteriorly than the pre sleep spectrum.

The energy shifts are as follows:

Pre sleep eyes-closed rest		Post III eyes closed rest	
2433	2821	2467	2413
2935	4052	3565	5813
Pre sleep task			
5345	5052	3420	2773
2791	965	1250	1038

Once more, we see that the right side has higher coherence at comparable locations at rest, and once again with task performance energy increases in frontal locations and decreases at posterior derivations. This holds for 3 locations in the

post sleep task (compared to eyes closed rest) the exception being the right frontal and temporal areas. Again, with one exception, the energy in the post sleep task is less than the energy in the pre sleep task. The exception is pre sleep low energy at the right posterior location. Once again, energy increases at posterior locations with resumption of eyes closed rest.

Coherences:

In the eyes closed rest situation, the largest peak is seen at 10 Hz with secondary peaks at 15 and 20 Hz. With pre sleep task performance, the peaks are sharply reduced, and again we see an increase in the 1-5 Hz band to the .6 level at $F_3 - T_3 \mid F_4 - T_4$. In general, coherence is lower during task performance. When compared to post sleep tasks, peaks emerge at 2,9,15,23, Hz at various locations. Coherence remains high at $F_3 - T_3 \mid F_4 - T_4$. It increases from pre-sleep levels at $P_3 - O_1 \mid P_4 - O_2$ to above .6. Post sleep coherences are higher than post sleep tasks in the eyes closed rest situation. Both pre and post sleep eyes closed rest coherences resemble each other with the main peaks respectively at 10 and 9 Hz.

*We should recall that the tasks in this exercise were the same pre and post sleep.

Stage IV

Finally, we examine spectral shifts following interruption of Stage IV sleep. Once again in the eyes closed rest situation, the alpha peak at 10 Hz is present anteriorly and posteriorly. This peak once again virtually disappears with task performance with small remnants visible anteriorly. With post Stage IV tasks, however,the peak becomes more evident at each location though still greatly diminished compared to the eyes closed rest peak which reappears post sleep when that state is assumed. The post sleep peak, however is approximately 1 Hz.

The quantitative energy shifts took place as follows:

Pre sleep ECR		Post sleep ECR	
2463	2998	2534	3214
2470	2963	3052	3578

	TASK		
7607	10803	7761	9141
5050	2707	1412	1232

Again we see that energy on the right side is higher at rest at both locations and the greatest at the right anterior derivation. Again, energy increases markedly at the right anterior location and decreases posteriorly on the right. Energy is still higher during post sleep tasks compared to pre sleep eyes-closed rest anteriorly, but not as high as pre sleep tasks. On the other hand, the posterior leads show decreases compared to pre sleep tasks. Post sleep eyes closed rest show increased energy at all locations compared to pre sleep eyes closed rest.

Coherences:

Coherences in the eyes closed rest at all pairs show large peaks at 10 and 15-16 Hz. Classically, the peaks disappear on task performance, and once again we see the large increase in 1-5 Hz band - nearly 0.8 again - at the $F_3 - T_3 \mid F_4 - T_4$ linkage. With that exception, coherences are in general lower in task performance during the post sleep task performance, a peak at 9 Hz emerges distinctly. It reaches 0.6 posteriorly, and $P_4 - O_2$ appears to be the source with a contribution from $P_3 - O_1$. Anteriorly, a 7 Hz peak is especially seen at $F_3 - T_3 \mid F_4 - T_4$. The previous high coherence here drops, but is still higher than in the eyes closed rest state. Once again, coherence at $P_3 - O_1 \mid P_4 - O_2$ increases in the 1-5 and 9 Hz band. Post sleep eyes closed rest resembles pre sleep but the largest peak is slightly lower.

Finally, we will briefly compare the spectra from the two subjects awakened in Stage II sleep. In the subject labelled s100, we see a prominent peak at about 10 Hz in the post sleep task period. A much larger alpha peak results, as expected, when the subject resumes post sleep eyes closed rest. The energy values associated with these changes are as follows.

Pre sleep task		Post III sleep task	
P_3O - 1	P_4 - O_2	P_3 - O_1	P_4 - O_2
1430	1378	1678	1286

Post sleep eyes closed rest	
P_3 - O_1	P_4 - O_2
7283	7270

The second subject showed similar findings with a slightly different montage - one which was close enough to reflect a strong alpha peak in the eyes - closed rest position.

C_3 (central location) RTM	Pre sleep task: C_4 - LTM
13030	13196
post sleep task:	
4213	4896
post sleep eyes closed rest	
8388	10750

Coherences:

On the first subject, on the post sleep task, we again see the high coherence from 2 - 7 Hz at the P_3 - O_1 | P_4 - O_2 pair

Figure 1. This is a graph of energy on the y axis with frequencies from 1-32 Hz on the X axis. Thus one can tell the energy distribution according to frequency. Note the large narrow band peak at about 10 Hz (cycles per second) with less energy contributions from the other aspects of the frequency band.

The abbreviation SUMSPEC refers to the sum of spectral energy which is represented by the number to the right, in this case 2518. An upward change in this number represents an increase in energy and a downward one a decrease.

The designations F_3 - T_3 identify the anatomic location of the electrode sensor on the scalp. F refers to a frontal location and T to a temporal location respectively. These areas of scalp overlie the frontal and temporal lobes and the odd number designates the left side. Conversely, even numbers refer to the right side. This convention holds throughout.

Figure 2. Note the even larger peaks from these posterior electrodes which overlie P for parietal and O for occipital lobes. Again the peaks are near 10 Hz and this is the well known alpha rhythm.

Figure 3. Note the disappearance of the previous peaks (and also note that the activity derives from the same set of electrodes) during task performance. Note also the energy increases which are pointed out in detail in the text.

Figure 4. The peaks are similarly absent here, but the energy has decreased over the resting record even though there is an obvious increase in the higher frequencies.

Figure 5. During this post REM sleep task performance, peaks remain absent but note that the energy is much increased over the pre-sleep energy. This is discussed in the text.

Figure 6. There is the merest hint of the previous peak here and, while the higher frequency activity is not as prominent as in the pre-sleep graph, the energy on the right has increased.

Figure 7. The peaks have now returned as expected in the eyes-closed rest state but casual inspection is deceptive. This peak is about 1 cycle slower than the pre-sleep peak in Figure 1.

Figure 8. The posterior peaks have also reappeared as anticipated but again these peaks are as much as 2 cycles slower than the ones seen in pre-sleep Figure 2.

Figure 9. These are plots of the shared electrical activity between the different wave trains recorded during the experiment. In each plot, the wave train from one set of bipolar electrodes is matched with a second wave train from another pair with respect to the degree of sharing. The y axis denotes the possible degree of sharing with a maximum of 1 and a minimum (not numbered but corresponds to the bottom of the graph) of zero with 1 indicating perfect sharing. The x axis again indicates the band of frequencies from 1 to 32 Hz. Thus, it is possible to identify the degree of sharing at a particular frequency. Thus we see in this eyes closed rest position, the peak near 10 Hz is almost perfectly shared, undoubtedly due to the activity we have seen on the energy graphs. For our present purposes, however, it is important to observe and compare throughout the following pairs: the one at the bottom right, most importantly the $F_3 - T_3 \mid F_4 - T_4$ pair and the top left, the $P_3 - O_1 \mid P_4 - O_2$ pair. Note the levels at 1 to 5 Hz.

Figure 10. See the dramatic rise in coherence with task performance in the pre-sleep state in the 1-5 Hz part of the band. It nears 0.8. This is a consistent finding throughout the data.

Figure 11. Note the not-so dramatic but definite increase in the coherence at 1 to 5 Hz in the $P_3 - O_1 \mid P_4 - O_2$ pair. This is also consistent. In this case, the $F_3 - T_3 \mid F_4 - T_4$ also remained high which was unusual: in all the other data, this decreases.

Figure 12. We now hav a return of the high peaks seen in the pre-sleep resting data. They are not quite as high and they are 1-2 Hz lower in frequency than the pre-sleep data, reflecting the shift seen in the energy spectrum.

TABLE 1

Tasks 1-4 Averages and F values.

	VER 1	VER 2	VER 3	VER 4	VER 5	VER 6	Multivariate F value
SK 1							
# CORRECT:	8.17	8.50	8.75	7.92	7.42	8.83	0.76
COR/TIME:	0.63	0.65	0.68	0.56	0.63	0.71	0.39
# CORRECT:	5.58	6.92	6.33	6.33	6.08	6.25	0.63	
COR/TIME:	0.42	0.44	0.39	0.39	0.44	0.43	0.25
# CORRECT:	10.83	9.88	10.67	10.42	10.58	10.00	0.49
COR/TIME:	0.55	0.52	0.55	0.53	0.58	0.50	0.25
TAL CORRECT:	24.58	25.29	25.75	24.67	24.17	25.08	0.24
# COR/TIME:	0.51	0.52	0.51	0.49	0.55	0.53	0.13
SK 2							
CORRECT:	1.67	1.58	1.83	1.50	1.67	1.58	0.48
IME:	5.05	9.51	9.36	11.53	10.18	7.33	1.20
SK 3							
CORRECT:	3.67	3.92	3.92	3.75	3.88	3.71	0.63
IME:	24.49	27.27	27.38	28.66	29.26	33.73	0.58
SK 4							
RRECT MOVES	73.83	75.17	77.17	72.50	69 33	70	2.59
WER. MOVES	2.83	1.75	1.50	1.17	0.50	0.83	0.59
R/TIME:	1.05	0.99	0.91	1.22	1.00	1.13	0.44
CESS MOVES:	4.83	4.17	7.17	3.50	15.33	15.00	8.44
TOTAL TIME	163.97	182.20	201.12	181.45	175.16	174.57	0.30

ALL ANALYSES COMPUTED ON [illegible] SCORES

Table 2

Tasks 1-4 Averages and F values.

	TRIAL 1	TRIAL 2	TRIAL 3	TRIAL 4	TRIAL 5	TRIAL 6	F value
TASK 2							
# CORRECT:	8.00	7.25	7.67	8.92	9.00	8.75	3.82
CORR. TIME:	0.45	0.48	0.58	0.80	0.76	0.79	5.17
# CORRECT:	5.42	6.17	6.25	6.42	6.92	6.33	0.81
CORR. TIME:	0.26	0.34	0.44	0.40	0.55	0.53	5.00
# CORRECT:	0.63	10.75	10.92	10.75	10.75	9.58	1.35
CORR. TIME:	0.38	0.54	0.61	0.59	0.59	0.53	2.25
TOTAL CORRECT:	23.13	24.17	24.83	26.08	26.67	24.67	1.33
TOTAL CORR. TIME:	0.35	0.44	0.55	0.56	0.62	0.60	6.50
TASK 3							
CORRECT:	1.42	1.58	1.75	1.83	1.50	1.75	1.00
TIME:	16.32	10.27	8.86	5.53	6.28	5.70	4.87
TASK 3							
# CORRECT:	3.71	3.79	3.83	3.92	3.92	3.56	0.80
TIME:	34.80	33.65	30.77	24.88	22.25	24.19	1.92
TASK 4							
CORR. MOVES TIME:	0.52	0.72	1.01	1.25	1.33	1.48	8.25
INCORRECT:	1.58	1.75	1.58	0.50	0.67	2.50	0.47
TOTAL TIME:	276.00	221.40	171.21	144.86	135.45	130.05	12.41

ALL AVERAGES COMPUTED OVER SAME 12 SUBJECTS USED IN ANOVA TABLE 4

37- Blank

TABLE 3

Task 5 Averages and F values.

	Trial 1	Trial 2	Trial 3	Trial 4	F value
JSCORE:	26	27.25	27.08	26.67	0.28
TSCORE:	74.67	75.33	71.50	71.92	0.24
PSCORE:	4.25	4.67	3.67	4.58	0.22
TIME:	334.28	311.92	271.25	274.65	0.96
EFFEC:	0.09	0.09	0.11	0.10	1.64

ABOVE AVERAGES COMPUTED OVER 12 SUBJECTS DOING TASK AT LEAST 4 TIMES.

J score: number of x's removed

P score: number of illegal moves

T score: number of moves to position cursor

	Trial 1	Trial 2	Trial 3	Trial 4	Trial 5	Trial 6	F value
JSCORE:	23.83	26.33	27.33	26.83	27	27.17	0.64
TSCORE:	65.67	71.17	69	71.50	69.67	73.67	0.23
PSCORE:	3.33	4.00	4.00	3.83	5.17	4.33	0.17
TIME:	255.48	257.83	210.55	233.13	239.37	204.83	0.62
EFFEC:	0.10	0.11	0.13	0.12	0.13	0.14	1.59

ABOVE AVERAGES COMPUTED OVER 6 SUBJECTS DOING TASK 6 TIMES EACH.

Table 4

Task 6 Averages and F values.

	TRIAL1	TRIAL2	TRIAL3	TRIAL4	TRIAL5	F value
SCORE:	78	70.33	69.67	69	65	1.48
SCORE:	182.33	163.67	173.67	173	161	0.30
SCORE:	9.33	6	12	12	8	0.44
IME:	505.73	416.67	397.73	347.17	314.57	2.11

ABOVE AVERAGES COMPUTED OVER 3 SUBJECTS DOING TASK 5 TIMES EACH.

J score: number of moves to interchange x and y.
T score: number of moves to position cursor.
P score: number of illegal moves.

	TRIAL1	TRIAL2	TRIAL3	Fvalue
SCORE:	80	73.60	76.40	0.58 ~~0.54~~
SCORE:	187.60	179.60	188.80	0.21
SCORE:	11.60	11.80	11.20	0.01
IME:	579.68	477.34	476.14	1.01

ABOVE AVERAGES COMPUTED OVER 5 SUBJECTS EACH DOING TASK AT LEAST 3 TIMES.

Table 5

Interrupted sleep study - Results for Tasks 1-3 & 5.

	1a 3-1-76		2b 4-1-76		2a 4-14-76		2b 4-20-76		2c 4-27-76	
	PRE	POST	PRE	POST	PRE	POST	PRE	POST	PRE	POST
TASK #1										
:) # CORRECT:	—	—	9	9	9	9	9	9	9	8
'ORR. / TIME:			0.19	0.46	0.34	0.11	0.16	0.33	0.65	0.45
) # CORRECT:	—	—	7	7	7	7	7	6	7	7
+CORR./TIME:			0.39	0.28	0.25	0.25	0.13	0.17	0.17	0.43
)# CORRECT:	11	11	0	11	11	10	11	11	11	11
#CORR/TIME:	0.40	0.41	0	0.43	0.45	0.30	0.39	0.38	0.39	0.58
TOTAL CORR.:	?	?	16	27	27	26	27	26	27	26
TAL CORR/TIME:	?	?	0.25	0.39	0.34	0.18	0.19	0.28	0.33	0.49
TASK #2										
# CORRECT:	1	1	2	2	2	2	2	0	1	1
TIME:	19.8	10.1	5.6	5.5	19	25.1	18.3	15.4	9.7	21.6
TASK #3										
# CORRECT:	4	4	4	3	4	4	4	4	3	4
TIME:	31.7	30.3	27.2	28.1	60.2	49.2	33.9	37.3	66	35.1
TASK #5										
# INCOR. MOVES:	0	0	0	0	2	0	2	2	0	0
#CORR/TIME:	1.81	1.74	0.55	0.42	0.89	1.40	1.04	0.99	1.33	1.93
OVERALL TIME:	100.30	87.0	241.2	291.7	240.6	266.4	258.0	218.2	211.5	151.4

Table 6

Interrupted sleep study results for Tasks 4 + 6.

	1		2b		2c	
	4-1-76		4-20-76		4-27-76	
	PRE	POST	PRE	POST	PRE	POST
TASK #4						
TSCORE	46	58	76	72	80	85
JSCORE	24	27	28	28	30	29
PSCORE	0	4	8	2	5	5
TIME	193.6	261.6	370.2	505.1	525	605.5
EFFEC.	0.12	0.10	0.08	0.06	0.06	0.05
TASK #6						
TSCORE	51	147	194	192	200	192
JSCORE	37	79	60	62	63	64
PSCORE	01	01	4	3	14	13
TIME	656.1	643.4	453.4	385.5	491.3	473.8

AIR FORCE INTERRUPTED SLEEP STUDY
REYNOLD YEE 4-1-76 PRE. SLEEP
EYES CLOSED RESTING

SUMSP = 2518
F3-T3

SUMSP = 3287
F4-T4

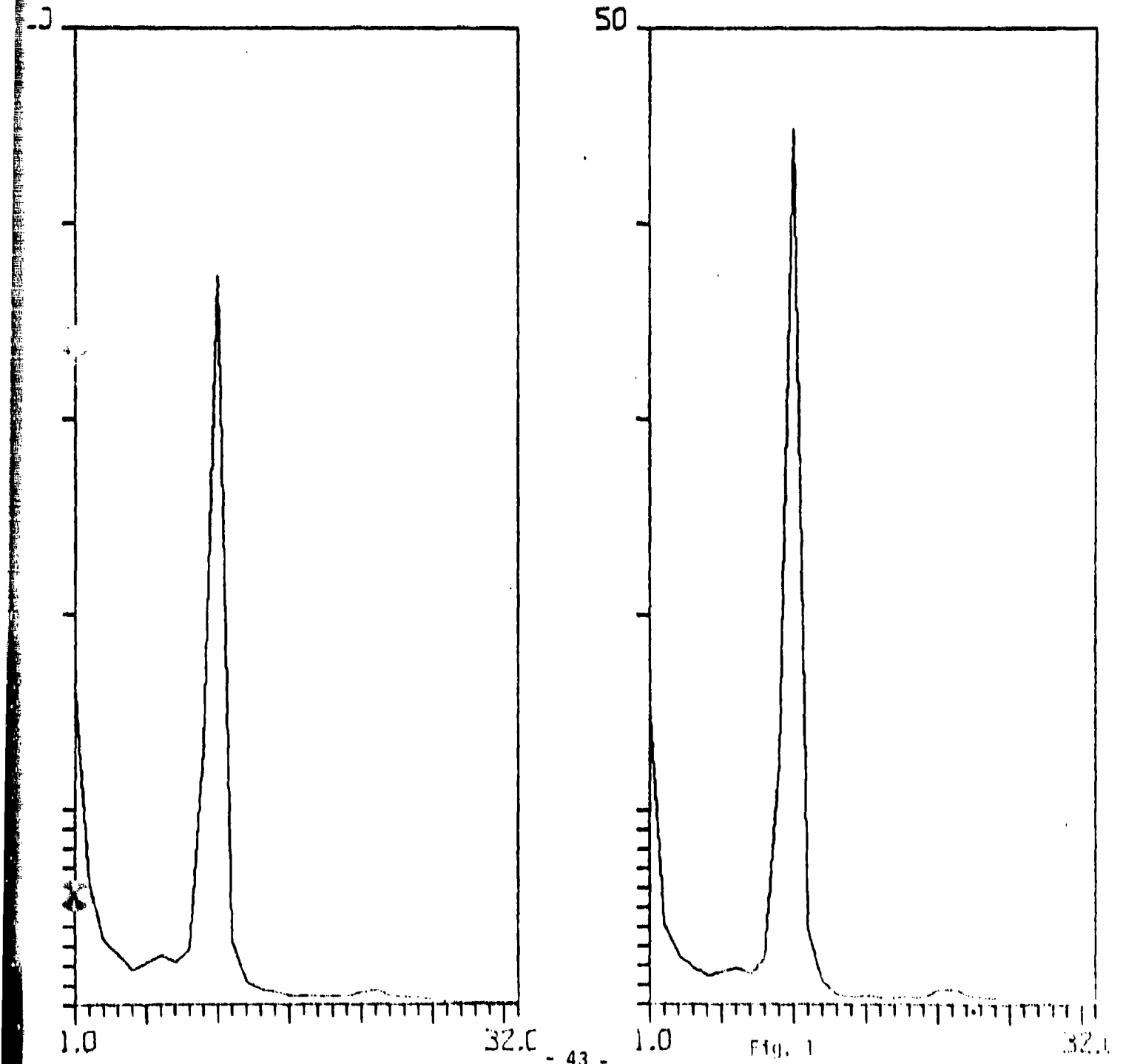

Fig. 1

AIR FORCE INTERRUPTED SLEEP STUDY
REYNOLD YEE 4-1-76 PRE. SLEEP
EYES CLOSED RESTING

SUMSP = 3017
P3-01

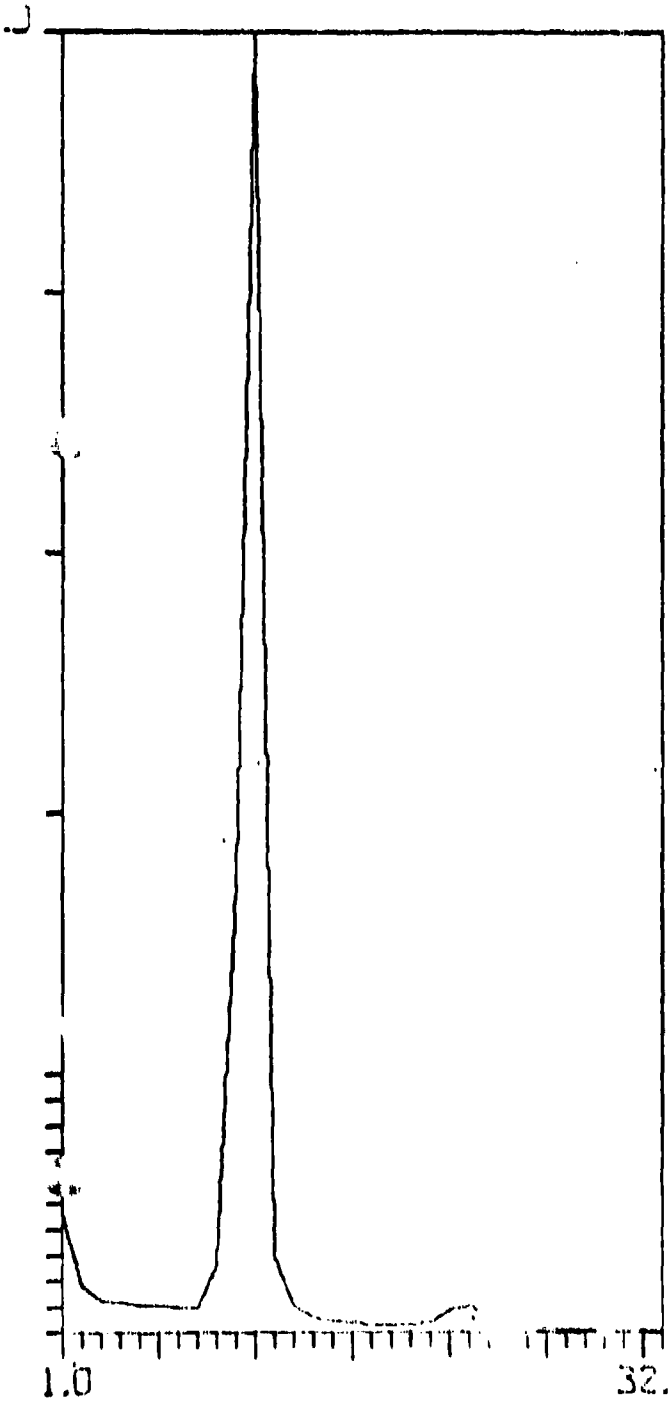

SUMSP = 2408
P4-02

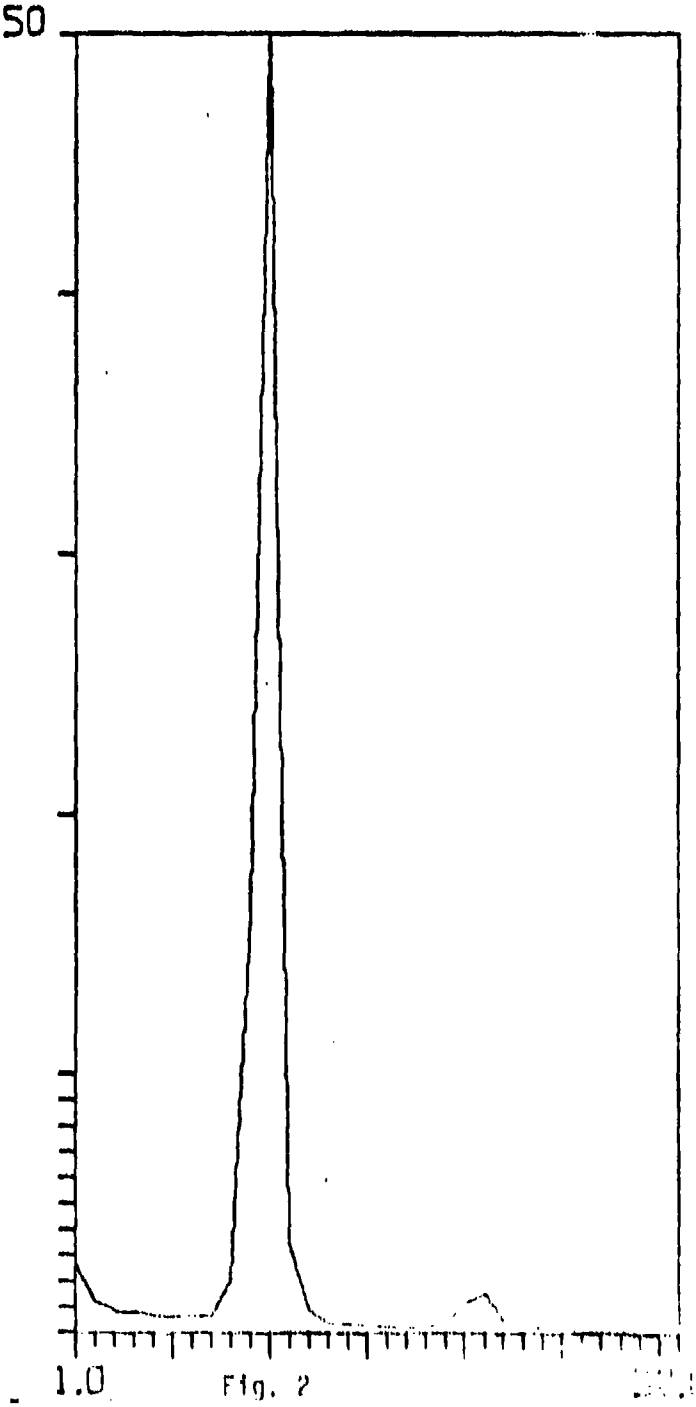

Fig. 2

AIR FORCE INTERRUPTED SLEEP STUDY
REYNOID YEE 4-1-76 PRE. SLEEP (N=50)
TASK

SUMSP = 3626
F3-T3

SUMSP = 6902
F4-T4

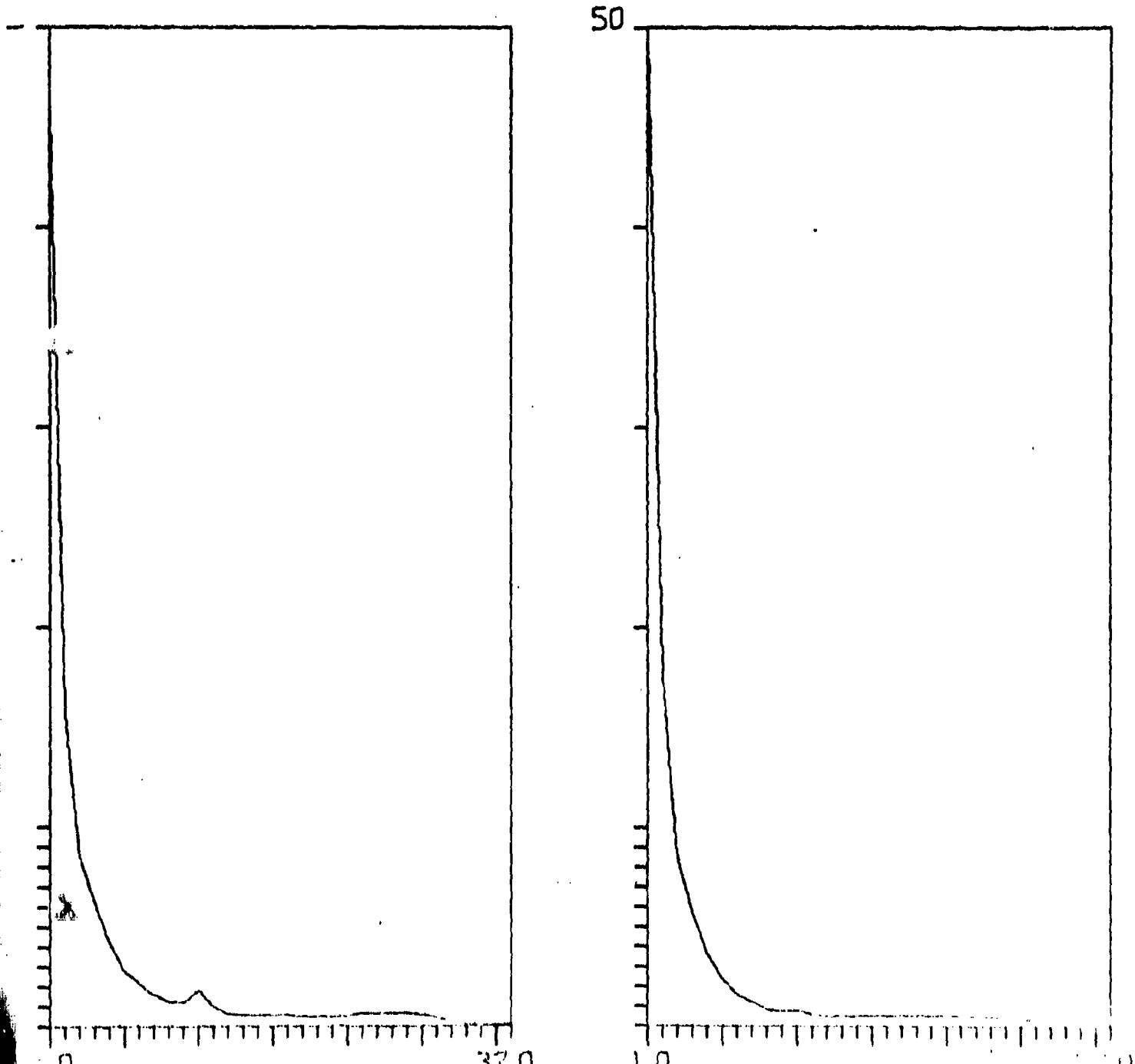

AIR FORCE INTERRUPTED SLEEP STUDY
REYNOID YEE 4-1-76 PRE-SLEEP (N=50)
TASK

SUMSP = 2088
P3-01

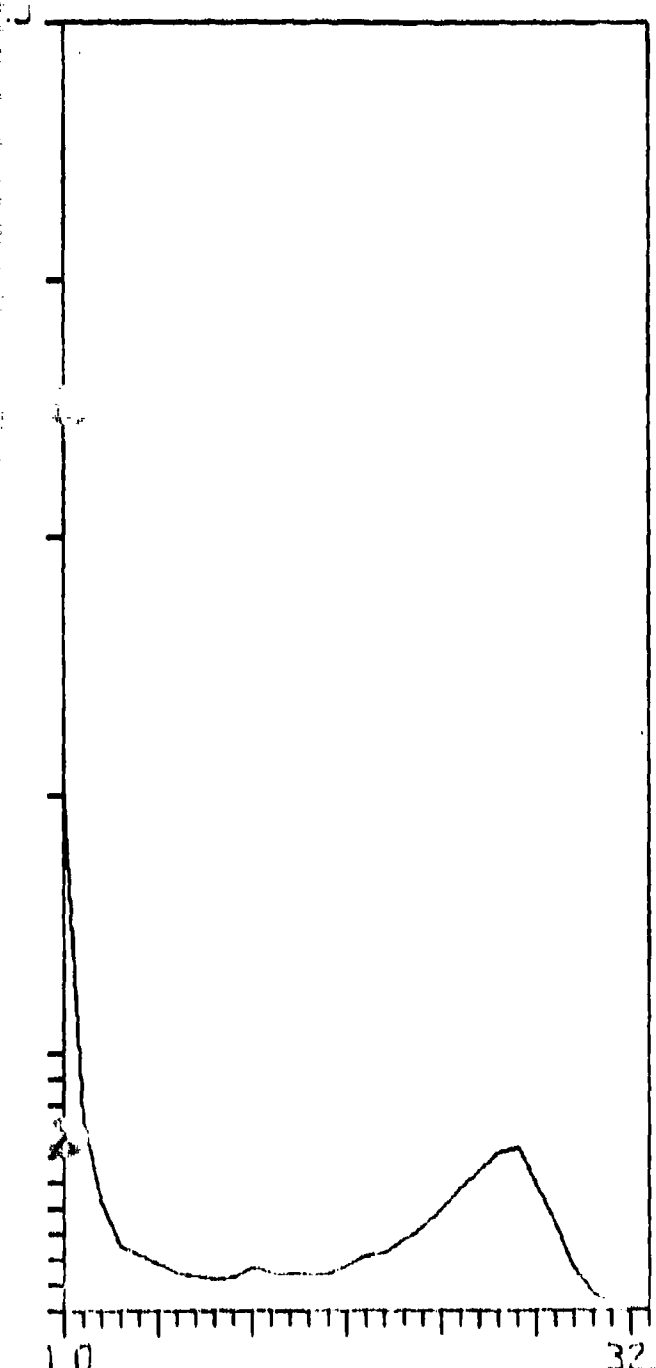

SUMSP = 768
P4-02

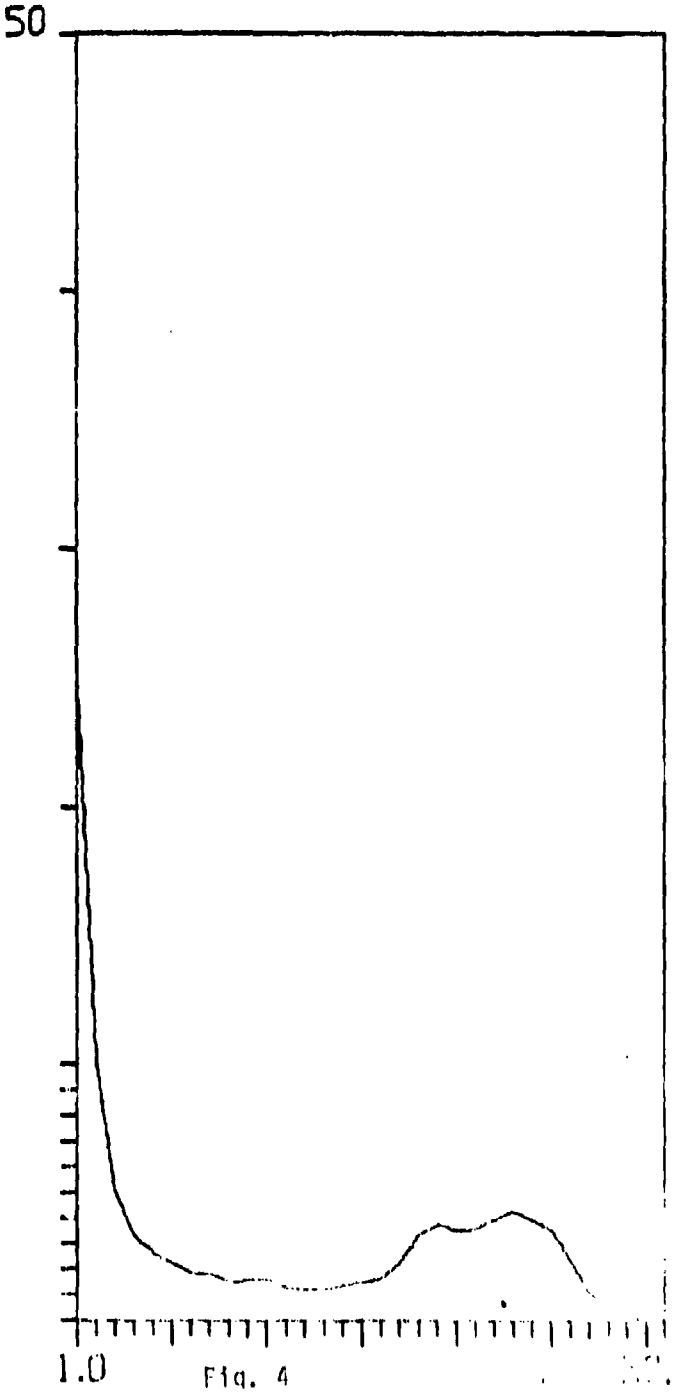

Fig. 4

AIR FORCE INTERRUPTED SLEEP STUDY
REYNOLD YEE 4-1-76
TASK POST REM SLEEP (N=50)

SUMSP = 6260
F3-T3

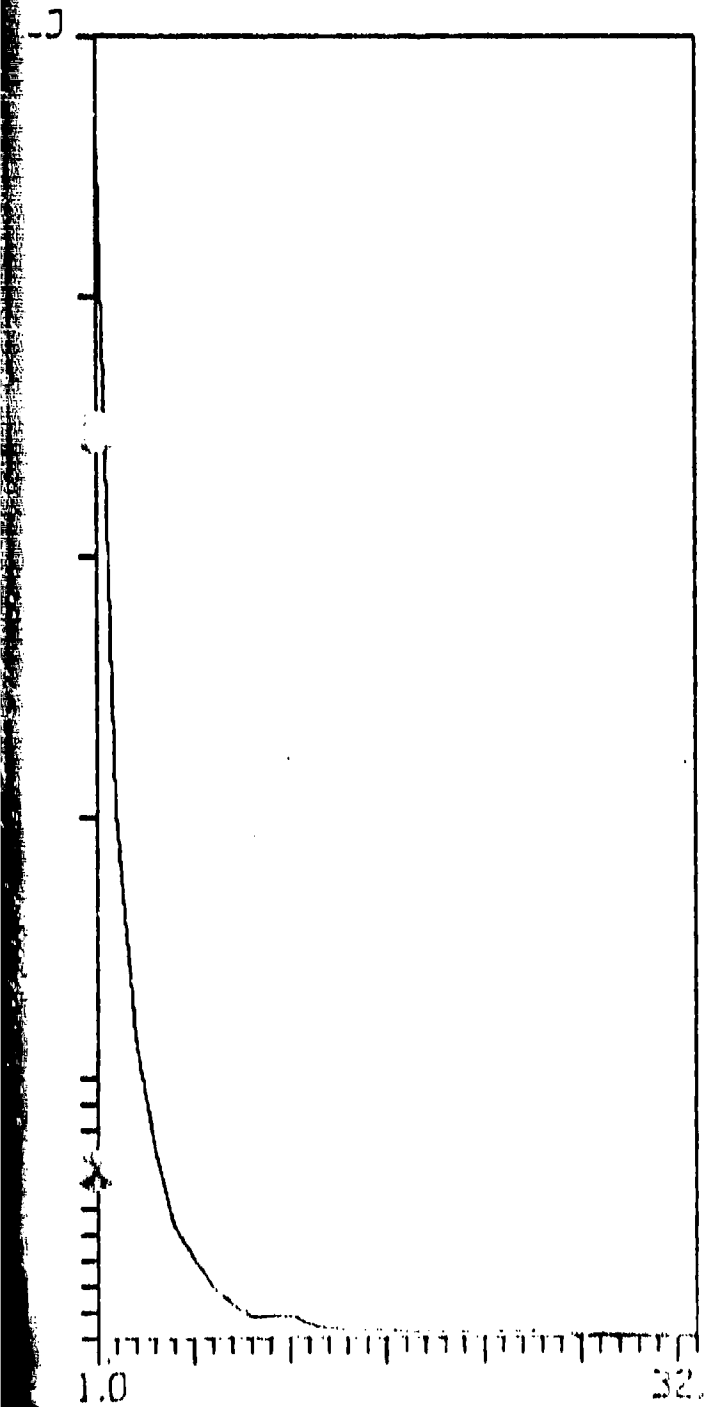

SUMSP = 9751
F4-T4

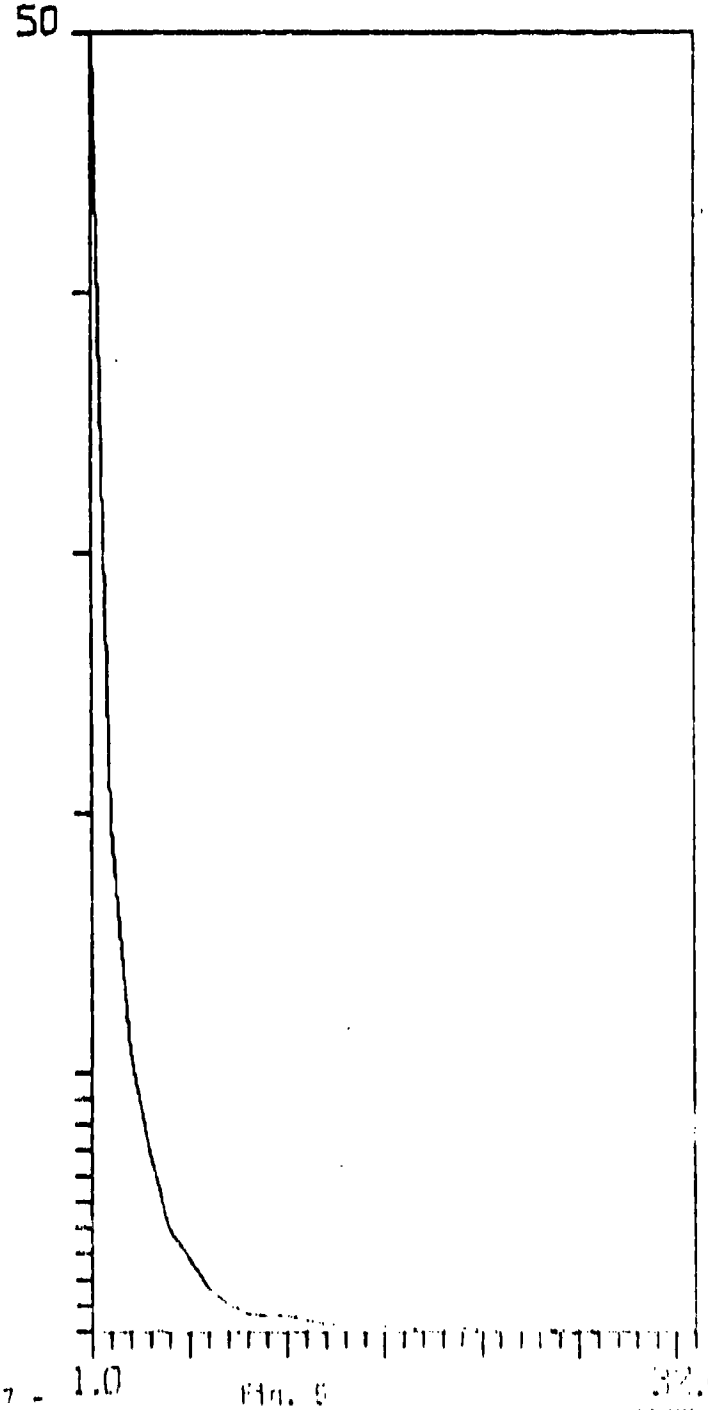

Fig. 5

AIR FORCE INTERRUPTED SLEEP STUDY
REYNOLD YEE 4-1-76 (N=50)
TASK POST REM SLEEP

SUMSP = 1456
P3-01

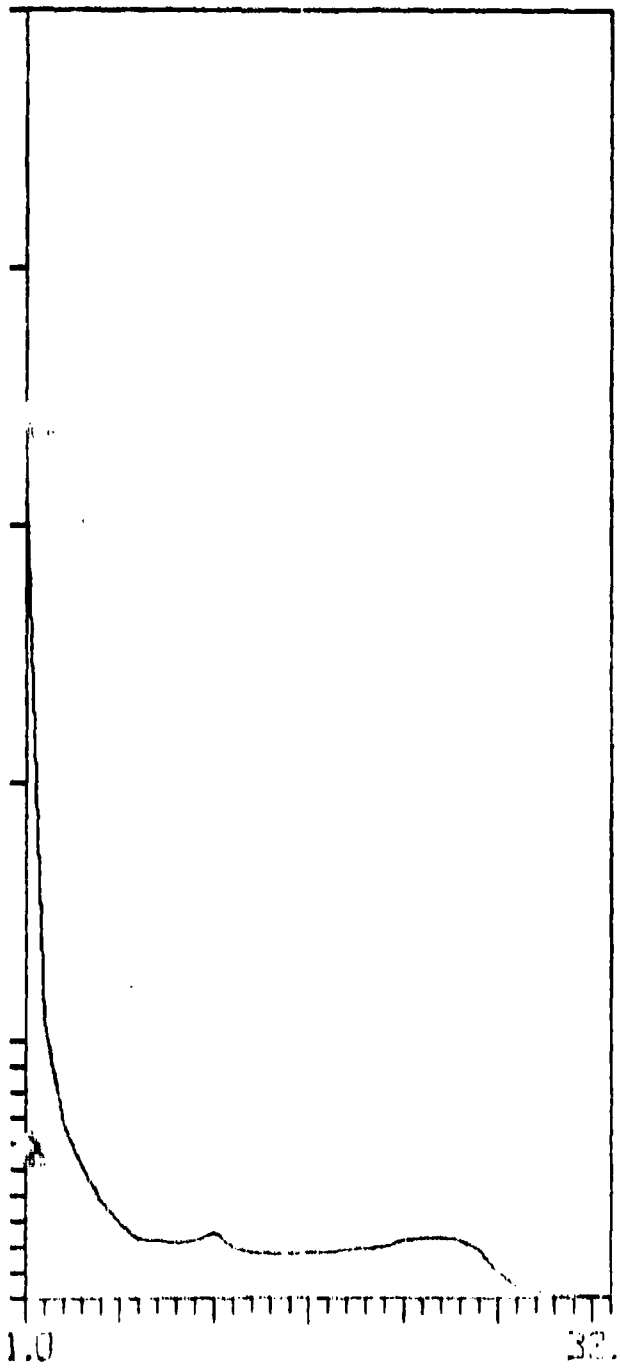

SUMSP = 1057
P4-02

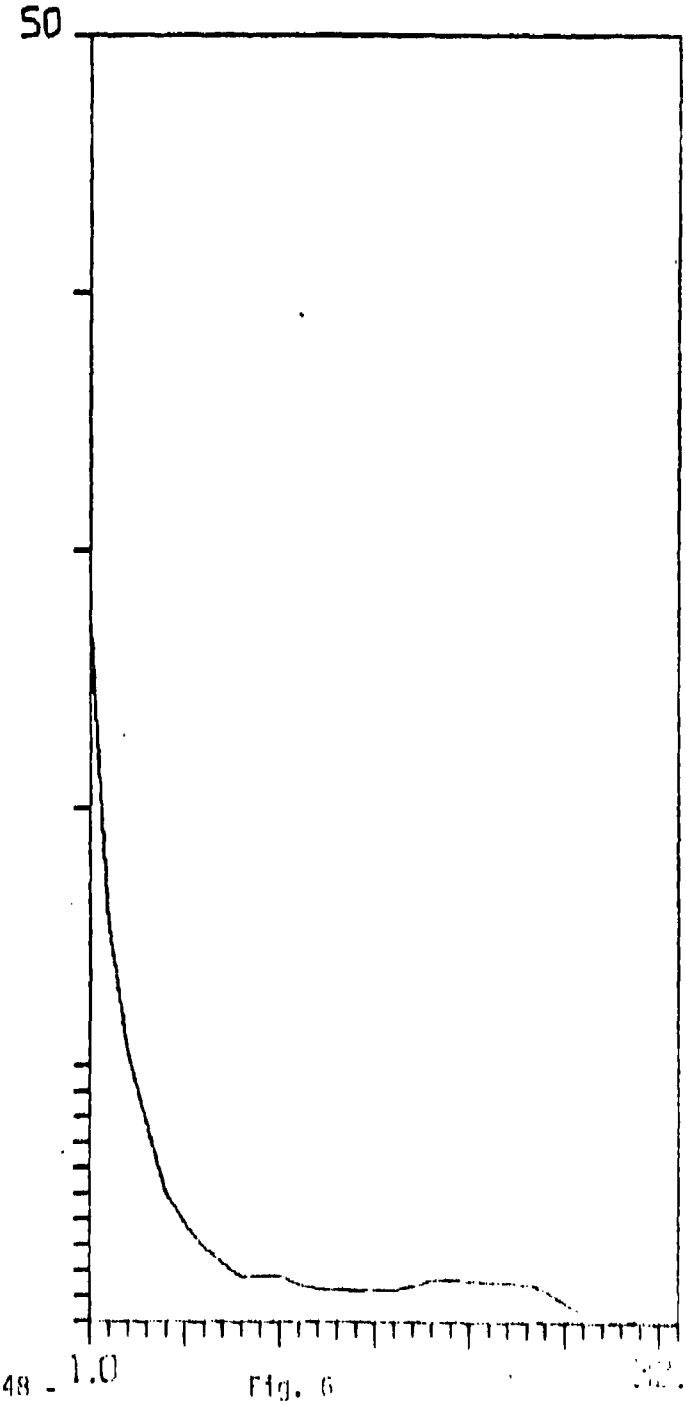

Fig. 6

AIR FORCE INTERRUPTED SLEEP STUDY
REYNOID YEE 4-1-76 POST REM SLEEP
EYES CLOSED RESTING

SUMSP = 3206
F3-T3

SUMSP = 3809
F4-T4

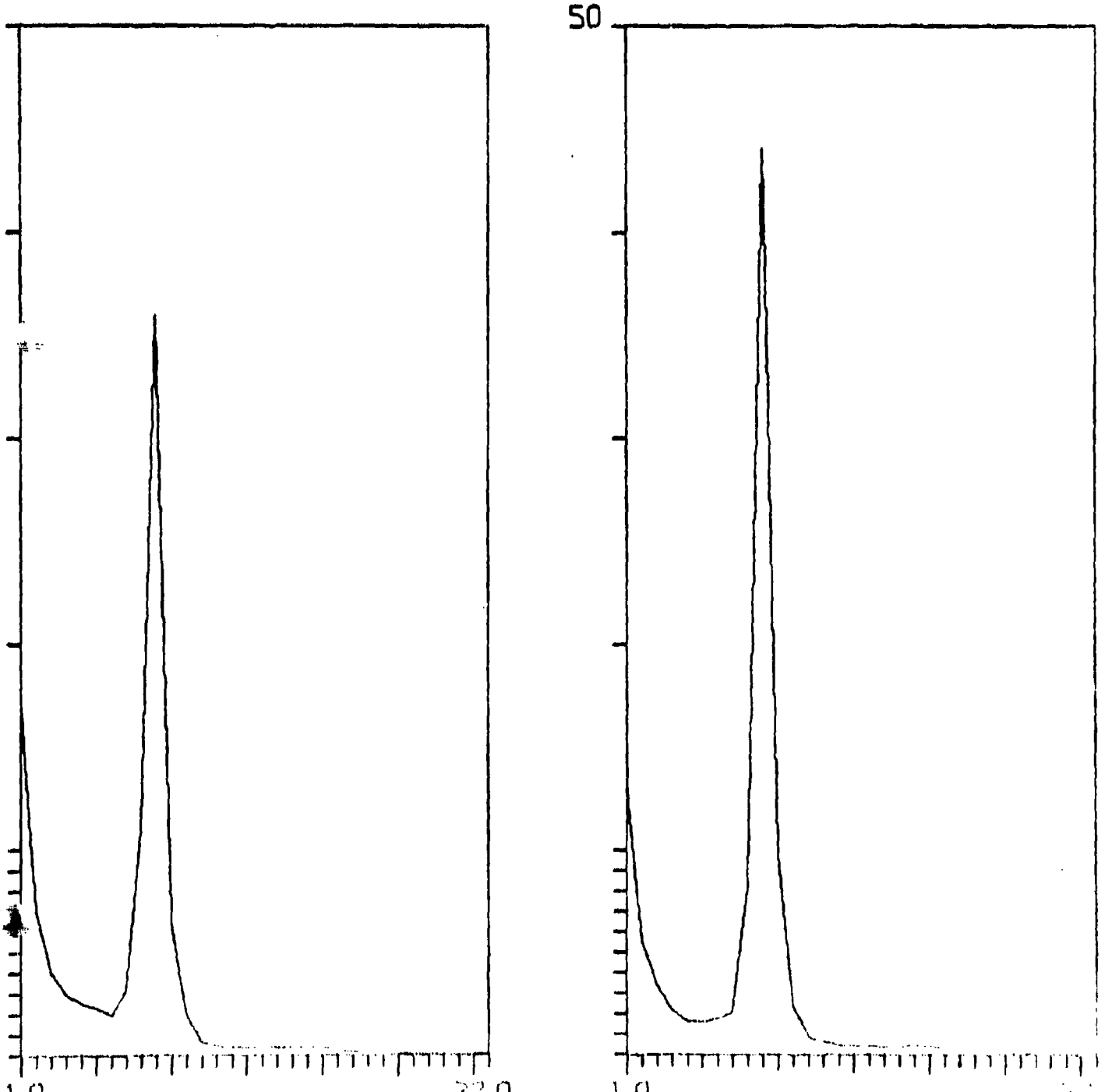

Fig. 7

AIR FORCE INTERRUPTED SLEEP STUDY
REYNOID YEE 4-1-76 POST REM SLEEP
EYES CLOSED RESTING

SUMSP = 4290
P3-01

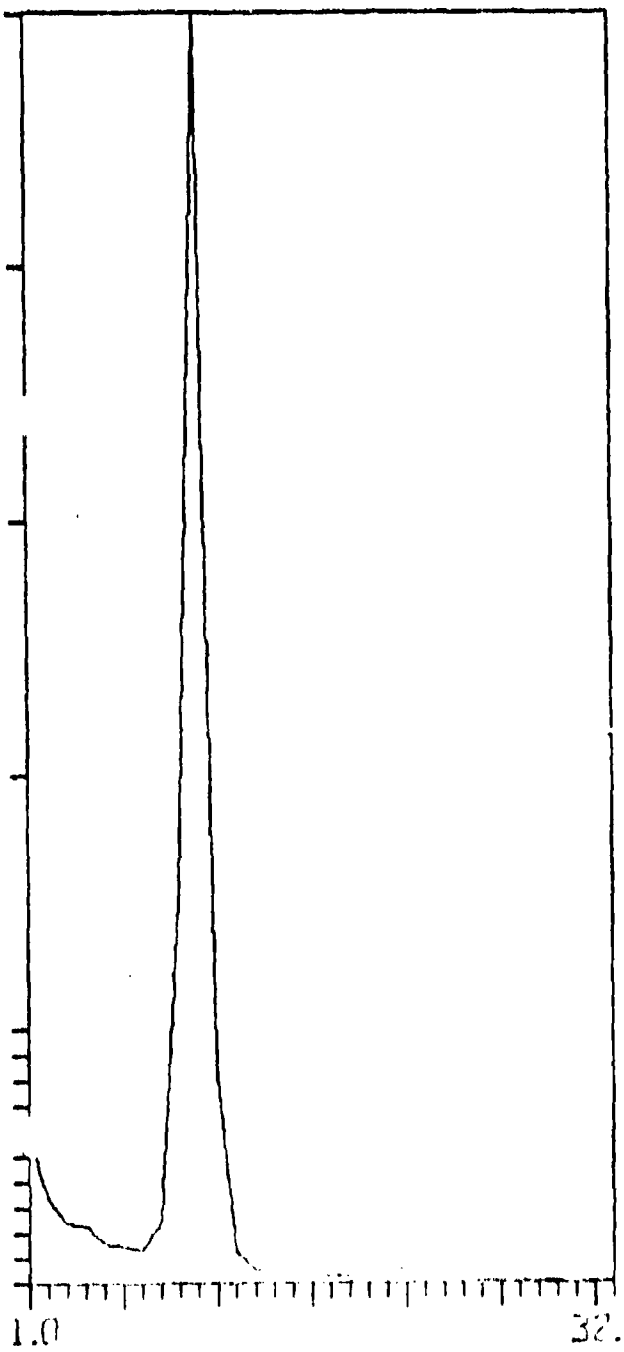

SUMSP = 5079
P4-02

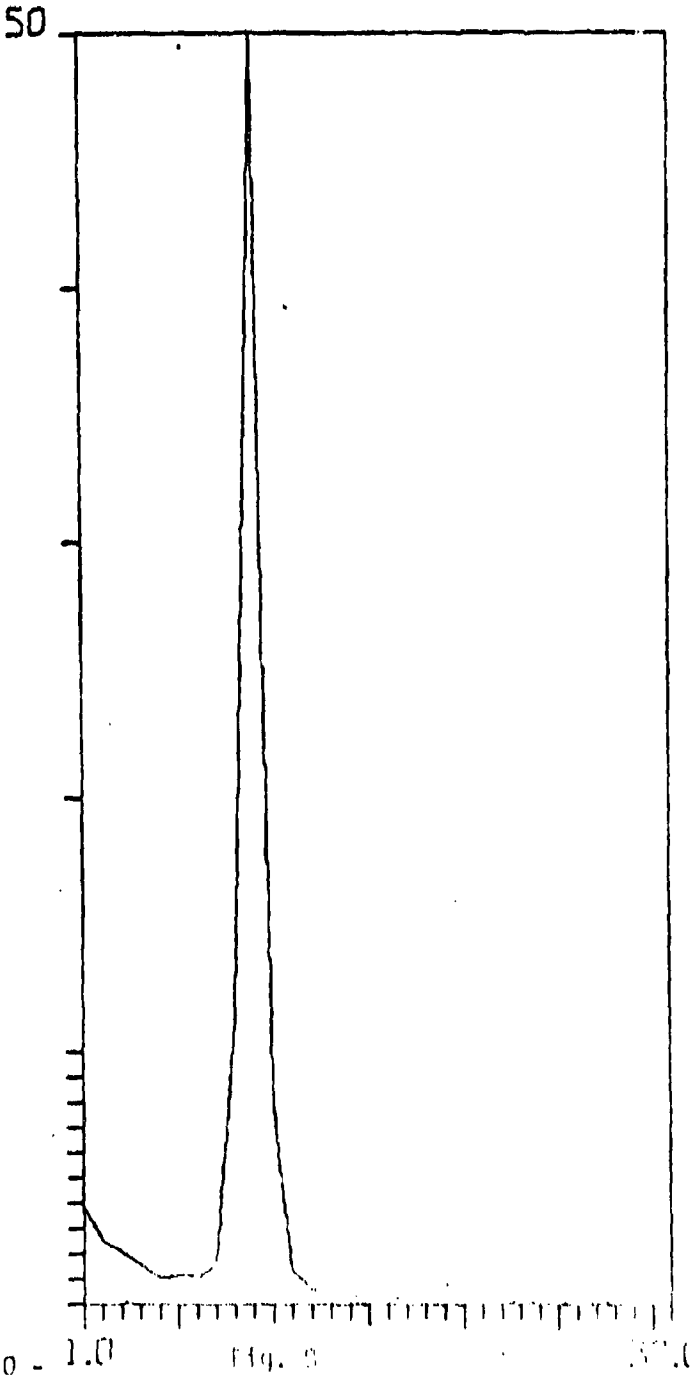

AD A083 208

Best available pages
p. 51, 52, 53, 54, 94, 95, 96, 97 + 98

12 Sep 84

1.0
F4-T4 / P3-01
32.0
1.0
P3-01 / P4-02
32.0
1.0
F3-T3 / P4-02
32.0
1.0
F4-T4 / P4-02
32.0

Fig. 9

1.0
F4-T4 / P3-01
F3-T3 / P4-02
P3-01 / P4-02
F4-T4 / P4-02

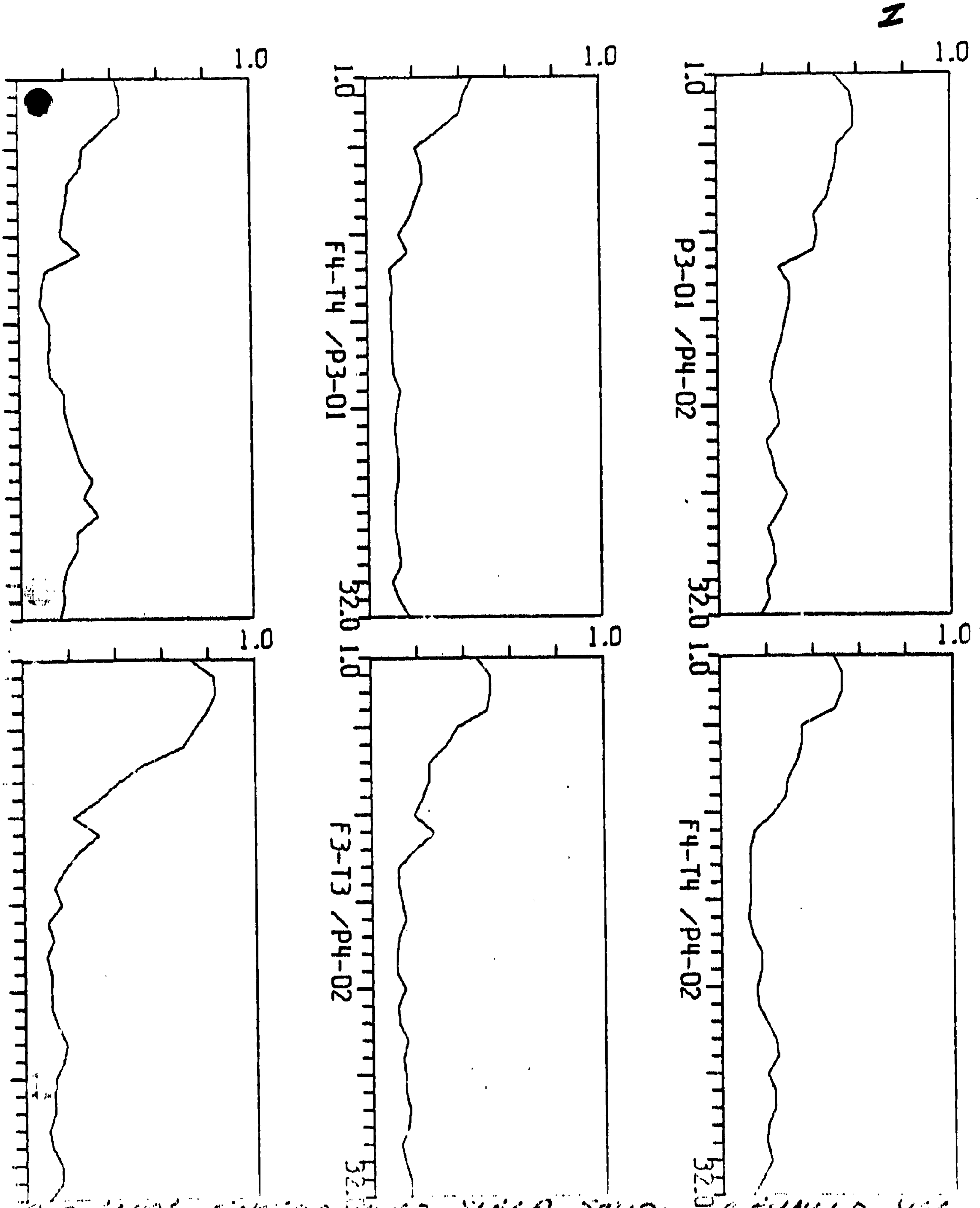

[illegible] SLEEP STUDY [illegible]

1.0
1.0
32.0
P3-O1 / P4-O2
1.0
1.0
32.0
F4-T4 / P3-O1
1.0
1.0
32.0
F4-T4 / P4-O2
1.0
1.0
32.0
F3-T3 / P4-O2
1.0
1.0
32.0
F4-T4 / P4-O2

Fig. 12

BIBLIOGRAPHY

1. Kleitman, N.: Sleep and Wakefulness, Chicago, University of Chicago Press, 1963.

2. Kety, S.S., Evarts, E.V. and Williams, H.L. (Eds.): Sleep and Altered States of Consciousness, Baltimore, Williams and Wilkins Co., 1967.

3. Kales, A. (Ed.): Sleep: Physiology and Pathology, Lippincott, Philadelphia, Pa. 1971.

4. Jovanovic, M.J. (Ed.): The Nature of Sleep, Stuttgart: Gustav Fischer Verlag, 1973.

5. Berger, H.: Uber das elektrenkephalogramns des menschen. Arch. Psychiat. Nervenkran. 87:525-570, 1929.

6. Kleitman, N.: Basic rest-activity cycle in sleep and wakefulness in: The Nature of Sleep, op. cit. reference #4.

7. Aserinsky, E. Physiological activity associated with segments of the rapid eye movement period in: Sleep and Altered States of Consciousness, op. cit. ref. #2.

8. Williams, R.L., Agnew, H.W. Jrs., and Webb, W.B.: Sleep patterns in young adults: An EEG study. EEG & Clin. Neurophysiol. 17:376, 1964.

9. Kales, A., Holdemaker, F.S., Jacobson, A., and Lichtenstein, E.L.: Dream deprivation: An experimental reappraisal. Nature, 204:1337-1338, 1964.

10. Webb, W.B.: Partial and differential sleep deprivation. Sleep: Physiology and Pathology.(Ed.)Kales, A. Lippincott, Philadelphia 221, 1969.

11. Pasnav, R.O., Naitoh, P., Stier, S., and Kollar, E.: The psychological effects of 205 hours of sleep deprivation. Arch. Gen. Psychiat., 18:496, 1968.

12. Edwards, A.S.: Effects of the loss of 100 hours of sleep. Am. J. Psychol., 54:80-91, 1941.

13. Webb, W.B. & Agnew, H.W.Jr.: Sleep: Effects of a restricted regime. Science, 150:1745-1747, 1965.

14. Wilkerson, R.T.: Muscle tension during mental work under sleep deprivation. Journal of Exptl. Psychol. 64:565-571, 1962.

15. Webb, W.B.: Partial and differential sleep deprivation. Sleep: Physiology and Pathology, Kales. A. (Ed.), Lippincott, Philadelphia, 221, 1969.

16. Zweizig, J.R., Kado, R.T., Hanley, J. & Adey, W.R.: The design and use of an FM/AM radiotelemetry system for multichannel recording of biological data. IEEE Trans. Biomed. Engr. BME 14:230-238, 1967.

17. Hanley, J., Zweizig, J.R., Kado, R.T., Adey, W.R. & Rovner, L.D.: Combined telephone and radiotelemetry of the EEG. EEG & Clin. Neurophysiol. 26:323-324, 1969.

18. The Intern and Sleep Loss, Friedman, R.C., Bigger, J.J. Kornfeld, D.S. New England J. Med. 4:201, 1971.

19. Hanley, J.: Optimizing Manpower Selection Final Report to AFOSR: Scientific Report 197 4H11, 1974.

20. Sklar, B., Hanley, J., & Simmons, W.W.: An EEG experiment aimed at identifying dyslexic children. Nature, 240:(5381)414-416, 1973.

21. Nathan, R.D. & Hanley, J.: Spectral analysis of EEG recorded during stimulation of the fovea. Brain Res., 91:65-77, 1975.

22. Hanley, J., Walter, D.O., Rhodes, J.M. & Adey, W.R.: Chimpanzee performance: Computer analysis of electroencephalograms. Nature, 220:879-881, 1968.

23. Brickner, R.M.: The Intellectual Functions of the Frontal Lobes. New York, Macmillan, 1936.

24. Penfield, W., Cameron, D.E., Prados, M.D. and Malmo, R.B.: Symposium on Gyrectomy. A. Res. New and Ment. Dis. Proc. 27:519, 1948.

25. Watts, J.W., and Freeman, W.: Prefrontal lobotomy; complications and treatment. J. Internat. Coll. Surgeons 11:343, 1948.

26. Ward, A.A., Jr.: The cingular gyrus: Area 24. J. Neurophysiol. 10:309-314, 1948.

27. Freeman, W.: Psychosurgery, Ch. 76, 1521-1540, In: S. Arieti (Ed.), American Handbook of Psychiatry, Basic Books, N.Y., 1959.

28. Klüver, H., and Bucy, P.C.: An analysis of certain effects of bilateral temporal lobectomy in the rhesus monkey with special reference to "Psychic Blindness". J. Psychol. 5:33-54, 1938.

28. Klüver, H., and Bucy, P.C.: "Psychic Blindness" and other symptoms following temporal lobectomy in rhesus monkeys. Am. J. Physiol. 119:352-353, 1937.

30. Klüver, H., and Bucy, P.C.: Preliminary analysis of the functions of the temporal lobes in monkeys. Arch. Neurol. Psychiat. 42:979-1000, 1939.

31. Terzian, H.: Observations on the clinical symptomatology of bilateral partial or total removal of the temporal lobes in man. In: Temporal Lobe Epilepsy, Baldwin, M., and Bailey, P. (Eds.), Charles C. Thomas, Springfield, pp. 510-529 ,1958.

32. Adey, W.R.: The organization of the rhinencephalon. In: H. Jasper (Ed.) "The Reticular Formation of the Brain". Boston, Little & Brown, 1958.

33. Elazar, Z. and Adey, W.R.: Spectral analysis of low frequency components in hippocampal EEG during learning. EEG and Clin. Neurophys., 23:225-240, 1967.

34. Elazar, Z., and Adey. W.R.: Electroencephalographic correlates of learning in subcortical and cortical structures. EEG & Clin. Neurophysol. 23: 306-319, 1967.

35. Grastyan, E., Lissak, K., Madarasz, I., and Donhoffer, H.: Hippocampal electrical activity during the development of conditioned reflexes. Electroenceph. & Clin. Neurophysiol. 11:409-430, 1959.

36. Berger, H.: Uber das elektrenkephalogramm des menschen. Arch. Psychiat. Nervenkr. 87:525-570, 1929.

37. Lindsley, D.B.: A longitudinal study of the occipital alpha rhythm in normal children: frequency and amplitude standards. J. Genet. Psychol. 55:197, 1939.

38. Grey Walter, W.: In: Electroencephalography: A Symposium on its Various Aspects. Hill, D. & Parr, G. (Eds.), Macdonald & Co., London, 1950, 184-191.

39. Davis, H. and Davis, P.: Action potentials of the brain in normal persons and in normal states of cerebral activity. Arch. Neurol. Psychiat. 36: 1214, 1936.

40. Rubin, M.A.: The distribution of the alpha rhythm over the cerebral cortex of normal man. J. Neurophysiol. 1:313, 1938.

41. Knott, J.R., and Henry, C.E.: The conditioning of the blocking of the alpha rhythm of the human electroencephalogram. J. Exp. Psychol. 28:134, 1941.

42. Jasper, H.H., and Shagass, C.: Conditioning in the occipital alpha rhythm in man. J. Exp. Psychol. 28:373, 1941.

43. Golla, F.L., Hutton, E.L., and Grey Walter, W.: Objective study of mental imagery: Psychological concomitants. J. Mental Sci. 89:216, 1943.

Table of Contents

Abstract

2. Visual Task Performance Under Conditions of Couch Tilt: An EEG Study.

This study investigated visual task performance by 7 subjects in a supinating couch-seat. The tasks consisted of recognition and recall of a variety of aspects of projected transparencies of aircraft. The transparencies were exposed in two time windows: 5 seconds and 3 seconds. The subjects were recorded with the seat at a 90° baseline (seatback vertical) and then in 45° and 70° of tilt. 4 slides were projected at each stage and time window for a total of 24 slides. Following the slide exposure, the subject was handed a sheet with 4 true-false questions pertinent to the slide. The subject marked off the choices of true, false, and don't know.

During control periods and task performance, the subjects' EEGs were recorded from bilateral frontal and posterior locations. Eye movements were recorded from electrodes placed at the outer canthus to assist in identifying artifact. The EEGs were stored on magnetic tape and subjected to spectral and discriminant analysis to identify effects of seat-tilt and correlates of poor vs. good performance on the tasks.

The results indicate that tilting the seat to the 70° position is associated with significantly decreased performance, particularly in the 3 second tasks. Tilting the seat also has definite effects on the EEG, both at rest and during task performance. EEG features, in particular coherences - shared electrical activity between two wave trains from different locations on the scalp - were highly correlated with successful performance, achieving discrimination from poor performance as high as 83% to 95%.

2. Visual Task Performance Under Conditions of Couch Tilt: An EEG Study.

Introduction:

The limitations on modern aircraft in the high performance class are no longer in the aircraft itself, but relate to the G-loading the pilot can sustain. The maintenance of vision and consciousness by well trained subjects at levels of 9 +Gz for up to 45 seconds has been possible with the aid of anti-G suits and the combination of muscular and respiratory maneuvers which have proven value in sustaining +Gz (1)(2)(3). This maintenance is however exhausting and places grave limitations on other pilot activities. Recently, therefore, the tilt-back cockpit seat, which has previously been demonstrated to have value in acceleration protection (4), has again been evaluated for this quality (5)(6). The tendency for mammals, from small animals to man, when confined in a supine position, is to lose alertness and even to go to sleep. This is not to suggest that skilled pilots of high performance aircraft will fall asleep at the controls simply because they are reclined. Rather, there may be trade-offs in fine degrees of alertness required in modern aircraft operations and the degree of tilt desired. This study examines the performance of visual recognition tasks and their EEG correlates under 3 couch conditions: No tilt baseline, for convenience called 90^{c}; 45^{c}; and 70^{c}. It should be emphasized here that only the condition of tilt per se and not the +Gz force was examined.

Subjects

The subjects were 7 young adult men. An eighth subject was also recorded but the EEG was unsuitable for the Discriminant Analysis procedures. His visual task scores are, however, available.

Procedure:

The subjects on arrival at the laboratory were instrumented with EEG telemetry. The electrode montage was similar to that used in the sleep-interruption study: Frontal-temperal bipolar pair bilaterally and parietal occipital pair bilaterally. In the internationally used 10-20 system these are designated F_3-T_3, F_4-T_4; P_3-O_1 and P_4-O_2 with the convention of odd numbers representing the left hemisphere and even numbers the right.

The subjects were seated in a supinating couch-chair. Baselines were obtained in the eyes-open rest situation with the subject gazing at a blank screen at the no-tilt (90°), 45° of tilt, and 70° of tilt positions. The subjects then saw projected on the screen 35mm transparencies of aircraft of various types. In one series they were given 5 seconds to observe the slide and were then handed a sheet with pertinent questions written on it. Subjects answered true-false questions by marking a choice on the written question sheet. No time constraints were placed on the answer interval. On completion, the next slide was shown. In all, 4 slides were projected at each position for 5 seconds a slide and at total of 12 slides were used in this series. In a second series, the same procedure of tilt was undergone but the time for slide observation was cut to 3 seconds. Time control over the slide exposure was achieved by use of three decade interval timers (Hunter MFG Co. Model III C). More detail on the time sequencing will be given in an appendix.

During baseline and task performance the subjects EEGs were telemetered to a Beckman Type R Dynograph ink-writer for visual analysis and stored simultaneously on an FM magnetic tape recorder (AMPEX CORP. FR 1300) for computation. These analog reels were digitized at a rate of 256 samples per second. The digitized data was then subjected to spectral analysis which generates estimates of autospectral intensity, which is related to energy,

mean frequency in the band under consideration, (in these studies the bandwidth extended from 1 to 30Hz), bandwidth within the band (we divide the total band width into clinically conventional bands i.e. Delta (1-3Hz); theta (4-7Hz); alpha (8-13Hz) and the beta bands 14-19Hz; 20-25Hz and 25-32Hz (For discriminant analysis, we arbitrarily limit the data at the 25Hz band). These measurements are made on all single channels. Then two measurements are made on cross-channel data: phase angle which gives relative lead, lag, or in-phase information for two given wave trains, and coherence which is an indicator of the amount of shared electrical activity between two given wave trains. These spectral estimates are then used as input to Stepwise Discriminant Analysis a program which is a hybrid of pattern recognition techniques and classical statistical discriminant techniques (7)(8)(9). This program selects those features in the EEG which consistently identify the situation in which they were recorded. These programs have been extensively described in a previous AFOSR final report (10) and are implemented on an IBM 360-91 General Purpose Computer.

Summary of Results

1. Performance on the 5 second task according to degree of tilt:

Tilt	% Correct	
90° (baseline)	43.7	
45°	64.0	55.2 overall
70°	58.0	

Subjects indicated that they had a learning response to the slides during the presentations at 90° so the decrement in performance from 45 to 70 is even more significant.

2. Performance on the 3 second task according to degree of tilt.

Tilt	% Correct	
90°	51.6	
45°	60.1	52.5 overall
70°	46.0	

Again we see a learning effect followed by a significant deficit because of tilt.

3. Successful performance in 5 second tasks was correlated with high values for coherence-shared electrical activity - in 4-7Hz band from the bilateral posterior pair P_3-O_1/P_4-O_2 at the baseline 90° ; Mean frequency decrease at 4-7Hz from left posterior location P_3-O_1 at 45°; and mean frequency increased at 14-19Hz from this same location at the 70° location.

4. Successful performance in 3 second tasks was correlated with high values for coherence in the 4-7Hz band from the F_4-T_4/P_3-O_1 pair at 90°; Mean frequency decrease in 8-13Hz alpha band from the right frontal F_4-T_4 location at the 45° tilt; and a phase difference of 69° between the two frontal locations

F_3-T_3/F_4-T_4 with the left side leading the right.

5. Tilt alone without task performance can be distinguished by EEG correlates and the computer analyses discriminated between 90° and 45° of tilt; 90° and 70°; and 45° and 70° in both the 5 second data and 3 second data. The highest degree of discrimination was between 45° and 70° with 70% success.

Inspection of the graphs of spectral energy also reveal obvious differences between degree of tilt. These are illustrated in the text.

6. Comparison of the eyes open-rest state versus slide observation shows that decreased energy in the 8-13Hz alpha band is associated with slide observation regardless of baseline or tilt condition. It does less well with tilt, however, than with baseline. Visual inspection of graphs of spectral intensity show that in the eyes open rest state consistent presence of a narrow band 10Hz alpha peak. This is in agreement with our previous experiments as discussed in the text. The peak is eliminated during observation of slides.

7. It was also possible to identify baseline and degrees of tilt during slide observation without regard to correctness of recognition and recall by EEG correlates in both the 5 second and 3 second data. The greatest % difference was between 90° baseline and 70° of tilt. Evidence for these summarized findings are presented in the body of the appendix.

Importance of These Findings For Air Force Goals.

The decrement in performance from baseline to 70° of tilt in a couch-seat in visual recognition tasks which have time window of 5 seconds and 3 seconds warrants serious consideration before employing this degree of tilt to lessen the +Gz acceleration force on pilots of high performance aircraft. The fact that 45° of tilt was not associated with such decrement and was associated with better task performance is also of interest but because of learning curve phenomena this experiment cannot be said to have established that the tilt alone is advantageous and this requires further investigation.

Since posterior activity in the EEG was frequently selected as a correlate of performance, it is worthwhile raising questions about pressure of the seat on the neck and possible inference on the vertebral-basilar circulation especially in view of the poor performance at 70° of tilt. Consistent findings in the virtually spontaneous EEG that are too rapid to be accounted for on the basis of changing circulation might relate to vestibular activity difficult to assess in conventional EEG tracings.

Further investigation of degrees of tilt less than 70°, together with studies of different seat configurations in the neck area would be worthwhile in view of the above findings. The changes in EEG activity both automatically selected by computer and by visual inspection of spectral energy graphs give credence to the view that performance has a neurophysiological substrate that is quantifiable.

Finally, these studies indicate that it may be possible, with parallel studies under appropriate +Gz loading to dissect out the effects of the tilt itself and permit examination of trade-offs between degree of supination and performance.

Appendix.

Results of the Stepwise Discriminant Analysis Procedures:

All subjects (7) were included in this study

1a. Baseline tilt only: no slides: Eyes Open Rest, looking at screen. Position 1 (90) versus 45 of tilt with 3 parameters, the program achieved 72% success in separating these two positions. It should be emphasized here that 72% success does not mean that each separate selection had a 72 percent chance of being correct. It means that 72% were wrongly classified.

The parameters were:

90° vs. 45°

1a Channel	Parameter	Band	Success (%)	Behavior
P_3-O_1/P_4-O_2	Phase	1-3Hz	63	48° difference
F_3-T_3/P_4-O_2	Phase	1-3Hz	67	39° difference
F_3-T_3/F_4-T_4	Phase	8-13Hz	72	11 difference

These three were chosen from 120 variables (The addition of variables could continue; we have arbitrarily chosen to stop at 3).

1b. No slides: Eyes Open Rest, looking at screen.

Position 90° vs. 70°

Channel	Parameter	Band	Success (%)	Behavior
P_3-O_1/P_4-O_2	Coherence	4-7Hz	60	70° Increased
F_3-T_3/F_4-T_4	Coherence	14-19Hz	69	70° Increased
F_3-T_3/F_4-T_4	Phase	20-25Hz	73	30°

1c. No slides: Eyes Open Rest, looking at screen position: 45° vs. 70°

Channel	Parameter	Band	Success (%)	Behavior
P_3-O_1/P_4-O_2	Coherence	20-25Hz	68	Higher at 70°
F_3-T_3	SUMSPEC	20-25Hz	76	Lower at 70°
F_3-T_3/P_3-O_1	Phase	20-25Hz	75	38° difference

Thus, the greatest difference because of position is seen between the 45° and 70° of tilt. All 3 situations reveal an influence of posture definitely greater than chance. We postpone an analysis of these results for the moment and turn attention to the question of epoch length. In the above analysis, we used 10 second epochs of EEG data because it has been well established statistically that this is a reliable time base for confidence (11)(12). Since our experimental design calls for the briefer epochs of 5 seconds and 3 seconds we reduced the epochs selected from the baseline experiment to those times. We now tabulate those results.

2a. 5 seconds. 90° versus 45°

Channel	Parameter	Band	Success (%)	Behavior
P_3-O_1/P_4-O_2	Phase	1-3Hz	58	42° difference
F_3-T_3	SUMSPEC	14-19Hz	61	Greater at 45°
P_3-O_1	SUMSPEC	14-19Hz	65	Less at 45°

2b. 90° versus 70°

Channel	Parameter	Band	Success (%)	Behavior
P_3-O_1/P_4-O_2	Coherence	4-7Hz	64	Greater 70°
P_4-O_2	SUMSPEC	4-7Hz	64	Greater 90°
F_3-T_3/F_4-T_4	Coherence	20-25Hz	66	Greater 90°

2c. 45° versus 70°

Channel	Parameter	Band	Success (%)	Behavior
P_3-O_1/P_4-O_2	Coherence	4-7Hz	67	Greater 70°
P_3-O_1/P_4-O_2	Phase	8-13Hz	69	7° difference

So, with the 5-second data, the program does not do quite as well, the trend is identical with the best separation between 45° vs. 70° and the most difficult between 90° and 45°. In all 3 discrimination procedures, all choices were still higher than chance, and in discrimination 1a compared to 2a the same parameter was chosen first, and this was also true for 1b and 2b. Although this is not the case in 2c, the discriminant features are from the lower part of the spectrum and we note that coherence is higher posteriorly at 70° of tilt in the 4-7Hz band and this accounts for 67% success in selection. Although not selected, coherence is also higher in the 1-3Hz band, and we recall that in the study of interrupted sleep, the post-sleep task coherences at this location were also higher in the band from 1-5 and 1-7Hz and this was thought to be associated with decreased alertness.

Next we examine the results from the briefest EEG epoch: 3 seconds.

3a. 90° versus 45°

Channel	Parameter	Band	Success (%)	Behavior
P_3-O_1/P_4-O_2	Phase	1-3Hz	61	45° difference
F_3-T_3/P_3-O_1	Phase	14-19Hz	62	35° difference
F_4-T_4/P_3-O_1	Phase	4-7Hz	70	31° difference

3b. 90° versus 70°

Channel	Parameter	Band	Success (%)	Behavior
F_3-T_3/P_3-O_1	Phase	14-19Hz	61	42° difference
F_4-T_4/P_3-O_1	Coherence	14-19Hz	61	Greater 70°
F_3-T_3	FBAR	20-25Hz	68	Higher 90°

3c. 45 versus 70

Channel	Parameter	Band	Success (%)	Behavior
P_3-O_1/P_4-O_2	Coherence	4-7Hz	66	Greater 70°
P_3-O_1/P_4-O_2	Phase	1-3Hz	67	47° difference
P_3-O_1	SUMSPEC	4-7Hz	72	Greater 45°

Thus we see a consistency in the coherence measure, and, despite the brevity of the epoch, consider that these are difference in the EEG due to tilt, and in order of greater differences 45° vs. 90° is the greatest; 90° vs. 70° next with one exception; and 90° vs. 45° a very close third with again one exception.

Results of Baseline Eyes Open Rest vs. Observing Slides.

90° versus 90° 5 seconds

Channel	Parameter	Band	Success (%)	Behavior
P_4-O_2	SUMSPEC	8-13Hz	85	↓Slides
P_4-O_2	Mean Frequency	4-7Hz	91	↓Slides
F_4-T_4	Mean Frequency	8-13Hz	91	↓Slides

90° versus 45°

P_4-O_2	SUMSPEC	8-13Hz	77	↓ Slides
P_3-O_1/P_4-O_2	Coherence	8-13Hz	77	↑ Slides
F_3-T_3	SUMSPEC	8-13Hz	81	↓ Slides

90° versus 70°

P_4-O_2	SUMSPEC	8-13Hz	80	↕ Slides
P_3-O_1	SUMSPEC	14-19Hz	78	↓ Slides
F_3-T_3/P_4-O_2	Coherence	20-25Hz	84	↓ Slides

Discussion of Eyes Open Rest vs. Slides at 5 Second Exposure Time.

As anticipated from the interrupted sleep experiment there is a sufficient decrease in energy with slide presentation at the parieto-occipital location to provide a high degree of discrimination between Eyes Open Rest and slide observance. Moreover, visual inspection of the graphs of autospectral intensity reveal the existence in the Eyes Open Rest of high, narrow-band alpha peaks at about 10Hz posteriorly. This peak virtually vanishes during slide observation, adding more evidence to our demonstration that alpha is not blocked with light but only attenuated (13) and further, the fact that it is blocked with performance of a task gives a further EEG differentiation of state.

Again, we see that there is a difference due to tilt, with a somewhat greater difference between the 90° and 70° positions. Next, we compared the effects of tilt during slide observation. Again, the program was successful in identifying the different tilt positions. Here, the situation is more complex with the EEG features of phase, bandwidth and mean frequency - all visually inobvious on inspection of the paper trace - being selected. Once again, the greatest disparity is 90° vs. 70° with an 88% separation.

Results of Slides vs. Slides:

90° versus 45° 5 seconds

Channel	Parameter	Band	Success (%)	Behavior
F_3-T_3	Bandwidth	20-25Hz	72	↓ 45°
F_3-T_3/F_4-T_4	Phase	14-19Hz	72	↓ 45° (27°) phase difference
F_3-T_3/P_4-O_2	Phase	8-13Hz	80	↑ 90° (41°) " "

90 versus 70

P_3-O_1	Mean Frequency	14-19Hz	68	↑ 70°
F_3-T_3/P_4-O_2	Coherence	8-13Hz	84	↑ 70°
F_3-T_3	Mean Frequency	4-7Hz	88	↑ 70°

45 versus 70

F_4-T_4	Bandwidth	4-7Hz	69	↑ 70°
P_4-O_2	SUMSPEC	1-3Hz	76	↑ 70°
F_3-T_3/P_4-O_2	Phase	8-13Hz	80	↓ 70° (35°) phase difference

3 Second Slides: Baseline vs. Slide

90 versus 90

Channel	Parameter	Band	Success (%)	Behavior
P_3-O_1	Bandwidth	8-13Hz	69	↑ Slides
F_4-T_4/P_3-O_1	Coherence	4-7Hz	88	↑ Slides

(Best selection at 2 steps)

90 versus 45

P_4-O_2	SUMSPEC	8-13Hz	78	↓ Slides
P_3-O_1/P_4-O_2	Coherence	8-13Hz	82	↑ Slides
F_3-T_3/F_4-T_4	Phase	4-7Hz	88	↑ Slides

90 versus 70

P_4-O_2	SUMSPEC	8-13Hz	77	↓ Slides
P_3-O_1/P_4-P_2	Coherence	1-3Hz	79	↑ Slides
F_3-T_3/P_4-O_2	Coherence	1-3Hz	85	↓ Slides

Again, as with the 5-second data, posterior activity in the alpha band is effective in separating Eyes Open Rest from viewing slides. Again there is an effect with tilt - the poorest differentiation with one parameter - 69% - is found at the no-tilt position of 90°. Increased coherence, with one exception, with the slide task is consistent with the pre-sleep task data in our previous experiment.

Results of Slides vs. Slides: 3-Second Exposure.

90 versus 45

Channel	Parameter	Band	Success (%)	Behavior
F_4-T_4	Bandwidth	8-13Hz	58	↓ 45°
F_4-T_4	Mean Frequency	14-19Hz	73	↓ 45°

(This is the best discrimination achieved)

90 versus 70

P_3-O_1/P_4-O_2	Phase	1-3Hz	60	46° shift
P_4-O_2	SUMSPEC	8-13Hz	71	↓ 70°
F_4-T_4/P_3-O_1	Coherence	4-7Hz	78	↓ 70°

45 versus 70

F_4-T_4	Bandwidth	8-13Hz	58	↑ 70°
P_3-O_1/P_4-O_2	Coherence	1-3Hz	64	↑ 70°
F_3-T_3/P_4-O_2	Coherence	1-3Hz	72	↓ 70°

Like the 5-second exposure, successful discriminant features are, in general, visually not obvious ones of bandwidth, phase, coherence, and mean frequency. The discrimination is not as good as the 5-second data, but the trend is the same: 90° vs. 70° provides the greatest disparity.

Results of the task performance according to score: 0-2 ranked as low score; 3 & 4 correct as a high score (4 highest possible).

90^{o}: 5 seconds tasks

CHANNEL	PARAMETER	BAND	SUCCESS	BEHAVIOR
P_3-O_1 | P_4-O_2	Coherence	4-7 Hz	83%	↑ High score

(highest discrimination attained)

45^{o}: 5 second tasks

P_3-O_1	Mean frequency	4-7 Hz	80%	↓High score
F_3-T_3	SUMSPEC	4-7 Hz	84%	↑ High score
F_3-T_3 | F_4-T_4	Coherence	8-13 Hz	92%	↑ High score

70^{o}: 5 second tasks

P_3-O_1	Mean frequency	14-19 Hz	65%	↑ High score
P_4-O_2	SUMSPEC	8-13 Hz	80%	↑ High score
F_4-T_4 | P_4-O_2	Phase	8-13 Hz	95%	56^{o} shift high score 21 - 35 low high

Discussion of Results of EEG Correlates of Low vs. High Performance: 5-second task.

It was possible with a high degree of success, more than 80 and 90%, to separate the low scores from the high scores by EEG parameters in both the five-second exposure tasks and the three-second exposure tasks. It was also possible to differentiate low and high scores during the different degrees of tilt. Thus we see that at baseline of 90°, 83% was achieved with the 5-second tasks by the coherence measure in the 4-7Hz band at the P_3-O_1/P_4-O_2 pair. Coherence increased with high performance. We recall here again that high coherences were noted in successful readers during reading tasks, particularly at symmetrical locations across the hemisphere, in previous research supported by AFOSR ( ). Inspection of the overall 5-second data (all tasks regardless of tilt) we see that coherence at 14-19Hz bifrontally and 4-7Hz posteriorly were chosen as the first and second EEG features of high performance with increased values versus low performance.

92% success was achieved at the 45° tilt with three parameters. Mean frequency in the 4-7Hz band decreased with correct performance and this shift to slower frequencies was accompanied by an increase in energy in that band at frontal locations, that feature being chosen second. We recall here increased frontal energy with good performance on the sleep interruption tasks. Third choice was frontal coherence in the 8-13Hz band: Again, this increased with high performance, similar to the choice in the overall results in the 14-19Hz band.

The greatest separation was attained at 70° of tilt. Here, 95% was achieved with three parameters. Chosen first was mean frequency posteriorly on the left: in the higher band of 14-19Hz, the mean frequency increased.

This increase with high task performance is not unexpected with the true alpha blocking associated with task performance, but it is interesting in terms of high versus low performance. When this feature was selected previously at the 45 degree of tilt, in the lower frequency band of 4-7Hz, it decreased with high performance - this probably relates to a redistribution of energy in the band.

Finally, the phase relationships between the frontal and posterior locations on the right contributed to the separation with the frontal wave train (F_4-T_4) leading the posterior wave train (P_4-O_2) by 56°.

Results of the task performance according to score: 0-2 ranked as low score; 3 & 4 correct as a high score (4 highest possible).

90^{0}: 3 seconds

CHANNEL	PARAMETER	BAND	SUCCESS	BEHAVIOR
F_4-T_4 | P_3-O_1	Coherence	4-7 Hz	66%	↑ High score
P_3-O_1	Bandwidth	4-7 Hz	88%	↑ High score
F_3-T_3 | P_4-O_2	Phase	4-7 Hz	94%	23^{0} phase difference 126^{0} - 149^{0}

45^{0}: 3 seconds

F_4-T_4	Mean Frequency	8-13 Hz	73%	↓ High score
F_4-T_4 | P_3-O_1	Phase	4-7 Hz	73%	-8^{0}- 36^{0} 44^{0} shift
P_3-O_1 | P_4-O_2	Phase	1-3 Hz	86%	11^{0}-2^{0} 13 shift

70^{0}: 3 seconds

F_3-T_3 | F_4-T_4	Phase	1-3 Hz	75%	186^{0} 117^{0} 69^{0} shift
P_4-O_2	Bandwidth	1-3 Hz	89%	↓ High score
F_3-T_3 | P_3-O_1	coherence	8-13 Hz	89%	↓ High score

Results of 3-second task performance: EEG correlates of low vs high performance.

At the 90° baseline position, 94% success was achieved with EEG correlates of low vs high performance. Associated with high performance were the features of coherence, bandwidth, and phase. Coherence at the F_4 - T_4 P_3 - O_1 pair in the 4-7 Hz band once again increased with high scoring. The bandwidth within the 4-7 Hz band at P_3 - O_1 widened with high vs. low score: This is the first time bandwidth has been selected. In general, bandwidth expresses the stability of the dominant frequency, and the narrower the bandwidth the more sinusoidal is the signal. The third choice, phase between dissimilar locations - frontal on the right parietal on the left had a 23° difference with the left leading the right side.

At 45°, mean frequency, and two phase measurements provided 86% discrimination. At the frontal location on the right, mean frequency in the alpha (8-13Hz) band decreased with high performance. Mean frequency on the left posteriorly also decreased in the 4-7 Hz band in the 5-second data in the 45° tilt position, and was also chosen first in that discrimination. Mean frequency is close to the dominant frequency in the band under inspection. Phase relations from right frontal and left posterior locations had a diference of 44°, with the posterior left side leading the right. The next phase difference is at the bilateral posterior pair P_3-O_1 / P_4 - O_2; it is a 13 degree difference with the left hemisphere leading the right once more.

At 70° of tilt, phase, bandwidth and coherence provide an 89% discrimination. Bifrontal phase at F_3-T_3 / F_4-T_4 has a 69° difference with the left side once more leading the right at 1-3 Hz. Bandwidth in this same band decreases with high performance on the right posteriorly at P_4-O_2. The third choice coherence between

F_3-T_3 / P_3-O_1 in the alpha band decreases.

These features were selected in both the 5 second tasks and 3 second tasks from a total of 120 parameters. Activity at the left posterior P_3-O_1 location was selected most frequently, and the most common frequency band involved was 4-7 Hz. This activity in the lower frequency bands is in dramatic contrast to the classic visual impression that faster frequencies are involved in mental effort. There is accumulating evidence however, that theta band activity (4-7 Hz) is involved as the dominant frequency band in environments which are novel and in orienting to novel stimuli (14) (15) (16). Theta band activity was also the most important band of significant activity in our previous work with the chimpanzee in which it was possible to predict correct performance (17).

Inspection of the results also reveal that the coherence function was frequently selected in both the 5-second tasks and the 3-second tasks. It is of interest to note that its value increased with correct performance when the shared activity involved both hemispheres but decreased when the shared activity was within the same hemisphere. We again recall that in our previous dyslexia experiment(10), good readers had higher coherence across the hemispheres during reading tasks, whereas the dyslexia poor readers had higher within the hemisphere coherences while attempting reading.

Another frequently selected cross-term measure, the phase difference between two given wave trains, was also selected several times. Here the situation appears complex. With symmetrical placements, the left hemisphere leads the right both when frontal phases and posterior phases were selected. In the one cross—hemisphere asymmetrical choice, the right posterior wave train leads the left frontal train.

All slides correct: Low vs. High: 0-2 correct vs. 3-4 Correct (4 highest possible) 5 seconds (regardless of tilt).

Channel	Parameter	Band	Success	Behavior
F_3-T_3 | F_4-T_4	Coherence	14-19 Hz	60%	↑High
P_3-O_1 | P_4-O_2	Coherence	4 - 7 Hz	74%	↑High
P_3-O_1	Mean Frequency	14-19 Hz	77%	↑High

In the one within hemisphere measure, the right frontal wave train led the right posterior activity.

From the single channel data (autospectra) mean frequency was chosen most often. It increased in the theta band and decreased in the higher bands, once more at some variance with classical visual observations and assumptions. The two other autospectral measures, SUMSPEC (autospectral energy) and bandwidth were chosen the least frequently. The energy increased in both the theta band and the alpha band with high scores. Bandwidth on opposite sides of the head behaved differently at different frequencies: in the 4-7 Hz theta band, the band widened at the left posterior location; in the 1-3 Hz on the right, posteriorly, it widened.

Finally, in considering the data without respect to tilt and then relating it to tilt we find at 5 seconds, coherence in the 14-19 Hz band at bifrontal locations is chosen first. This is not seen in either the 90^{0} baseline or the tilt situations. The next band was chosen 3rd at 45^{0}, however: at 8-13 Hz, coherence improves discrimination from 84% to 92%. Next, we see that coherence in the 4-7 Hz theta band from the bilateral posterior location improves the selection from 60% to 74%. This was chosen at the 90^{0} baseline and as the best selection, achieved 83% success. In all circumstances, coherence value increased with high scores. The third feature chosen, mean frequency in the 14-19 Hz band at the P_3-O_1 posterior location which raised the selection to 77%, was chosen first at the 70^{0} tilt position. Here, on this one step, 65% success was attained.

In comparisons at the 3 second interval in the overall data regardless of tilt, the F_4-T_4 | P_3-O_1 combination was chosen all 3 occasions. First, coherence in the 4Hz - 7Hz band at this pair was picked. Its increase during high scoring permitted a 69% discrimination. At the 90^{0} baseline, this was also chosen first and provided 66% selection. Next, coherence at 20-25Hz was chosen. Its value

decreased with high performance. This parameter is not seen in the tilt data; nor is there other activity in this high frequency band. The final selection was phase angle in the 4-7Hz band were the left posterior wave train leads the right frontal activity. This same parameter appears in the 45^{o} tilt selections as a second choice.

Thus, four out of six parameters from the overall data are seen again in the tilt data, reflecting a high degree of consistency in the results. Moreover, though there is a range in the percent success in this tilt study from 83% to 95%, not only are these much better than chance findings, even the initial single selections are significantly better.

Though the parameters of bandwidth, phase, and mean frequency are difficult to see in the raw and transformed data, the changes in the energy spectrum are visually observable due to tilt and due to true alpha blocking as we have described. The changes can be seen even in the 3-second data which we illustrate in Figures 1-6.

Finally, we illustrate the consistent increase in coherence in lower frequencies at the F_3-T_3 | F_4-T_4 bifrontal location with increasing success from none correct to a maximum of 4 correct at the 90^{o} baseline level. This data is taken from the 10 second epoch group.

Figure 1. This is the distribution of energy over the frequency band of 1 to 32 Hz from electrodes positioned at the back of the head in the parieto-occipital linkage. The narrow-band peak at 10-11 Hz is the well-known alpha rhythm. The subject is in the eyes-open rest state, looking at the blank screen. The seat is not tilted. Note the energy listed as SUMSP=1488 on the left and SUMSP=1971 on the right. This is the sum of spectral intensity or energy in the signal.

Figure 2. These are the same leads as Figure 1. Note that the alpha peak is really "blocked", that is, it disappears and that the energy decreases on both sides. This was also true in our pre-sleep data during task performance. Here, the subject is looking at a projected slide on the screen with the seat in the baseline 90^{o} position.

Figure 3. The seat has now been tilted to the 45^{o} angle. Notice that the alpha peak, though evident, is much smaller than in the comparable eyes-open-rest spectra at the 90^{o} position. Though it is not easy to see, the peak is also at about 1Hz slower and the base of the peak, comparatively, is broader. The alpha peak also was at about a 1-2 Hz slower frequency in the post-sleep resting state. Note also that energy is sharply decreased.

Figure 4. The subject is now observing the projected slide and we see again that, except for the barest hint of a peak at P_4-O_2, the alpha activity is blocked. Note also that the energy during observation has increased over the 45^{o} baseline (even though) it is still less than the 90^{o} position). This was also true of the post-sleep task data.

Figure 5. The seat is now tilted to the maximum used in the study: 70^{o}. The alpha peaks are truncated and broader at the base, in the eyes open rest position as compared to 90^{o} baseline. Energy is still reduced from that seen at 90^{o}.

Figure 6. The alpha peaks are again blocked, except for the merest hint at P_3-O_1, in the 70° position. Once again, energy is lower than in the 90° task data, with only slight changes when compared to the 70° eyes open rest state. Spectral "profiles" tend to look alike during task performance, but the energy data as we have seen is quite different. This is further discussed in the text.

Bibliography for Tilt Experiment

1. Parkhurst, M.J., Leverett, S.D., Jr., and Shurbrooks, S.J., Jr. Human tolerance to high, sustained + G_2 maneuver. Aerospace Med. 43:708-712, 1972.

2. Wood, E.H., and Code, C.F. The physiologic basis of voluntary (self-protective) maneuvers capable of increasing man's tolerance to positive acceleration. XVII International Physiol. Congress, 311-312, 1974.

3. Watson, J.F., and Cherniak, N.S. Effect of positive pressure breathing on the respiratory mechanics and tolerance to forward acceleration. Aerospace Med. 33:583-588, 1962.

4. vonBeckh, H.S. G protective tilting aircraft seats. NADC-72063-CS., 1972.

5. Burns, J.W. Re-evaluation of a tilt-back seat as a means of increasing acceleration tolerance. Aviation, Space, and Environmental Medicine 46(1): 55-63, 1975.

6. Burton, R.R., Leverette, S.D., Jr., and Michaelson, E.D. Man at sustained + G_2 acceleration: a review. Aerospace Med. 45(10)1115-1136, 1974.

7. Anderson, T.W. Introduction to Multivariate Statistics. Wiley, New York, 1960.

8. Nilsson, N.J. Learning Machines. McGraw-Hill, New York, 1965.

9. Dixon, W.J. Ed., BMD Biomedical Computer Programs, Univ. of California Press, Berkeley, 1970.

10. Hanley, J. Optimizing Manpower Selection, Final Report, AFOSR: Scientific Report, 197 1974-11.

11. Blackman, R.B. and Tukey, J.W. The Measurement of Power Spectra. New York, Dover, 1959.

12. Jenkins, G.M., and Watts, D.G. Spectral Analysis and Its Applications. Holden-Day, Inc., San Francisco, 1969.

13. Nathan, R.D., and Hanley, J. Spectral analysis of the EEG recorded during stimulation of the human Fovea. Brain Research, 91:61-65, 1975.

14a. Elazar, Z. and Adey, W.R. Spectral analysis of low frequency components in the electrical activity of the hippocampus during learning. EEG & Clin. Neurophysiol. 23:306-319, 1967a.

14b. Elazar, Z., and Adey, W.R. Electroencephalographic correlates of learning in subcortical and cortical structures. EEG & Clin. Neurophysiol. 23: 306-319b. 1967.

15. Zweigig, J.R., Adey, W.R., Hanley, J., Hahn, P.M., Pilmanis, A.A., Given, R.R., & Cockett, ATK. EEG monitoring of a free-swimming diver at a working depth of 15 meters. Aerospace Med., 43:403-407, 1972.

16. Sokolov, A.N. Higher nervous system functions: the orienting reflex. Ann. Rev. Physiol. 25:545-580, 1963.

17. Hanley, J., Walter, D.O., Rhodes, J.M., and Adey, W.R. Chimpanzee performance: computer analysis of electroencephalograms. Nature. 220:879-881, 1968.

I

AIR FORCE COUCH TILT STUDY
ALL SUBJECTS 90° BASELINE
FOR 3 SECOND EPOCHS (N=24)

SUMSP = 1488
P3-01

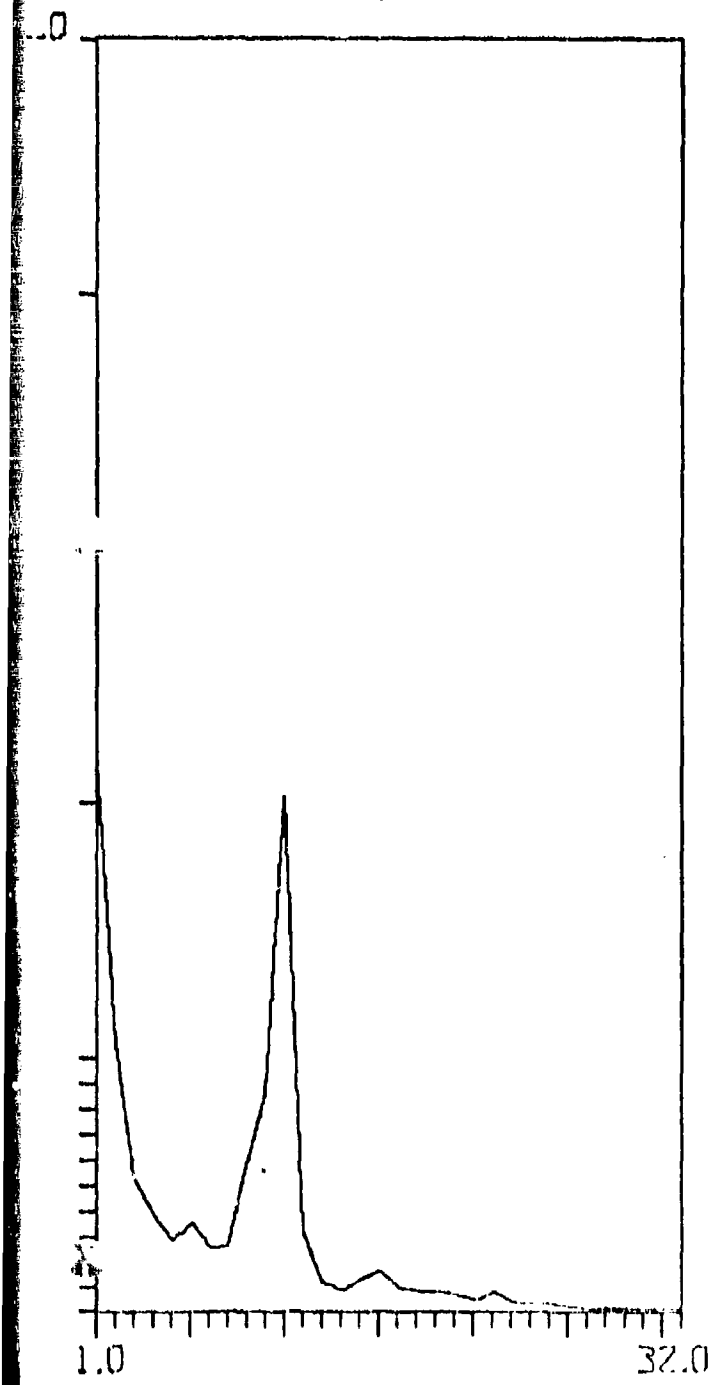

SUMSP = 1971
P4-02

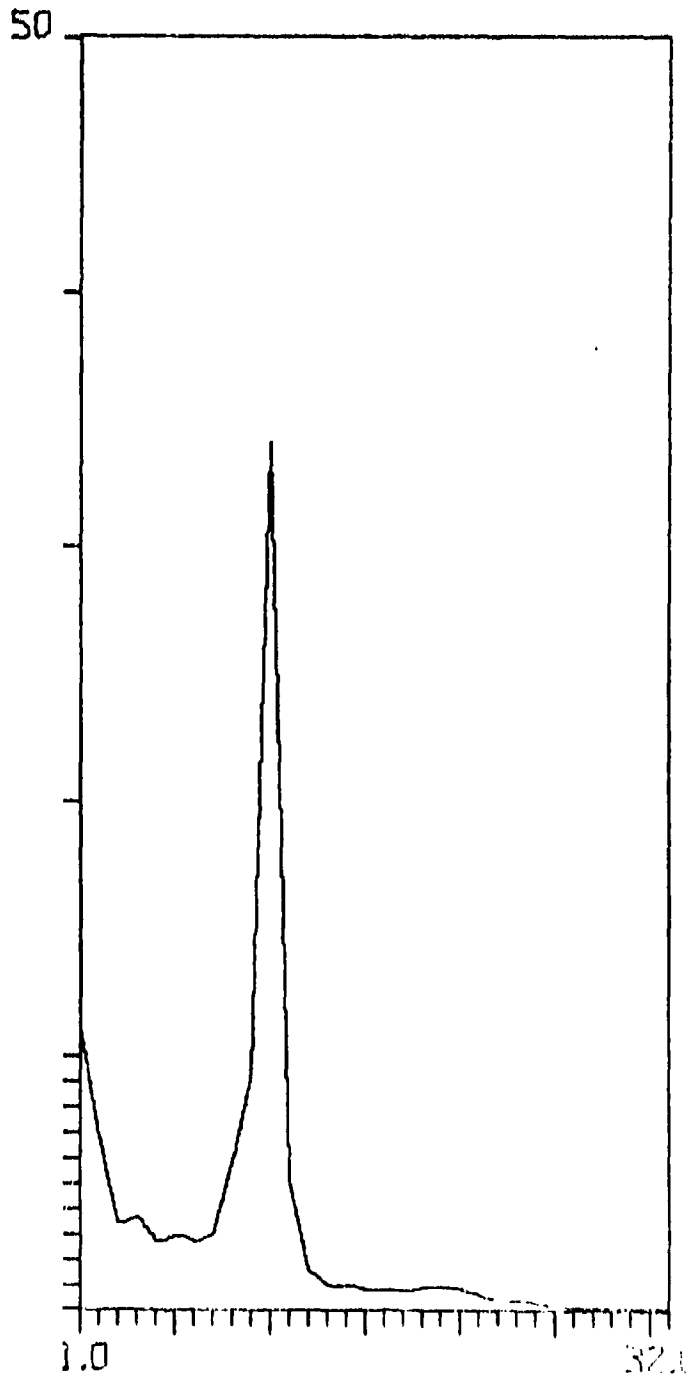

AIR FORCE COUCH TILT STUDY
ALL SUBJECTS 45° BASELINE
FOR 3 SECOND EPOCHS (N=28)

SUMSP = 899
P3-01

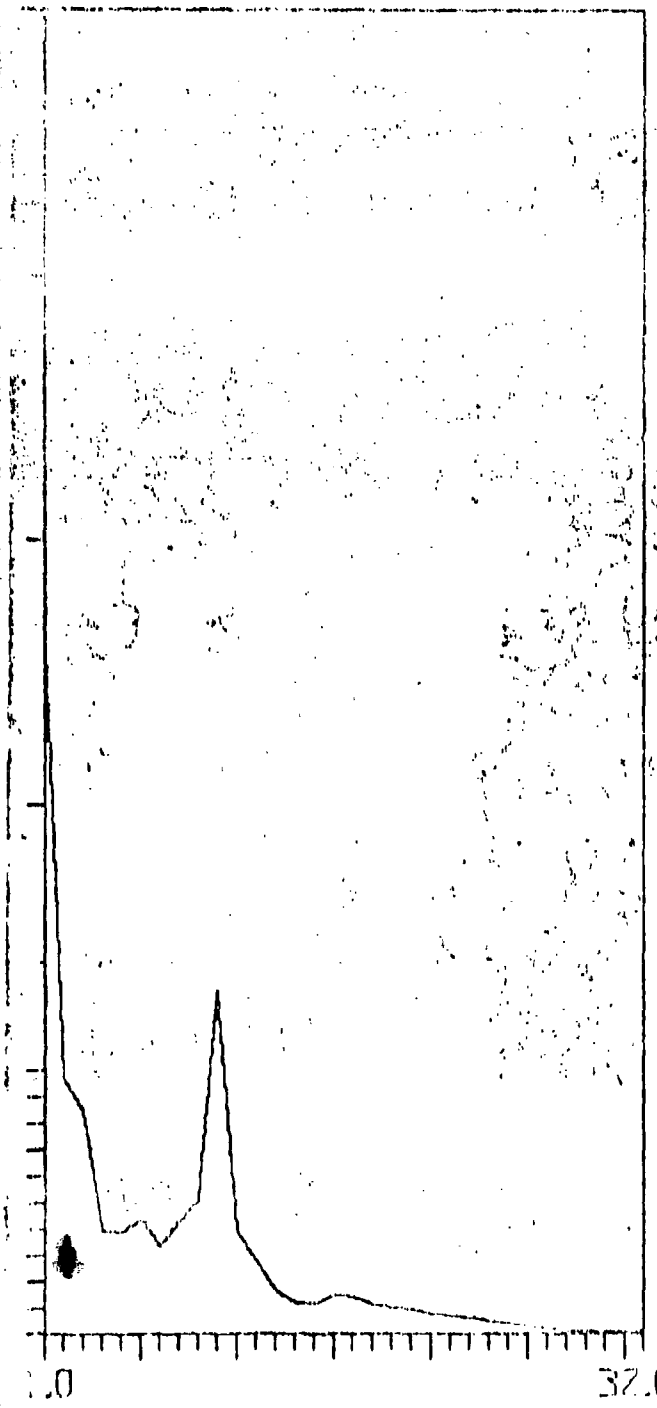

SUMSP = 599
P4-02

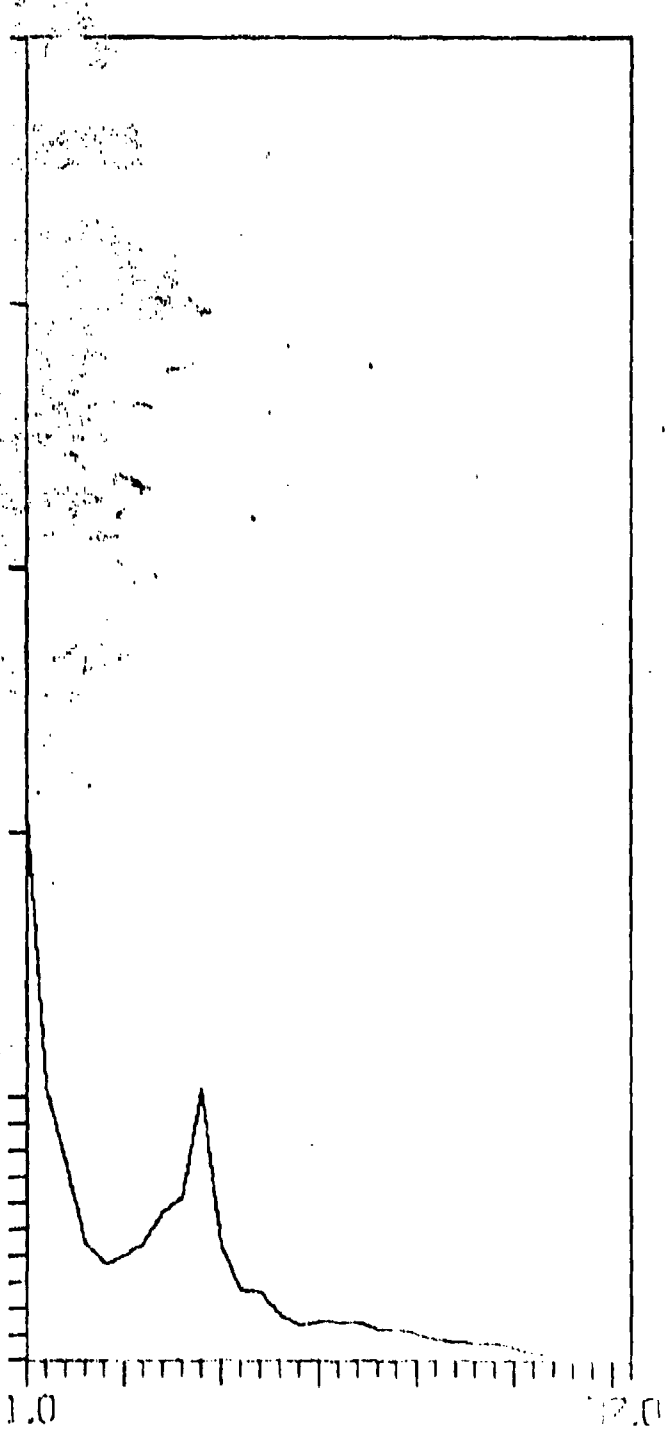

AIR FORCE COUCH TILT STUDY
ALL SUBJECTS 70° BASELINE
FOR 3 SECOND EPOCHS (N=26)

SUMSP = 856
P3-01

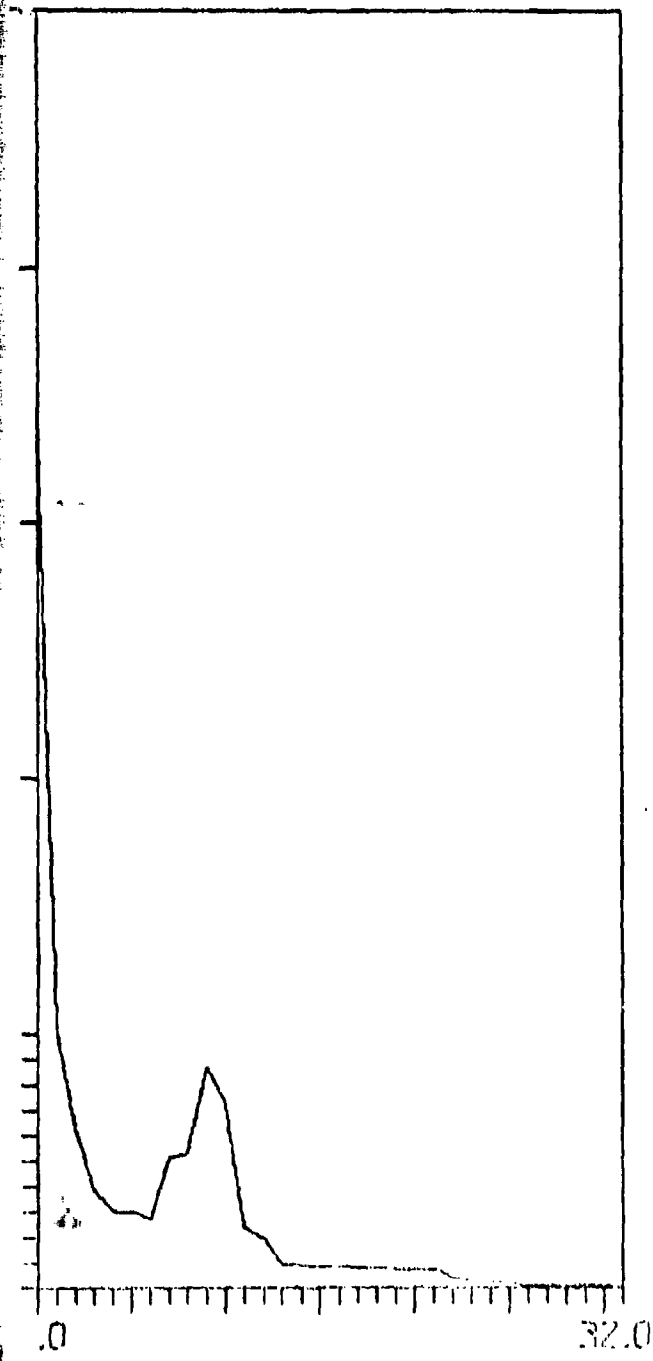

SUMSP = 786
P4-02

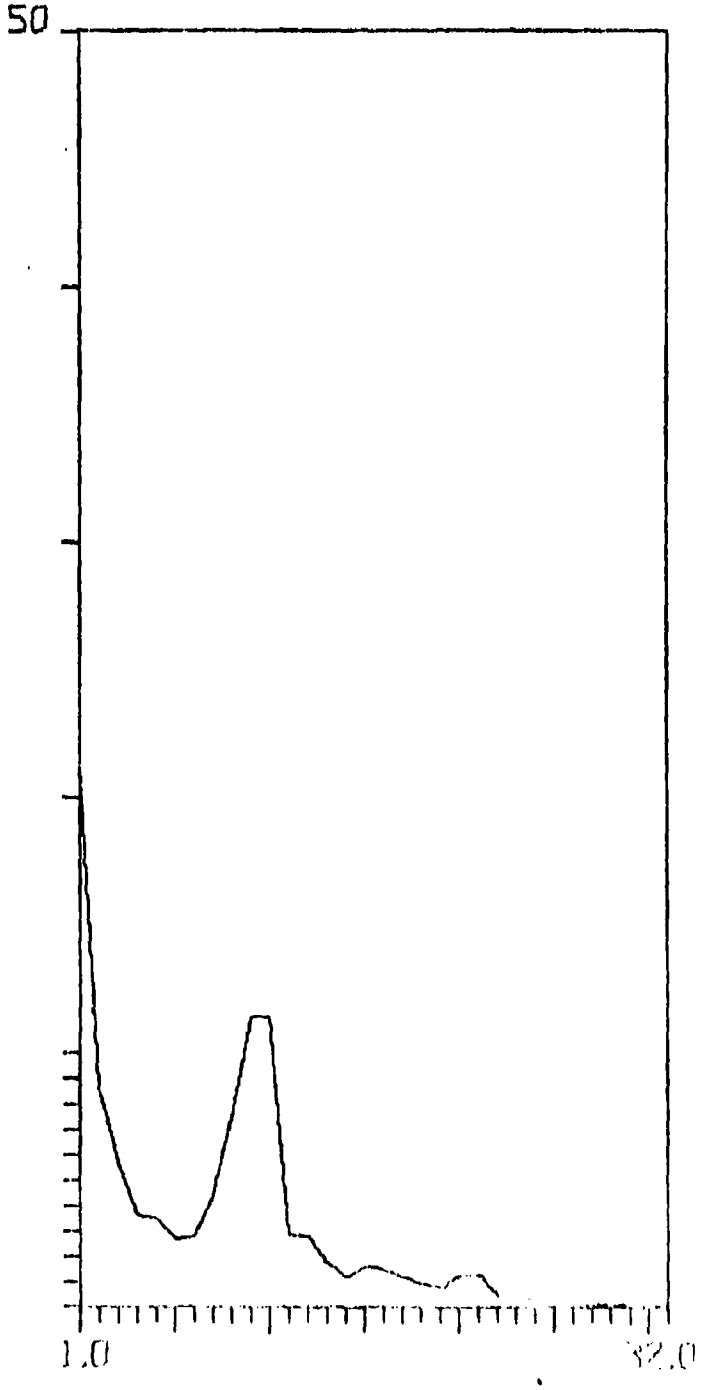

AIR FORCE COUCH TILT STUDY
ALL SUBJECTS 90°
SLIDES 3 SECONDS (N=18)

SUMSP = 1165
P3-01

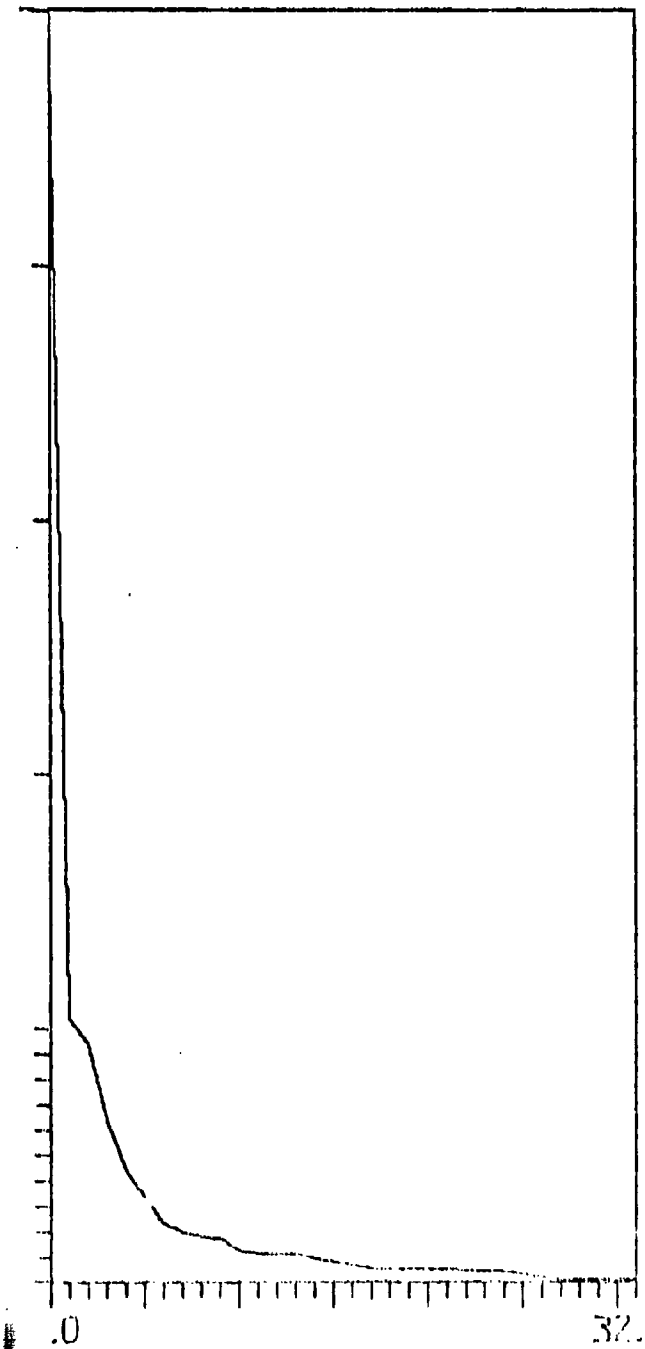

SUMSP = 1036
P4-02

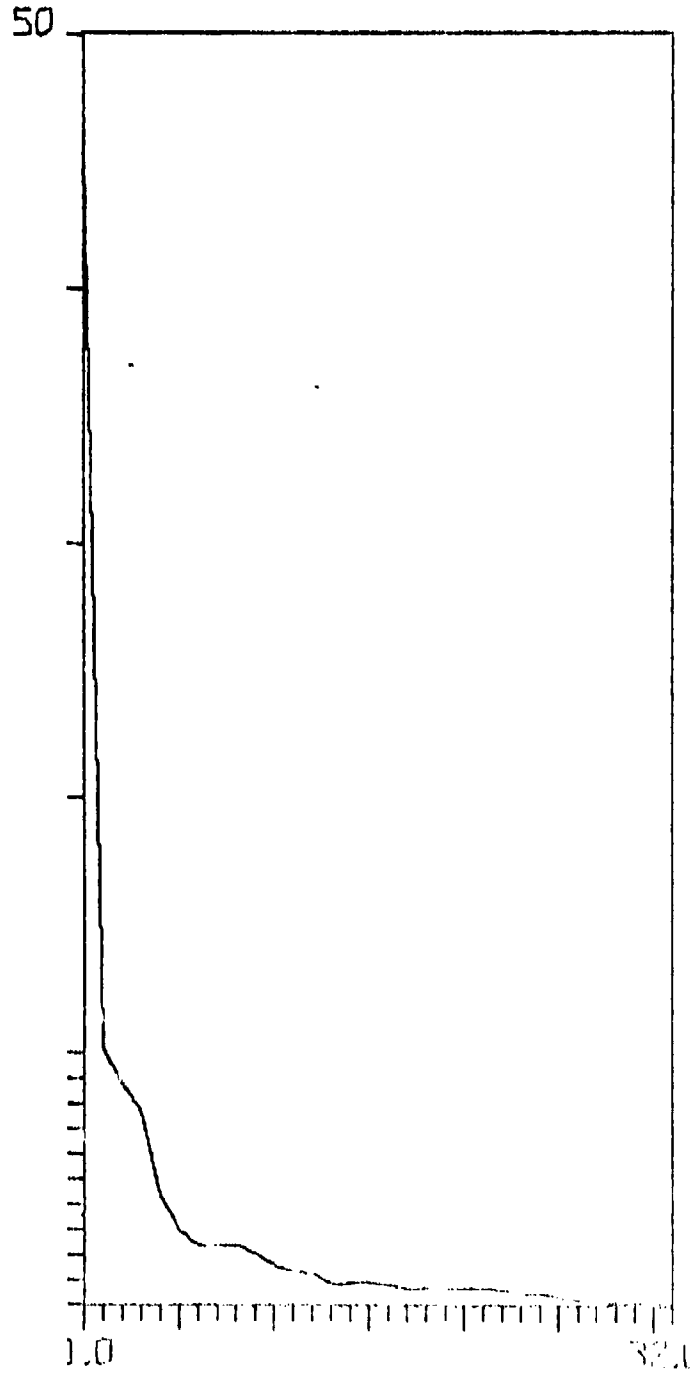

AIR FORCE COUCH TILT STUDY
ALL SUBJECTS 45°
SLIDES 3 SECONDS (N = 23)

SUMSP = 1100
P3-01

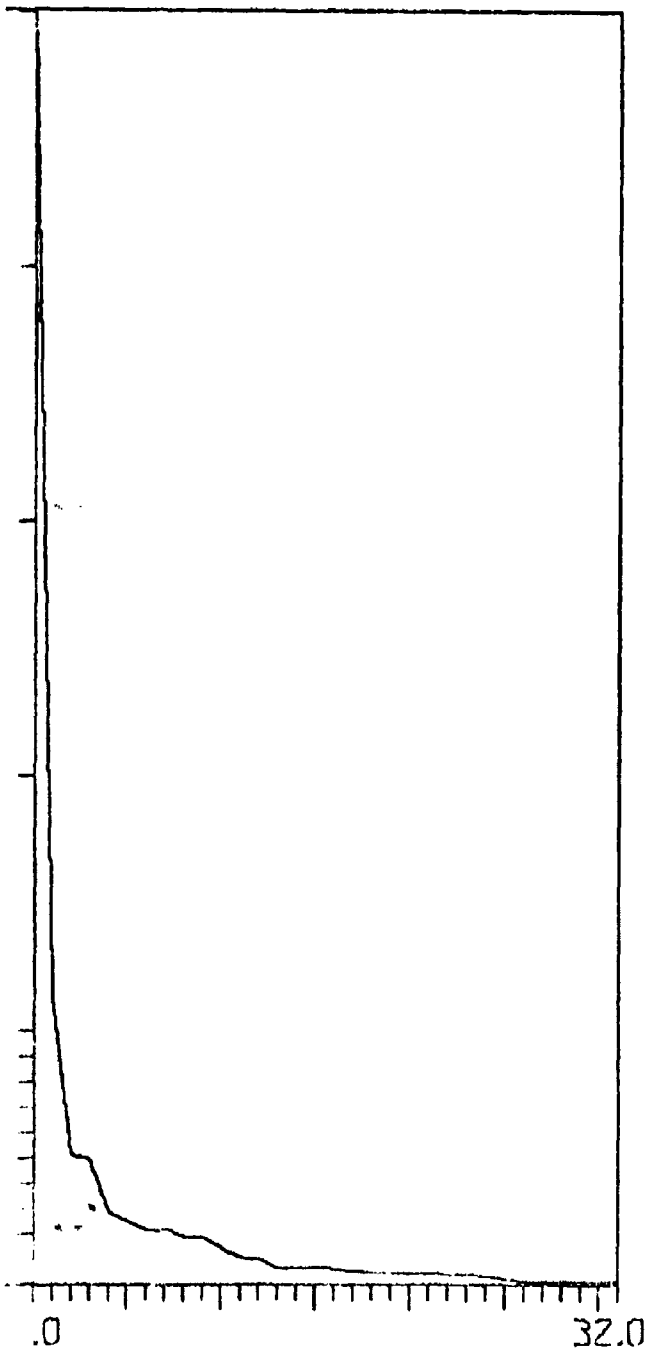

SUMSP = 757
P4-02

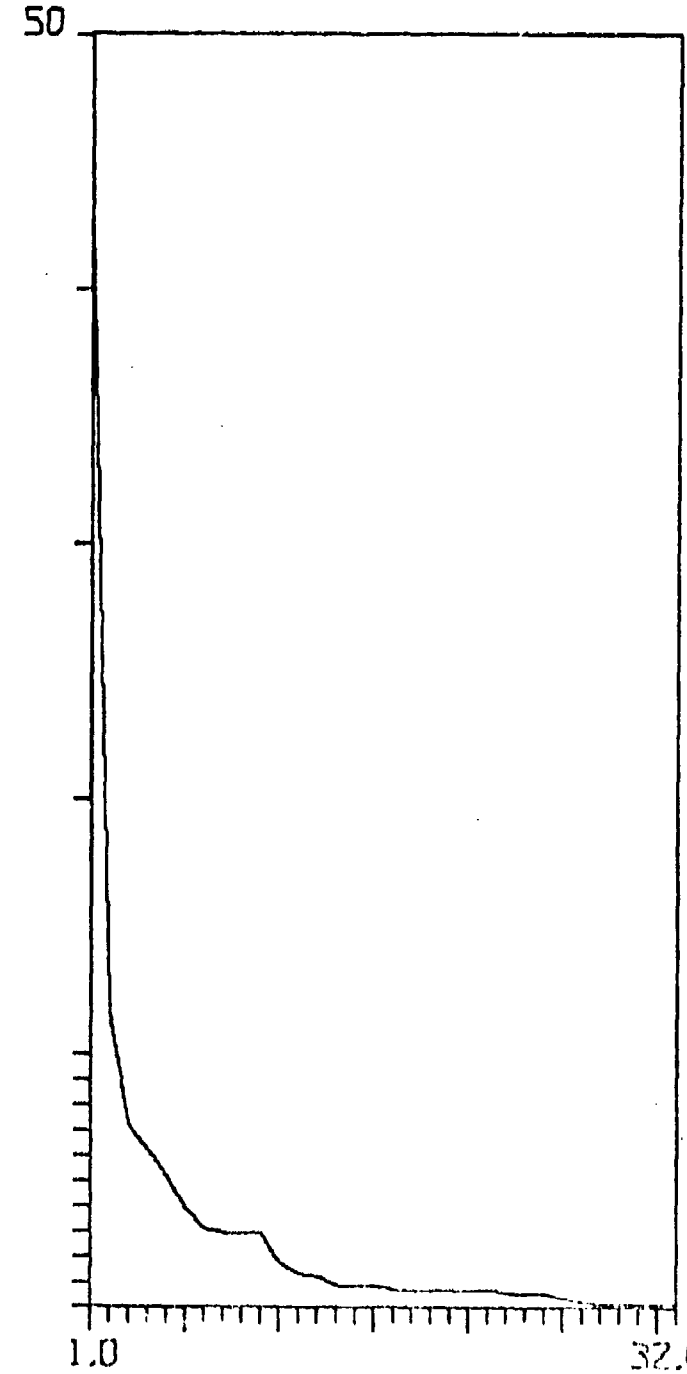

AIR FORCE COUCH TILT STUDY
ALL SUBJECTS 70°
SLIDES 3 SECONDS (N=28)

SUMSP = 826
P3-01

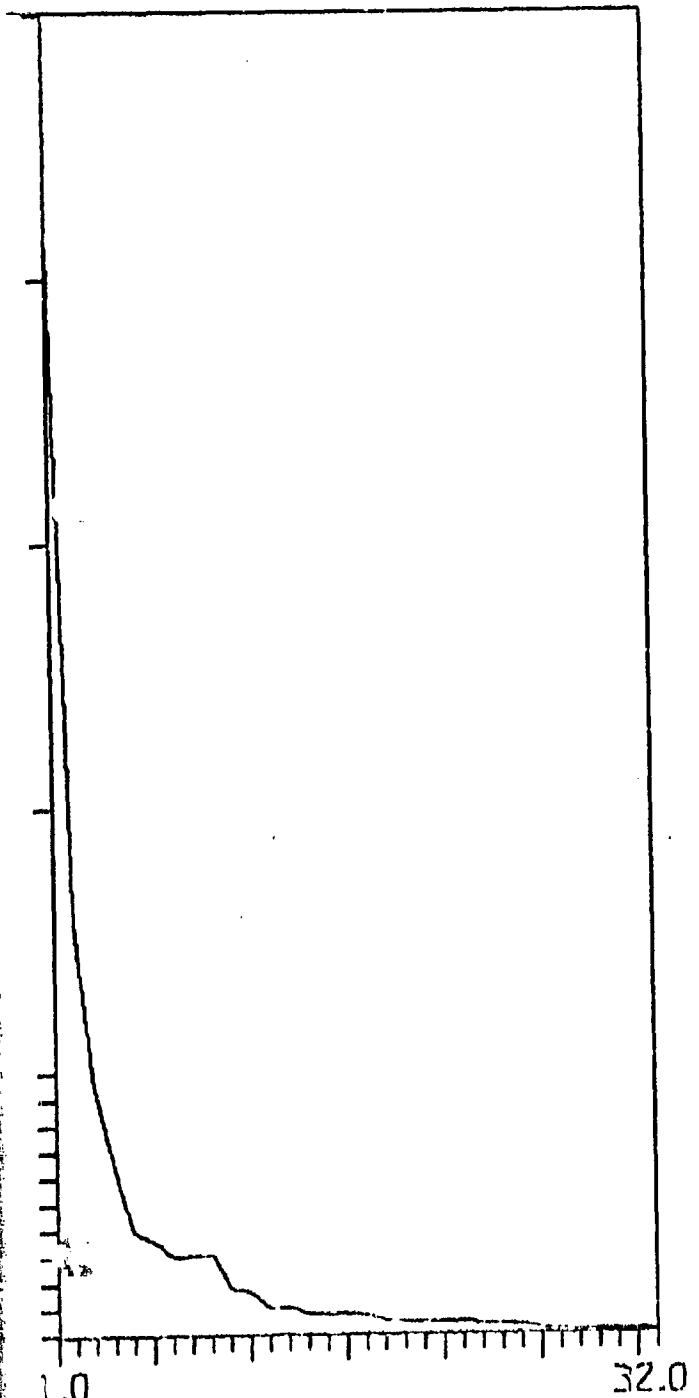

SUMSP = 848
P4-02

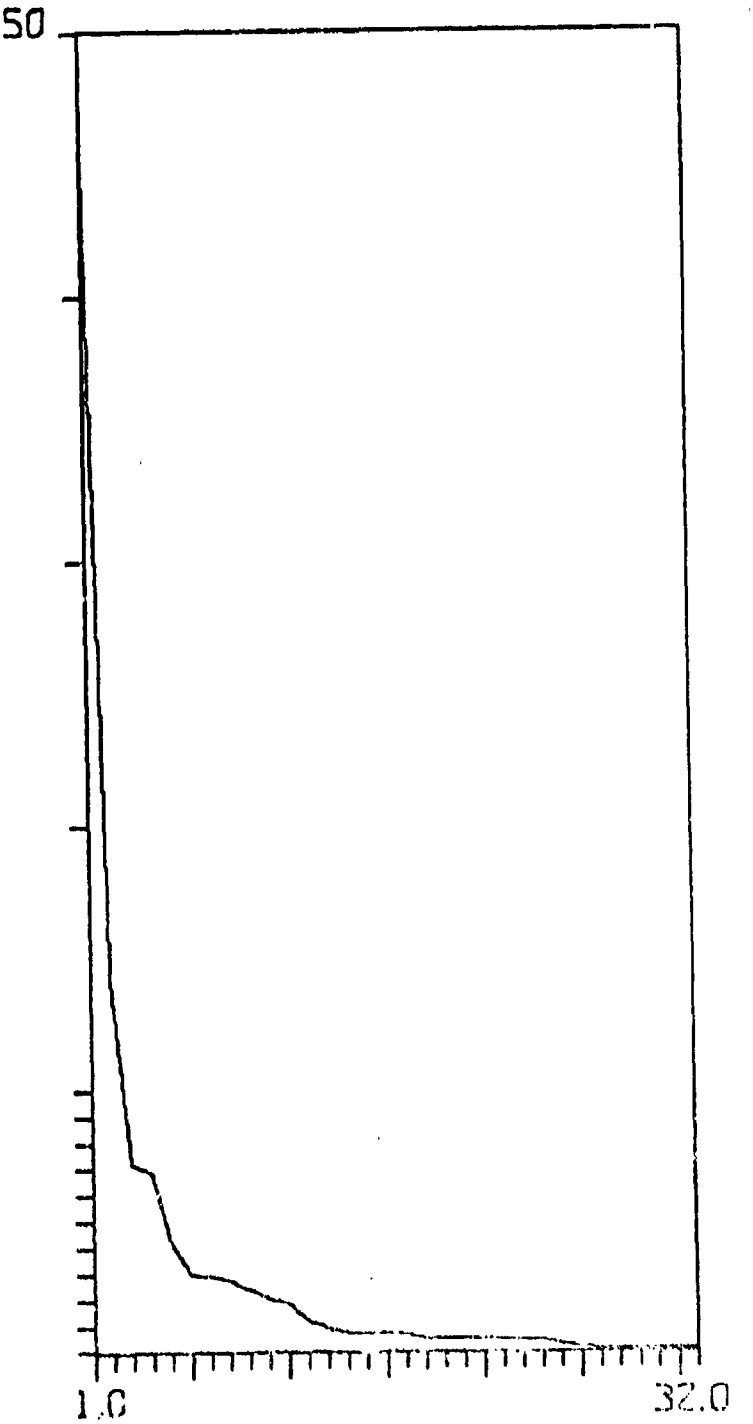

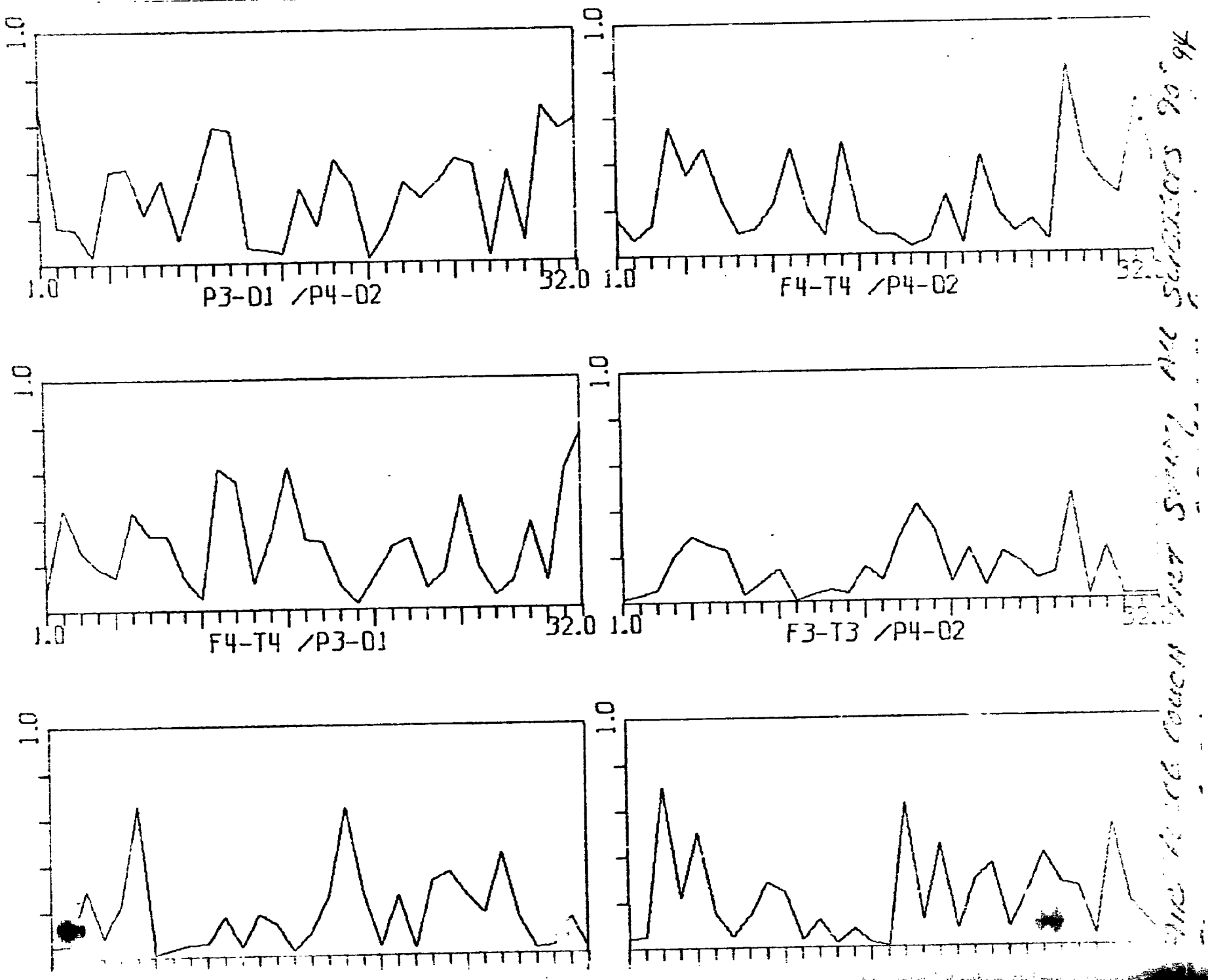
1.0
1.0
32.0
P3-O1 /P4-O2
1.0
1.0
F4-T4 /P4-O2
1.0
1.0
32.0
F4-T4 /P3-O1
1.0
1.0
F3-T3 /P4-O2
1.0
1.0

AIR FORCE COUCH TILT STUDY All Subjects 90°

SLIDE #2 S 202, 206 SLIDE #4 ... 200, 207

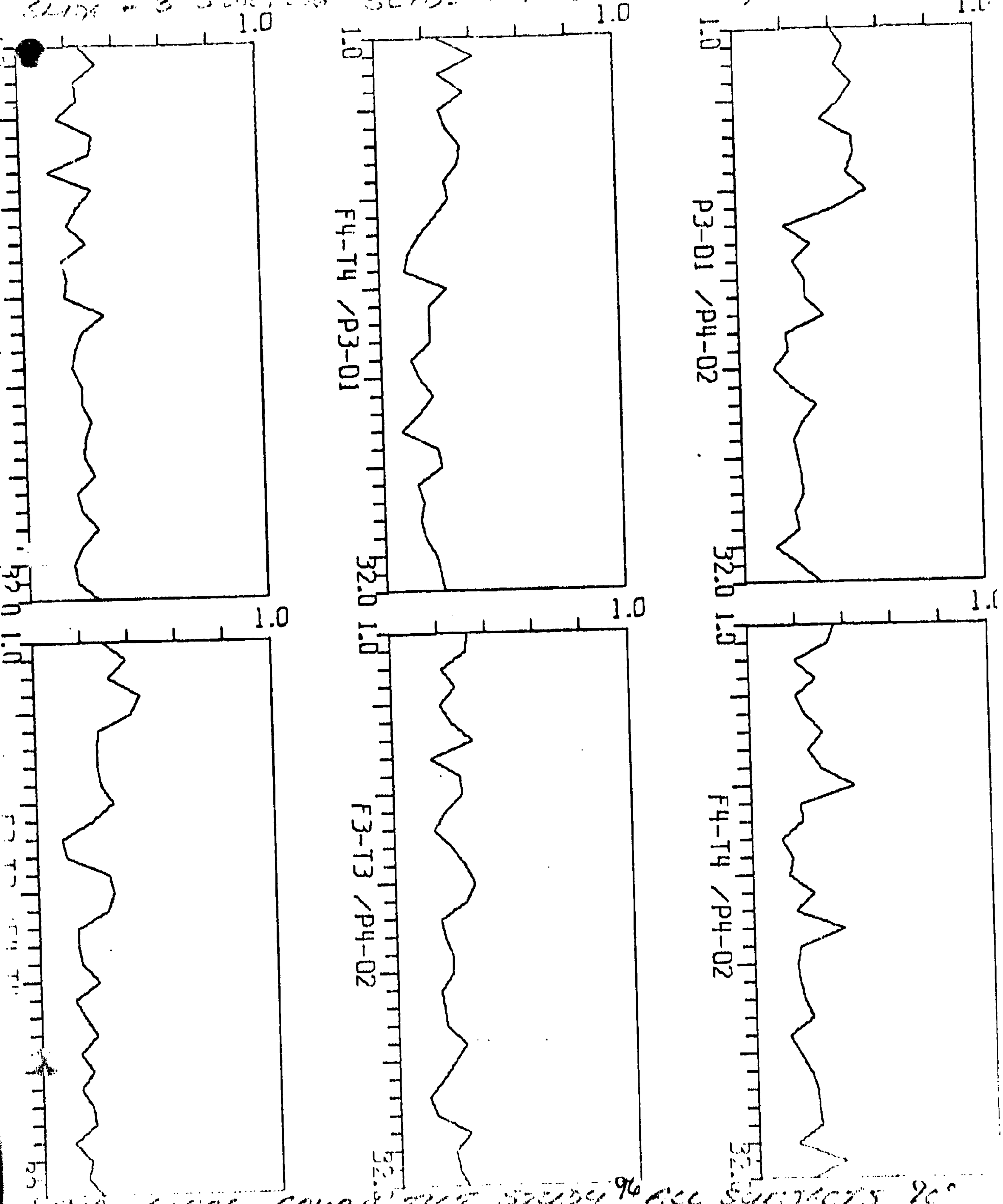

AIR FORCE COUCH MCT STUDY 96 ALL SUBJECTS 96

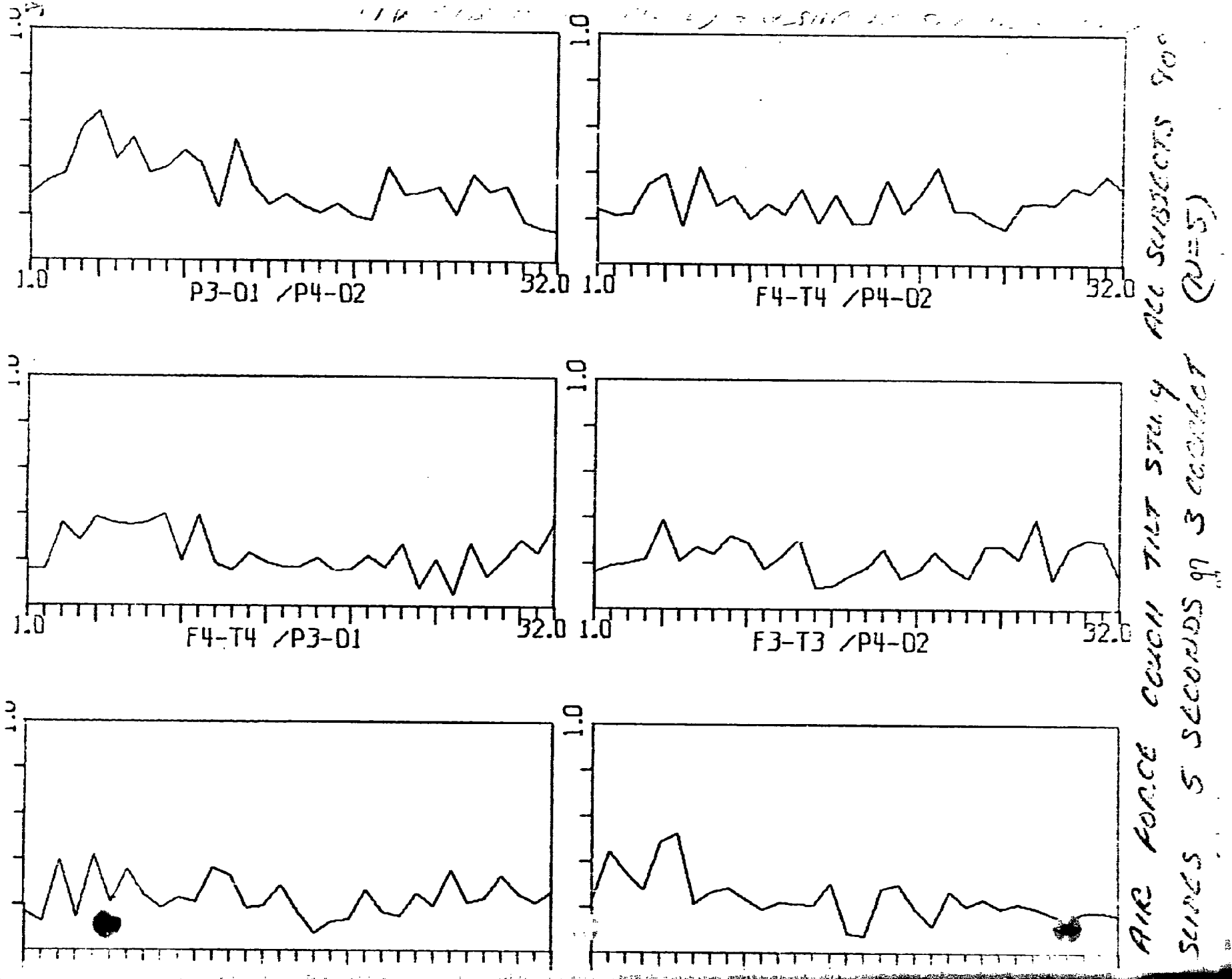

AIR FORCE COUCH TILT STUDY
SERIES 5 SECONDS @ 3 CM/SEC
ALL SUBJECTS 90°
(N=5)

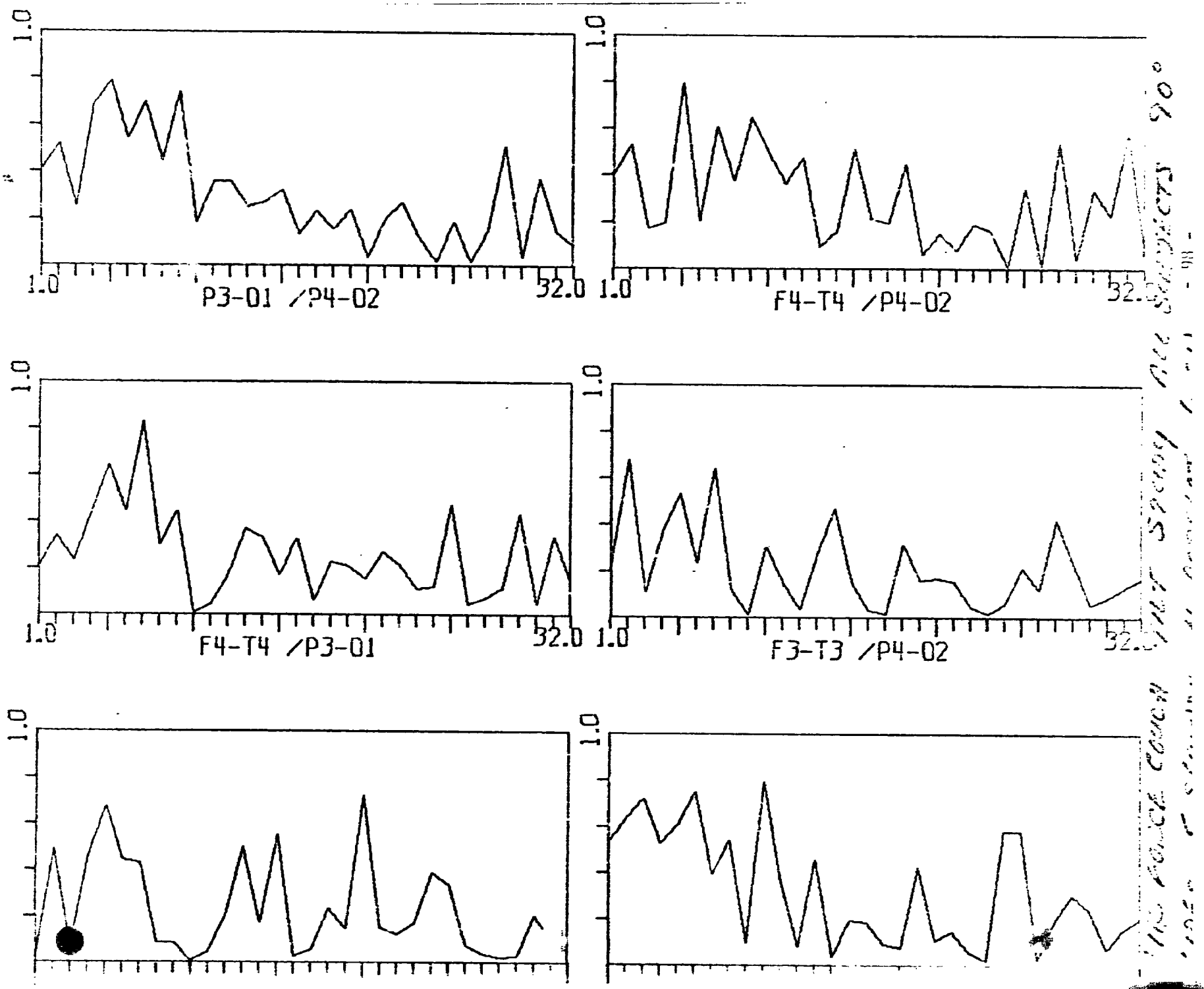
1.0
1.0
32.0
P3-01 /P4-02
1.0
F4-T4 /P4-02
1.0
1.0
32.0
F4-T4 /P3-01
1.0
F3-T3 /P4-02
1.0
1.0

SECTION II

BEHAVIORAL NEUROPHYSIOLOGY IN SUBHUMAN PRIMATES

2. Behavioral Neurophysiology

a. Effects of simulated cockpit noise on monkey visual discrimination and EEG activity (S. Moise, Ph.D., and A. Costin, M.D., Ph.D.).

Human performance in skilled tasks deteriorates in high environmental noise levels. This deterioration is not limited to tasks involving auditory signals, where there may be direct interference with perception of essential cues. It also characterizes performance of visual tasks.

More precise data on brain mechanisms that might be involved requires direct examination of electrical activity in deep brain structures in sensory and associative systems that participate in decision making on visual cues in the presence of high levels of interfering noise. New knowledge on these interference effects would serve a double purpose. It would assist in development of mitigating procedures to minimize effects of high noise in operational environments. It would also lay the groundwork for mazimizing interference with visual perception, as in sniper fire against low flying aircraft.

Five pigtail macaque (Macaca nemestrina) monkeys have been tested on a visual task during intercurrent exposure to two different auditory stimuli. Test procedures were designed to detect possible impairment of performance and concurrent altered electrical patterns in particular brain structures.

Auditory stimuli were presented at a level of 90 db. Two different auditory stimuli were tested. One was a recording of B52 cockpit noise presented continuously during the test period. The other was white noise pulsed at 4, 10, 40 and 400 Hz. For EEG recording, bipolar electrodes were implanted in the hippocampus, lateral geniculate body, visual cortex, temporal neocortex and the caudate nucleus.

The monkeys were presented with a delayed matching-to-sample task for a food pellet reward. The task was presented under control of a PDP-8-I computer.

b. Proactive effects of stimuli, delays and response position during delayed matching-to-sample in monkeys.

Numerous studies in recent years have revealed functional similarities between short-term memory in monkeys and man. In particular, retroactive interference effects have been shown to be important determinants of memory task performance in monkeys as well as in man. The role of proactive interference factors have been more difficult to assess. Because of the considerable theoretical importance of proactive interference for an understanding of memory in man, it is an important phenomenon to investigate in the context of human memory problems in operational environments, as well as for models of animal learning.

Possible proactive effects were sought in 4 female pigtail macaques performing a 2-choice delayed matching-from-sample task. The display involved the 3 x 3 matrix of symbols described under (a) above. Effects of the nature of the sample stimulus, the duration of the delay, and the position of the test symbol embedded in the matrix of the final display were all evaluated, testing their role in trial n-1 on trial n. The results are interpreted as indicating proactive interference with retention of sample stimuli on trial n when the stimulus used in trial n-1 differed from that in trial n. The control situation used the same stimulus in trials n-1 and n. In addition, when the same stimuli were used in trials n-1 and n, and trial n-1 was incorrect, greater interference occurred than when trial n-1 was correct.. Evaluation of performance as a function of delays on trial n-1 and trial n support the

hypothesis of d'Amato (Psychonom. Sci. 1971, 25:179-180) that delayed matching occurs as a temporal discrimination.

c. Computer technology: an automated system for primate instruction in complex behavioral tasks.

In recent years, there have been numerous descriptions of hardware and software systems for facilitating use of minicomputers in psychological and physiological research. These systems can offer flexibility in the management of options and contingencies essential in testing sophisticated behavioral capabilities in man and subhuman primates. They permit rapid modification of sequential tasks not possible by intervention of the experimenter. Nevertheless, we have not formed a system suited to our needs in a primate training and data acquisition system, based on the widely used PDP-8-I computer. Our requirements were for a system which would (1) act as a task controller for a large number of experimental paradigms (operant conditioning to complex decision making behavior) (2) collect behavioral data in a well organized format for subsequent analysis (3) monitor and record physiological data (EEG, EKG, EMG, etc.) for on-line analysis during the experiment and (4) permit computer control of a large number of experimental parameters (i.e. brain stimulators, noise generators, ambient lighting).

We have developed a flexible hardware/software system (ASPRIN) for use in behavioral neurophysiology (Moise, Olsen and Huston, 1974). A real time monitor was designed to facilitate development, debugging and modification of programs to run experiments. It relieves the programmer of the burden of dealing with hardware-dependent functions, such as handling interrupts and input/output routines. In addition, it provides the user with a large library of routines that can be called from storage in disc files to perform functions commonly needed in the course of experiments. The monitor is modular in design and can be expanded for use with many of the PDP-8 family of computers.

SECTION III

NEUROCHEMISTRY

3. Neurochemistry (L.K. Kaczmarek, Ph.D., A. Costin, M.D., W.R. Adey, M.D., I. Sabbot, M.S. and B.G. Bystrom, M.S.).

Changes in alveolar CO_2, together with decreased EEG amplitude and increased cortical temperature are well documented as reliable indices of arousal, or of the transition from synchronized to desynchronized sleep. In operational flying, modification of alveolar CO_2 levels are likely to occur in association with inhalation of oxygen through face masks, and in any situation where cockpit or cabin pressurization is associated with accidental or intentional changes in partial pressures of gas mixtures. We have investigated the correlates of release of macromolecular and putative amino acid transmitters from cerebral cortex in association with altered alveolar CO_2 levels and with modified extracellular ionic environments. We have also studied effects of thermal and swimming stress on calcium and magnesium uptake in pituitary gland, and in limbic cortex, diencephalon and brainstem.

a. Release of calcium, amines and amino acids from cerebral cortex during arousal in the cat; correlations with carbon dioxide, brain temperature and EEG.

The release of $^{45}Ca^{2+}$, $^{3}H_2O$, ^{14}C-carboxyl-inulin, ^{3}H-gamma-aminobutyric acid, ^{14}C-taurine, ^{3}H-5-hydroxy-tryptamine, ^{3}H-norepinephrine and ^{3}H-lysine from cerebral cortex into a superfusion medium has been studied in vivo, in locally anesthetized, immobilized cats.

Peaks in the rate of release of all these compounds from the suprasylvian gyrus could be correlated with a diminished amplitude of the cortical EEG, and with increases in brain temperature and levels of CO_2 in alveolar air. Peaks correlated with pCO_2 could still be observed after the topical application of 5×10^{-4} NaCN. Death produced by an overdose of pentobarbital, resulted in a 45 percent drop in the release of $^{45}Ca^{2+}$ and ^{3}H-GABA, followed by irregular peaks in efflux. Superfusion of the cortical surface with a low Ca^{2+} medium

resulted in very regular oscillations in the efflux of a number of isotopes, including ^{45}Ca and $^{3}H_2O$. These oscillations, which had a period of about 6 min, were best observed immediately before or after a train of seizures, while the efflux pattern during seizures was slightly more irregular. The ratio of $^{45}Ca^{2+}$ and $^{3}H_2O$ released at this time also rose and fell in phase with the oscillations in efflux. At each individual seizure, the $^{45}Ca/^{3}H_2O$ ratio fell to a minimum.

On two occasions, marked long term changes in the amplitude of the EEG were observed to correlate with a change in the amplitude of these oscillations. Hemodynamic factors are considered to affect the rate of release of isotopes into the superfusate, but cortical metabolism is also likely to play a role in controlling the rate of release, especially during the oscillations in efflux in low calcium media.

b. Extracellular release of cerebral macromolecules during potassium - and low-calcium-induced seizures.

Proteins and other macromolecular constituents of nervous tissue are in a constant state of synthesis and catabolism. The possibility of an interference with either one or both of these processes is possible during cerebral anoxia, with or without concurrent epileptic seizures. Chronic or repeated episodic anoxia associated with high altitudes may be considered as a possible trigger to or adjuvant to this sequence. Scheibel et al (Epilepsia, 15:55-80, 1974), in studies of the histology of hippocampal pyramids in temporal lobe epilepsy, reported a spectrum of degenerative changes ranging from the loss of dendritic spines to cell death. Their data suggest that these changes may be due to an active, ongoing process of degeneration, rather than having been caused by a discrete cortical injury.

Chemical evidence also supports this possibility, because cerebral protein synthesis is substantially inhibited by raised levels of potassium ions. An increased potassium concentration occurs in the extracellular medium during epileptic seizures. Using a superfusion technique, we have studied the turnover of cerebral proteins at the onset of seizure activity induced by potassium and by media deficient in calcium.

Cerebral cortex of cat was incubated *in situ* with ^{14}C-lysine and ^{3}H-glucosamine. Subsequent superfusion of the surface of the cortex resulted in the release into the superfusate of a variety of ^{14}C- and ^{3}H-labeled compounds, including proteins, glycoproteins, and gangliosides. The release of these macromolecules was considerably enhanced by topical addition of 40 mM K^{+}, which induced epileptiform EEG activity. Peaks in efflux could also be correlated with the onset of seizures induced by superfusion with low (0.75 mM) Ca^{2+} media. Control experiments in which the cortex was prelabeled with ^{14}C-carboxyl-inulin and $^{3}H_2O$ indicate that the release of macromolecules was not a direct consequence of the altered blood flow that may occur during convulsions.

c. Effects of physical stress on calcium and magnesium uptake in pituitary gland and brain tissue.

Calcium plays an important role in the secretory process of hormones, but there is relatively little information about the transport of this cation and of magnesium into pituitary tissue. We have therefore investigated the incorporation *in vivo* of ^{45}Ca and ^{28}Mg by the hypophysis of the rat during severe physical exercise (swimming), cold and heat. All these stress conditions induced a statistically significant increase in both ^{45}Ca and ^{28}Mg uptake. ^{14}C-inulin uptake was unchanged, indicating that this increase involved a change in the permeability of the barrier and not a modification of

the vascular bed or extracellular space. Monoamine oxidase inhibitors increased both ^{45}Ca and ^{28}Mg uptake, whereas reserpine affected only the ^{45}Ca uptake. This suggested an important contribution of the biogenic amine transmitters in the stress-induced changes. Furthermore correlated ultrastructural studies (see below) showed that the stress-induced increase in ^{45}Ca uptake strengthened mitochondrial membranes.

d. Ultrastructural changes in rat brain and pituitary tissues induced by chronic heat stress.

We have studied the regional distribution of uptake of radiolabeled calcium in the brain and pituitary gland of the rat under normal and chronic heat stress conditions (37C for 21 days). A third series of animals were exposed to cold stress (swimming in water at 4C for 30 min). Cerebral cortex were separated by ultracentrifugation into four fractions: 60 min at 1000 G, 55 min at 17,000 G; 60 min at 100,000 G, and 120 min at 100,000 G. In both heat and cold stressed animals, there were significant differences in organelles following ultracentrifugation at 17,000 G for 55 min.

Mitochondria from tissues of control animals appeared physically weaker than those from stressed animals. The proportion disintegrating in the pituitary (84%) and cerebral cortex (79%) was greater than in comparable samples from heat and cold stressed animals (pituitary 48%, cerebral cortex 50%). No differences in mitochondrial structure were evident at lower speeds of ultracentrifugation. The results are interpreted as indicating that the influx of calcium ions resulting from thermal stress had strengthened mitochondrial membranes.

SECTION IV

EFFECTS OF WEAK LOW FREQUENCY FIELDS ON CALCIUM EFFLUX FROM CHICK AND CAT BRAIN

4. Effects of weak low frequency fields on Ca efflux from chick and cat cerebral tissue. (Drs. S.M. Bawin and W.R. Adey).

In 1965 this Laboratory initiated studies to evaluate the possibility of direct interactions between environmental electromagnetic fields and the mammalian central nervous system. These first studies strongly suggested that very weak sinusoidal fields (2-10 v/m in air) at frequencies from 5 to 15 Hz shortened human reaction times of 200 msec by about 5 msec (Hamer, 1968). Our later studies in animals have confirmed the occurrence of subtle behavioral interactions. Estimates by monkeys of a 5.0 sec time interval are shortened by approximately 0.5 sec in the presence of fields from 7 to 75 Hz. Lowest thresholds occur at 7 Hz, with fields of 10 v/m (Gavalas, Walter, Hamer & Adey, 1970; Gavalas-Medici and Day-Magdaleno, 1976).

In recent years, our behavioral studies have been conducted concurrently with neurophysiological and biochemical observations on altered brain states in the presence of low frequency electric fields and radio frequency fields that are amplitude modulated at low frequencies (typically from 0.5 to 30 Hz). The findings have been summarized elsewhere (Adey, 1975; Bawin and Adey, 1976a and b). Neurophysiological effects have involved entrainment of electrical brain rhythms at the field frequency (or at the modulation frequency of a radio frequency field). This entrainment appears gradually from the onset of field exposure, and has been observed in monkeys, cats and chickens. Both low frequency and modulated radio fields altered binding of calcium in isolated cat and chicken cerebral tissue. From measurements of induced components of low frequency fields in tissue phantoms, field sensitivities in brain tissue from thresholds for altered calcium binding are of the order of 10^{-7} volts/cm. These sensitivities occur within amplitude and frequency "windows". The amplitude range for low frequency fields appears to be 10 to 100 volts/meter. In the frequency domain, both

cat and chicken cerebral tissue respond only in the range from 6 to 20 Hz. Finding of an amplitude window in the range 10 to 100 volts/meter is in good agreement with behavioral sensitivities noted in monkeys making subjective time estimates (Gavalas-Medici and Day-Magdaleno, 1976). Thresholds at 10^{-7} volts/cm are within an order of magnitude of sensitivities to environmental fields seen in sharks, rays and other marine vertebrates.

The long and difficult sequence of studies summarized above has led us to formulate a model of cerebral tissue in transaction and storage of information, based on the role of slow electrical oscillations in dendrites of cerebral neurons, and in the surrounding extracellular medium. It is proposed that transductive coupling of oscillating extracellular electrical gradients is significant in cerebral processes. The evidence supports the view that the extracellular gradients may be associated with recall of information stored from past experience. The extreme sensitivities described above are orders of magnitude greater than those characterizing classic synaptic excitation. The findings suggest that certain forms of cell-cell communication in brain tissue involve quantum amplification of low level energy exchanges in the binding of ions in the length of membrane surface glycoproteins. Our collaborative studies have given formal physical expression to some aspects of these hypotheses.

We have studied effects of weak low frequency electric fields on calcium efflux from isolated chick and cat brain. Freshly isolated chick cerebral hemispheres were equilibrated with a calcium Ringer's solution containing $^{45}Ca^{2+}$ for 30 min. washed tissue portions were then exposed to sinusoidal electric fields at either 1, 6, 16 or 32 Hz, with electric gradients of 5, 10 or 56 V/M in air for each frequency for 20 min. $^{45}Ca^{2+}$ efflux was then measured in 0.2 ml of supernatant, and compared with efflux from unexposed control samples. All tissues were maintained at 36C, and checked for specific activity

after the experiment. A frequency sensitive "tuning curve" showed sharply reduced efflux of 15 to 20 percent at 6 Hz ($p<0.05$) and 16 Hz ($p<0.01$). Similar but smaller reductions ($p<0.05$) occurred at 56 V/M. Threshold was around 10 V/M, but non-significant trends occurred at 5 V/M. No effects were seen at 100 V/M. There are thus both frequency and amplitude windows for this effect.

Cat visual, auditory, suprasylvian and sensorimotor cortex tested at 1, 6, 16, 32 and 75 Hz also showed significantly decreased effluxes at 6 Hz ($p<0.05$) and 16 Hz ($p<0.01$), but with nonsignificant trends at all other frequencies tested. At 10 V/M, nonsignificant trends occurred at 6 and 16 Hz.

Oscillating ELF fields at 6 to 32 Hz thus reduce Ca efflux, whereas weak VHF fields amplitude modulated at the same frequencies increase efflux (Dawin, Kaczmarek and Adey, Ann. New York Acad. Sci. 247:74-81, 1975). A model for both effects based on cooperative interactions of Ca with fixed charges on stranded biopolymers is proposed. Tissue components of these fields in a phantom monkey head averaged 0.1 μV/cm. We have reported interactions of Ca, glutamic acid, GABA and taurine in cerebral tissue (Kaczmarek and Adey, Brain Research, 1973, 1974, 1975). The evidence supports an hierarchical model of excitation in cerebral neurons, with longitudinal Ca binding to membrane surface, macromolecules as an initial step before classical, secondary transmembrane events. Initial steps in Ca binding and release would involve cooperative interactions with fixed charges on surface polyanions. Intrinsic EEG signals are sufficient to elicit these effects and may relate to a "second signaling system."

SECTION V

BIOENGINEERING

5. Bioengineering (Dr. J. Hanley, M.D., S.L. Moise, Ph.D. and S.W. Huston)

Previous reports under this contract have described our development of an eight-channel personal biotelemetry system. The telemeter comprises amplifiers, multiplexer to provide PAM (pulse amplitude modulation), and an FM transmitter. In its application to studies in monkeys, this system was packaged in a fashion to minimize risk of damage by a monkey's digital manipulations when the pack is attached to the animal's head (Olsen, Moise and Huston, 1974).

In collaboration with Dr. T.J. Willey, Depts. of Pharmacology and Physiology, Loma Linda University School of Medicine, an improved version of this system with 12 physiological data channels is in routine use for studies of monkey drug addiction to methadone.

In collaboration with the staff of the UCLA Department of Anesthesiology, Dr. J. Hanley has evaluated the PAM and FM-FM telemetry systems in operating room and intensive care environments. Acquisition of high quality biomedical data, including EEG, EKG, and respiration, in this study has resulted in development of specific "staging" signatures in the course of general anesthesia with a series of inhalational anesthetic agents.

SECTION VI

CRYOMAGNETIC AND OTHER REMOTE MEDICAL MONITORING TECHNIQUES: A REVIEW

INTRODUCTION:

This section examines the feasibility of a magnetic field sensing device to monitor a pilot's physical and mental competence while he pilots the aircraft. Our evaluation is preceded by a review of the techniques and recent research results of magnetic field recording at the extremely low field strengths characteristic of heart and brain activity.

The initial attraction of a magnetic field monitor is that it reduces the wiring directly attached to the pilot and bypasses the usual problems of electrode contacts with the skin. Other advantages follow from the spatial specificity of the magnetic fields as discussed below.

The usefulness of such a monitor can be estimated by comparison with the properties of an ideal pilot monitor which we describe in Section A. The magnetic fields produced by the body and those found in the environment are described in Section B. Section C reviews the technology of measuring exceptionally small fields and explains the operation of a superconducting magnetometer. Following this background information on the body's fields and measurement techniques is a review of the information derived from such measurements (Section D). The potential use of such information in a cockpit monitor is presented in Section E, along with a speculative outline of the form a monitor might take. Section F addresses technological and scientific problems in an assessment of the possibilities for the actual development of a suitable device. Our final topic, in view of a rather dismal prospect for the near term development of any sophisticated device, concerns other non-invasive monitors which would be less than ideal but still of value.

Section A: Requirements of an ideal cockpit monitor of pilot well-being.

An ideal pilot cockpit monitor answers the common sense question, "Is the pilot physically and mentally capable of performing his tasks now

and in the immediate future." To give a useful answer the monitor should have these qualities:

i) Real time readout --- The device should operate so fast that the answer to the above question is available "immediately." Should the answer be negative, alternate courses of action could be taken in time to prevent errors or catastrophes.

ii) Predictability --- Knowledge of the pilot's present capabilities, while perhaps sufficient, is not as useful as a predictive statement of the pilot's capabilities over the next interval of seconds or minutes. The ability to predict allows greater flexibility in taking corrective measures and serves as an alarm to the pilot.

iii) Reliability --- The importance of the pilot's life, the aircraft and the mission require a highly reliable device. False positive answers are an obvious hazard and false negatives are of nearly equal importance. Secondly, the device must function continuously and be immune to environmental hazards of the cockpit environment, even to the point of damage to the aircraft, or failure of other systems.

iv) Non-ambiguous --- The answer's format should allow decisions on the course of corrective actions. Ambiguities would limit the device's usefulness because after all, placing a healthy person into a well designed aircraft already provides a conditionally positive answer to the question. Thus, the readout data should have strong correlations to well defined physiological and mental states and, still speaking ideally, there should be a translator to correlate the data with such other measures as blood pressure, nerve conduction velocity, scotopic flicker frequency, cognitive ability, etc.

v) Non-invasive --- This property assures that the monitor is not affecting the person and that the pilot is easily ejected from the aircraft if that is necessary. Also, a non-invasive probe eliminates the possibility of hook-up errors or disconnection and, in contrast with electrode probes, there are no electrode potential problems, or noise problems from the connecting wires.

vi) Output in telemeterable format --- The data should be available for decisions which may be made on the ground as well as on board the aircraft.

vii) Not Pilot-Specific --- Ideally, the monitor should work interchangeably on all persons without adjustments for personal idiosyncrasies of physiology or psychology. Considering the wide range of normal parameters in most physiological, neuro-physiological, and psychological variables, a practical requirement may be that the device set the criteria of normalcy on the basis of previous analysis of the individual.

Section B: Magnetic fields produced by the body; ambient fields

The body produces magnetic fields as a consequence of ionic currents related to the activity of nerve and muscle tissue. These fields are generally in the ELF (Extremely Low Frequency) portion of the spectrum and have magnitudes far less than the earth's DC field of approximately 0.5 Gauss. The presence of ferromagnetic materials in the body due to contamination from non-biological sources may also produce bodily magnetic fields but these will be DC fields.

The heart produces the most prominent magnetic field with a magnitude of 10^{-6} gauss (G) at the peak of its activity cycle (Cohen, 1975a). Upon contraction skeletal muscles give rise to fields which are lower in strength at about 10^{-7} gauss when recorded from a distance of about 4 cm (Cohen and

Givler, 1972). However, magnetic fields from the brain are very much smaller achieving peak values of only 5×10^{-9} G in the waking state although in sleep the brain field may be as large as 3×10^{-8} G. With the eyes closed fields of similar magnitude exist. In epilepsy, the brain's magnetic field can be larger yet, approaching 10^{-7} G (Cohen, 1975a).

These signals may be contrasted with typical levels for the ambient noise within the same frequency range as used for the recording of heart or brain fields. In the urban environment this background field is typically 10^{-2} G within the band from DC to 40 Hz (Cohen, 1972). Distinct from this man-made background there is a small background of natural origin present when the magnetic field spectrum is measured in rural locations. The noise from natural sources falls off steeply with frequency so that while 10^{-2} G may be typical at 1 Hz the noise at 40 Hz will be only 10^{-3} G (König, 1974). We have no information on the fields found in an aircraft cockpit but the use of 400 Hz AC power should make the cockpit quieter at ELF than if commercial frequency (60 Hz) power were used. On the other hand the profusion of electrical and electronic devices may make it a very noisy environment, perhaps far worse than the average laboratory. The aircraft's motion through a changing earth's magnetic field may introduce more noise but we have no data on the fine structure of the geomagnetic field at the amplitude sensitivity we are discussing. Finally, a complete consideration of the aircraft environment should consider the possibility that electrostatically induced currents in the aircraft's metallic skin could contribute additional noise. We have not given the question a numerical analysis.

Another noise source which concerns the experimenters who measure nanogauss* field levels is from ferromagnetic materials, especially when they are in motion with respect to the detector. The incredible sensitivity of the magnetometers used requires that even the noise contributed by

*a nanogauss is 10^{-9} G

ferromagnetic materials in the dyes of the person's clothing must be considered (N. Cuffin, personal communication).

In general it is necessary to use detectors sensitive to the field gradient - or even the second derivative of the field - to measure the localized body fields in the presence of a noisy magnetic environment which may have non-localized fields 10^6 times stronger than those to be measured.

Blood flow itself does not contribute a direct magnetic signal because the blood is electrically neutral. However, it is possible to measure blood flow electromagnetophoretically using an externally imposed pair of electric and magnetic fields (Kolin, 1968).

Section C. Magnetometry at field strengths of 10^{-5} to 10^{-9} gauss

In all the various schemes used to detect magnetic fields the initial coupling to the field is with a coil of wire. At the larger field strengths we are considering, down to approximately 10^{-6} G, a "flux gate magnetometer" may be used, e.g. to measure the heart's magnetic field. This device operates at room temperature. To achieve greater sensitivity, down to 10^{-9} G, the devices operate at liquid helium temperature (4 K) to obtain significant noise reduction and to utilize the unique properties of superconducting metals.

The device which has been successfully applied to measurements of the heart and brain fields is the RF SQUID (Radio Frequency Superconducting Quantum Interference Device). It is distinct from several other low temperature magnetometers which use related schemes. The RF SQUID magnetometer is enclosed inside a dewar (thermos bottle-like container) which retains a charge of liquid helium for up to several days. The entire "front end" of the SQUID, consisting of a flux transformer, superconducting ring, RC tank circuit and RF amplifier, is kept at liquid helium temperature and for this reason it is a reasonably bulky package although the actual working parts are only a

few cm in length and diameter. Presently available detectors have a spatial resolution of about one centimeter and are operated about 4 or 5 centimeters above the body. Outside of the dewar, which contains only the superconducting "front end" and a room temperature preamplifier, the SQUID involves a moderate amount of auxillary electronics -- an RF generator (typically at 19 MHZ), a mixer, an audiofrequency oscillator and a lock-in detector. The detector noise is one limit on sensitivity and in the state of the art the total detector noise can be as low as 1.6×10^{-10} G/$\sqrt{\text{Hz}}$ (that is, the total noise increases with the bandwidth). Future advances in SQUID technology are likely to lower the sensitivity below 10^{-10} G/$\sqrt{\text{Hz}}$, but the present devices are sensitive and quiet enough for many purposes. Reductions in overall size involve a tradeoff on dewar holding time but are limited by shielding needs and the requirements of a mechanical isolation from vibration.

The key elements of the SQUID detector is a block or film of niobium metal a square centimeter or so in area. It is adjacent to the coils of the flux transformer which are about 1 centimeter in diameter and a few centimeters in length, depending on the configuration of the flux transformer. The flux transformer may be made up of two coils of niobium wire wound on a plastic core of which one coil is the initial detector element and the other carries the flux into the SQUID or multiple coils and may be wound to achieve a detector sensitive to the field gradient ($\partial H/\partial x$) or even the second derivative of the field ($\partial^2 H/\partial x^2$) the "double gradiometer" configuration. To detect field gradients in the presence of large background fields the gradiometer and double gradiometer configurations are necessary however no change in the rest of the SQUID apparatus is required if the flux transformer configuration is altered.

The Physics of the SQUID

The basic physical principle utilized in the SQUID is that in a superconducting material phase information is maintained over macroscopic distances. This manifestation of the quantum nature of matter on a macroscopic scale (here, centimeters around the superconducting ring) comes into play when electrons are coupled into a collective state of macroscopic dimensions. This coupling is possible for certain metals at very low temperatures as a consequence of a subtle interaction between electrons and the crystal lattice in which they move. The principle phenomena of superconductivity are the properties of perfect conductivity of DC currents and perfect diamagnetism (total expulsion of a magnetic field from the bulk of the material). Related discoveries indicate that for large enough magnetic fields ("bigger than the critical field") superconductivity is destroyed and similarly for large enough currents a resistive current flow appears in parallel to this resistanceless supercurrent flow (i.e., above the "critical current" superconductivity breaks down locally). One of the most useful applications of superconducting properties comes about in the Josephson junction and related devices in which pairs of superconducting electrons pass through a thin barrier layer by quantum mechanical tunnelling. The pairwise tunnelling leads to the many important phase coherent properties of Josephson devices (Bloch, 1970; Deaver, 1973).

In the superconducting magnetometer a ring of superconducting material capable of carrying a large supercurrent is interrupted by a Josephson junction or other weak link through which only a much smaller supercurrent can flow. The supercurrent in the ring is determined by the properties of the weak link, which include a sensitivity to magnetic fields. The discussion to follow is clearer if we specify a Josephson junction as the particular form for the weak link but actual devices may use a point contact 10^{-10} cm^2 in

area that allows a maximum supercurrent of 10^{-5} A or a similar constriction made by deposition of a narrow film of metal. In the junction the supercurrent is determined by a macroscopic wavefunction, $\psi(x)$, and its phase ϕ. $\psi(x)=/\psi(\ )/e^{c\psi}$ describes the collective electron state throughout the superconducting ring. There is a supercurrent I_s, through the junction in the ring when no voltage is imposed across the junction.

$$I_s = I_o \sin \Delta\psi \qquad (1)$$

where $\Delta\psi$ is a "gauge invariant phase difference" which expresses the difference in phase between x_1, and x_2 where x_1 and x_2 are at opposite sides of the junction. I_o is a constant which can be related explicitly to physical properties of the material.

In the RF SQUID device (the name is a misnomer because the quantum interference properties of multiple junction devices do not occur in this one junction device) a big enough voltage (at RF frequency) is imposed across the junction so that, in addition to the supercurrent, there is now an additional normal current (with ohmic losses). Thus, the current in the ring is, augmented by an RF current:

$$I = I_o \sin \Delta\psi + \frac{V}{R} , \qquad (2)$$

where the first term describes the resistanceless supercurrent and the second term describes the normal current. (We suppress the time variation of I in our notation.)

The device operates as a magnetic flux detector because the junction itself changes when in a magnetic field and the change in junction properties affects the supercurrent in the ring. The magnetic field causes a spatial variation in phase (more accurately, the "gauge invariant phase") in the plane of the junction. Thus the current I, which as shown in eqs. (1) and (2) depends on $\Delta\psi$, also depends on position in the plane of the junction,

indicated by writing, $\Delta\psi(\xi)$ for the position dependent phase.

$J_s = J_o \sin \Delta\psi(\xi)$ expresses the varying supercurrent density within the junction and for certain values of the magnetic field in the junction the net phase relation is such that the supercurrent is reduced to zero (when $\Delta\psi(\xi)$ is a multiple of 2π). At this point in the discussion it is necessary to introduce the flux quantum, Φ_o, a unit of flux which has a value of about 2×10^{-7} G-cm^2 determined by the fundamental relations between currents and fields in superconducting materials (of any size and shape). In terms of the flux quantum Φ_o, and the applied flux Φ, produced by the sum of external field to be measured and the RF field, the junction current now has this form

$$I = I_o \sin \Delta\chi(o) \quad \frac{\sin(\pi\Phi/\Phi o}{} + \frac{V}{R} \qquad (3)$$

where $\Delta\chi(o)$ is the phase difference measured in the center of the junction plane (where $\xi = o$). Assuming a choice of applied flux plus RF current that sets $\sin \Delta\psi(o)$ to a value of near unity, the second sine function indicates that the supercurrent is periodic with period Φo.

The practical details of the magnetometer to be discussed below concerns techniques for measuring the changes in supercurrent caused by the external field and although several schemes have been used we discuss just one which is characterized by use of negative feedback to establish a particular operating point at which the RF voltage is a maximum.

In the practical designing of a point contact device Zimmerman, Thiene and Harding (1970) used a single block of niobium containing just one weak link but having two holes in which flux is trapped when the material is rendered superconducting. See Figure 1. Because the total flux is kept constant in the interior of a superconductor the introduction of flux into one hole by

a coil of wire alters the flux difference $(\Phi_2 - \Phi_1 = \Phi)$ but not the total flux $(\Phi_1 + \Phi_2)$. The flux difference enters into equation 3 and thus can be measured. This configuration has the advantage that it is insensitive to external fields which affect both holes reducing shielding requirements.

The coil of wire which introduces the flux to be measured into the hole is one of a pair which are kept at liquid helium temperatures and wired in series in an arrangement known as a flux transporter or flux transformer. This efficient technique of introducing the field to be measured can be complicated with additional coils wound in arrays sensitive to only the field gradient or the second derivative. The gradiometer and second order gradiometer flux transporter detectors have been successful in measuring nanogauss fields in the presence of background noise many times larger. Thus, although the weakly linked ring is the sensitive element in the system the flux transporter is the initial detection element.

The development of the output signal is most simply discussed in terms of a superconducting current which has an inductance in the nanohenry range, shunted by a resistance of roughly one ohm (the normal current), coupled to an RF coil of nanohenry inductance which is resonant in a tank circuit of very large Q. (See Figure 2.) All these components operate at liquid helium temperature to reduce noise effects although superconductivity properties are necessary only for the ring and the flux transporter. As discussed immediately following eq. 3, the total magnetic flux in the junction determines the supercurrent and in this way the coupling between the coils is altered. See Figure 2. A change in flux changes Q, changes the resonant condition of the tank circuit, and changes the RF voltage across the tank circuit $(L_1\ C_1)$.

It is more practical to fix the system at a flux condition which gives the largest RF voltage (for the chosen circuit elements and RF frequency). This is achieved by using a feedback loop to alter the ring current so that whatever the flux introduced by the flux transporter tries to do to the supercurrent it is corrected by a quasi-DC current fed back into the device. See Figure 3. The feedback voltage is derived from sensing the RF voltage and this feedback voltage, rather than the tank voltage, becomes the analog signal which is finally amplified by conventional (FET input) low noise amplifiers as an indication of the flux at the detector.

One final engineering detail which was incorporated into the successful design is a further modulation of the flux in the hole by a fixed amplitude audio frequency (10 kHz) current through the tank coil. In this way the shifts in RF voltage to generate the feedback current may be sensed with a phase sensitive (lock-in) amplifier operating at the audio frequency.

Webb (1972) summarizes the device as "a weakly superconducting ring coupled to an L-C tank circuit resonant at 1 to 30 MHz with both at liquid helium temperature. The tank circuit is driven by an RF oscillator and an audiofrequency amplifier. The RF voltage across the tank circuit is amplified with a RF amplifier, mixed with a reference signal from the oscillator and phase sensitivity detected with a lock-in detector at the flux audio modulation frequency. For high sensitivity, continuous, linear flux measurements, the output of the phase sensitive detector is amplified and fed back into the tank coil to provide a fixed operating point for the superconducting ring."

The magnetometer's sensitivity is in part due to the intrinsically small size of the flux quantum (Φ_o) which enters into equation 3. Flux changes less than one-thousandth of the flux quantum (perhaps as little as 10^{-5} Φ_o is possible in theory) can be detected with the practical limitation coming from Johnson noise* in the ring. The Johnson noise has contributions from

*Johnson noise is due to thermal fluctuations of the electrons

the inductive component (including the supercurrent) and the resistive component (normal current) and is about equal in importance to the noise in the room temperature amplifiers which amplify the RF signal.

Shielding:

The sensitivity of the SQUID and the large background flux at the frequencies of interest make it necessary to use either of two techniques to extract useful data from the noise. In the first a shielded environment reduces the ambient fields to allow real-time recording of data. The most elaborate such room has been constructed at the Francis Bitter National Magnet Laboratory associated with MIT in Cambridge, Massachusetts. A reduction of 10,000 in the ambient low frequency fields is obtained with layers of a highly permeable alloy (permalloy) and thick aluminum plates. Static and low frequency fields parallel to the surface of the metal are attenuated in the permalloy by a large counterfield developed in the metal and the highly conducting aluminum reduces the AC components of the incident field by virtue of the eddy currents which cause counterfields. But, to achieve a still better degree of shielding these two techniques of passive attenuation are augmented by an active system which senses field changes outside the room and causes an opposing field to be created in sets of wire coils which surround the chamber's exterior. The net result is a room inside of which the ambient field is below the SQUID noise of $1.6 10^{-10}$ G/$\sqrt{Hz}$ (RMS) at 2-40 Hz with a rapid increase above SQUID noise at frequencies below 2 Hz (Cohen, 1975b).

A simpler and cheaper shielded room has been constructed at the National Bureau of Standards at Boulder, Colorado using only eddy current destruction of the external fields. Aluminum plates 4 mm thick, are welded together to create a structure inside of which the field gradient is 10^{-10} G/cm$\sqrt{Hz}$. The

aluminum structure is itself shielded by a 3 mm shell of soft iron which, like the permalloy---but to a much lesser extent---shields with a large induced magnetization field. The soft iron is a DC shield for the earth's field but is also effective at low frequencies (Reite et al, 1976).

In the second technique to deal with the noise, as an alternative to a shielded room the measurements are made in a noisy environment ($\sim 10^{-4}/G\sqrt{Hz}$) and signal averaging is used to extract the signal from the noise. Of course the ability to make real-time measurements is sacrificed and in the application made so far, up to several hours have been needed to acquire data on evoked response patterns. Thus in situations where real time data is not needed, noise can be tolerated up to the limit imposed by excessively long averaging periods.

Review of Research Findings to Date:

Magnetocardiography

In the first recording of the heart's AC magnetic signal (of the order of 10^{-6} G) a magnetocardiogram (MCG) was made using wire coils wound on a core (Baule and McFee, 1963; 1970). The MCG is the magnetic correlate of the electrocardiogram (ECG) and may be recorded at various locations on the chest and limbs. It shows the same PQRST pattern of depolarization and repolarization as the ECG. The main difference between the AC coupled MCG and ECG is the spatial localization possible with the MCG. In contrast, the ECG uses leads located far from the heart. The relative amplitude of the various portions of the PQRST waveform also differs. A major finding with magnetic methods is the information found in DC coupled recordings which indicate a steady current of injury associated with ischemia (inadequate blood flow)--whether an ischemia produced by infarction ("heart attack") or as in angina. Furthermore it has been possible to establish that the DC current of injury is the direct cause of the "S-T segment shift" which has long been used as a diagnostic test of coronary pathology. The S-T shift was seen in both ECG and MCG records of dogs subjected to experimental ischemias and the DC level shift has been directly observed magnetically (Cohen and Kaufman, 1975) by moving the dog's chest toward and then away from the magnetometer.

Magnetoencephalography

Magnetic recordings of the brain (magnetoencephograms or MEGs) show the alpha rhythm, already known from EEGs, the abnormal spikes found in epileptics, and evoked responses (in which the subject's brain waves show a particular pattern in response to an impressed stimulus, e.g., a flashing pattern on a screen). MEG patterns have been evaluated by Reite et. al.

(1966) by comparison of simultaneously recorded EEGs and MEGs. They found similarities in the EEG and MEG alpha rythms with respect to location and their response to blocking by visual stimuli. The MEGs and EEGs tracked in amplitude: subject's with large EEG signals had large MEG signals. The spectral distribution (power density at a given frequency) of the electric and magnetic records was similar but distinguishable by some differences. These authors also noted the lack of an MEG eyeball motion artifact in contrast with electrical recordings.

Evoked responses have been observed by three groups (Brenner, Williamson and Kaufman, 1975; Reite, et al., 1976; Teyler, Cuffin and Cohen, 1976). In these studies the responses to many (100 or more flashes of light are averaged to demonstrate that a particular brain activity occurrs upon presentation of the light. Teyler Cuffin and Cohen (1975) established that the magnetic signal is dependent on stimulus intensity and that, as in the electrical recording of evoked responses, there are no components at high frequency (above 100 Hz). Their study also investigated the location of the brain's current generators with the conclusion that the evoked response signal is generated in the occipital lobes (in agreement with EEG data). They speculate that some small discrepancies between the electrical and magnetic records are due to the nature of the current generators in the brain and their location. The lack of high frequency components is not conclusively demonstrated because the internal noise of the SQUID (1.6×10^{-10} G/$\sqrt{Hz}$) limits detection at higher frequencies. The quieter SQUIDs that may be available will soon allow measurements in a wider bandwidth. Brenner and Williamson achieved their evoked response data without any shielding and with somewhat greater spatial resolution. Their measurements at various frequencies of the photic stimulus show that 16 Hz gives the peak response (Williamson,

personal communication) and in their reported results at 10 Hz (Brenner and Williamson, 1975) the spatial studies indicated that the magnetic field reverses phase between measurements made at opposite sides of the head (across a line about 5 cm from the midline of scalp). They also find a high degree of spatial localization along a few centimeters of scalp near the occipital lobe.

Cohen's original report on MEGs (Cohen, 1968) was the result of data taken with a non-superconducting device (a coil of about 1 million turns). Data was averaged for a period of several minutes at the same time as an EEG was recorded. He observed definite magnetic signals which had a different phase on opposite sides of the head (across the scalp's midline) and he was also able to show that the orientation of the field vector varied over the skull. At the back of the head there was no signal from the normal component although there was a horizontal component.

Cohen's initial report of a SQUID measured MEG (Cohen, 1972) established the existence of MEG signals in real time, i.e. without averaging, and their apparent similarity to EEG records. However, it was immediately obvious that the MEG did not show slow theta waves simultaneously present on the EEG. This has been explained in terms of the probable location of the theta rhythm generator deep within the brain (at the hippocampus?) in correspondence with other indications from animal experiments using implanted electrodes.

EEG and MEG records of seven normal and eight diseased human subjects is reported by Hughes et al. (1976). The data were taken in the MIT shielded room using the SQUID magnetometer. Extensive frequency analyses of the magnetic and electric records are discussed for waking activity, wake and sleep, and sleep (slow waves, spindles and vertex sharp waves). The authors establish that the MEG signals are certainly of neural origin and that the

EEG/MEG correlation is best at 10 Hz and generally good throughout the alpha frequencies. At other frequencies the MEG/EEG correlation was less clear or absent and an explanation is not given. The absence of spindles in the sleep records of the MEG is the most interesting discrepancy noted. The authors suggest that these spindle rhythms are the consequence of a diencephalic-cortical circuit. The same theory has been suggested from the evidence of spindles recorded in anesthetized animals.

The interpretation of EEG/MEG correlates is made difficult because one must remember that the data analyzed represents only the normal component of the magnetic field and so indicates only the current sources positioned in the cortex parallel to the scalp. Thus, the evidence of EEG/MEG correlation at 10 Hz is an indication that the 10 Hz rhythm is produced by tangentially arranged generators in the cortex -- but does not exclude the existence of a radial generator to which the MEG probe is blind.

The phase reversal at opposite sides of the head, first reported by Cohen (1968) was noted again by Hughes et al, and in addition they found strong evidence of a variable phase difference between the EEG and MEG which may support some earlier ideas of a travelling wave phenomenon in brain activity. Cohen found no MEG theta (slow) waves when they were seen in the EEG but Hughes et al., find MEG theta rhythms when they are absent or weak in the EEG. The later group also finds the opposite condition (agreeing with Cohen) but with much lower incidence.

These first details of MEG analysis indicate that there is certainly a great deal that may be learned about brain activity with this new tool and that at the present time only the very first steps have been taken.

Other Bodily Magnetic Signals

The lung is a third organ producing magnetic signals but here the magnetic

field is primarily due to a DC field from contamination of the lung by ferromagnetic particles. The studies performed to date show it may be practical to make measurement of lung burdens due to industrial exposure (Cohen, 1975a; 1975b) to asbestos which is accompanied by an exposure to magnetitic. The magnetite levels in asbestos worker's lungs is a more sensitive test of the amount of inhaled asbesto dust than is possible using radiographic tests. Potentially lung function may be measured by inhalations of small amounts of magnetic dust in a clinical setting but this idea has not yet been developed. Lung measurements can be performed using the simpler fluxgate magnetometer and do not require a shielded room although it is likely that any clinical use involving humans would require the use of shielding and the SQUID in order to expose the person to the smallest possible amount of magnetite dust However, Cohen (1975a) states that magnetite is "harmless in the lung even in gram amounts".

Finally, skeletal muscles also produce magnetic fields the recording of which is "magnetomyography". In this case the signal is of the order of 10^{-7} G during muscle contraction and falls in a frequency range below 200 Hz (dependent on the muscles involved) with a distribution fairly sharply peaked around 40 Hz for the muscles of the elbow region and around 70 Hz for muscles of the palm (Cohen and Givler, 1972). Some DC signals persist long after the arm muscles are relaxed. Additionally, MMG's may be useful in measuring the current of injury in muscle.

Theoretical Studies of the Sources of Biological Magnetic Fields

A number of theoretical questions are raised by the new experimental evidence of magnetic recordings of biological fields. The direction of the theoretical studies is to identify current generator configurations with the

resulting field patterns. Current sources are best discussed in terms of the idealized current dipole which is analogous to the electric dipole, but distant from the current loop more usually encountered in electrodynamics. The current loop is defined as the product of a current, i, and a differential length, dl, such that the product idl is constant in the limit of infinitesimal dl.

The magnetic field produced outside of a volume of conducting material in which such a current dipole is embedded consists of a direct contribution from the dipole, B_d and a contribution from currents set up in the volume of conducting medium, B_v. An important simplification which has been recognized is that the contribution from the volume, B_v, may be ignored in certain idealized cases because, by symmetry arguments, it vanishes. In practical cases, it is still prudent to simplify the solution by ignoring B_v as one obtains a quite accurate result nonetheless.

A current dipole embedded in a semi-infinite conductor is the first model used in modelling the heart in the chest. A dipole oriented parallel to the surface produces a magnetic field whose component normal to the surface is due entirely to the dipole and one can totally ignore the volume field B_v. If the dipole in a semi-infinite medium is oriented perpendicular to the surface the total field is zero (Cuffin and Cohen, in press).

Using a sphere to model the brain one finds a similar simplification because a radially oriented dipole produces no normal field components and only dipoles oriented tangent to the surface need be considered (Cuffin and Cohen, in press). In the simplest case considered, a dipole is placed parallel to the x axis at a point on the z axis above the xy plane. Once again, the volume conductor field contribution can be ignored to the extent that it produces no radial (i.e. normal) component so that the entire normal field can

be discussed in terms of the dipole's contribution alone. Similar investigations have been carried out for prolate and oblate spheroidal geometrics (Cuffin and Cohen, in press). In these cases the dominance of the dipole contribution occurs only on the surface and near to the dipole. At points on a prolate spheroid which are distant from the dipole the volume field is significant but this is not the case for an oblate spheroid.

The next step in these theoretical studies considers the fields developed by a distribution of several dipoles throughout the volume of the conductor (brain or torso). Cuffin and Cohen (preprint) have considered several arrangements of dipoles, beginning with a pair of dipoles aligned anti-parallel, and proceeding to several dipoles arranged radially along the circumference of a circle or arranged in various ways along straight lines or on the surfaces of sheets. Finally, they consider the fields which result from random alignments of the current dipoles in several geometries. In all these cases, only the dipole fields are considered since it is quite reasonable to ignore the volume produced fields in practical measurements which show only the normal components. The aligned dipole models are applicable to heart and the random dipole models to the brain.

The development of these ideas will increase the power of magnetic field measurements especially in the interesting questions of brain activity where knowledge of the location and distribution of the current generators is of great interest. Using EEG information alone this problem is very difficult for unambiguous answers are not possible. Although MEG data is ambiguous in other ways the combination of the two is much more powerful. In due course, greatly expanded knowledge of brain rhythms and brain activity may result from continued investigation. It is very early in this line of research and the extent to which these techniques prove useful is unknown but very promising.

E. What are the Potential Achievements?

The combined use of electric and magnetic recording of brain activity promises to give a significant amount of information on the location of the generators of brain rhythms. This line of questioning has been pursued, up to now, through the use of implanted electrodes. Due to the limitations of surgical procedures and the fixed location of the electrodes the information which can be obtained in this way is achieved quite laboriously and is quite specific to the placement of the electrodes. The MEG technique may allow a more rapid development of information and a broader picture may develop because of the reduced dependence on fixed electrode location. Of course, on the microscopic level, electrode implants will maintain their unique ability to record events from the region of just a few cells or when recording intracellularly, from just one cell.

Of direct application to the question of cockpit monitoring, we can foresee that particular MEG patterns, associated with specific cortical areas could be identified and thus provide a signal for monitoring. The likelihood of using signals from deeper within the brain is markedly reduced because, as mentioned above, a current source located radially inside a spherical volume produces no external field. This is, to some extent, a serious limitation, which may still be overcome by recognition of higher order effects in the MEG. Recordings from deeper in the brain may be advantageous, e.g., to monitor functions of the medulla or cerebellum because of their association with more basic physiological processes in contrast to the higher functions of the cortex. It is, however, too early to say whether magnetic information from both levels of brain function can be obtained.

F. Evaluation of Prospects for a Magnetic Monitor of Pilot Competence by Recording the Body's Magnetic Field

A monitor which indicates a pilot s overall competence will be exceedingly difficult to realize -- if it can be done at all. The first serious obstacle which must be overcome is the difficulty of making a good quality recording in the cockpit envirorment -- under the best of circumstances. Although we have no data on the actual magnetic field levels in the cockpit it appears that the numerous electrical devices located in close proximity to the pilot make this a very noisy magnetic environment requiring at least some degree of shielding between the probe and the cockpit. It is not obvious that the sources of magnetic interference (that is, every current carrying wire, motor, solenoid, etc.) could be adequately shielded without increasing the craft's weight excessively but this question should be addressed directly by an engineer familiar with aircraft electrical systems. Perhaps some balance might be struck between limited shielding of both the sources of noise and the probe. The requirement that vibration of the probe be kept very low is another very serious obstacle. Again, we have no data on the amplitude and frequency of vibrations in the cockpit but they are certainly too high for operation of the SQUID probe without extensive acoustical isolation. For comparison, the MIT shielded room isolates the floor from the probe because vibrations of the probe raise the SQUID's noise figure substantially. The third environmental difficulty is of relative movement between the source (pilot) and the probe. Assuming that the probe, which, with it's liquid helium dewar is quite massive, must be fixed to the craft any movement of the pilot's head, as in turning to read a dial or set a control, will destroy the data flow at that time.

In general terms, the instrumental difficulties described above lead one to speculate that a cockpit monitor would be useful only if it used different-

ial information from several probes each of them operating in the gradiometer configuration which strongly discriminates between background fields and localized sources. The use of several probes would reduce the dependence on exact orientation of the pilot's head and the probe providing much more data, from different regions of the cortex but making data analysis astronomically complex.

We are then brought to a discussion of the possible techniques by which such a massive influx of real time data could be analysed to produce an output statement to answer the question, "Is the pilot O.K.?" We envision a rather large onboard computer capable of analysing each channel (probe) in order to recognize particular patterns of amplitude and frequency as they develop in real time and then to make a horribly complicated cross-correlation of the analyses of the patterns extracted from each channel. Although the pattern recognition of a real time signal (which must be "memorized", at least in part, for several seconds) -- combined with a frequency analysis of a signal over a bandwidth of perhaps 20 Hz involves a considerable amount of computation it seems at least feasible to consider a computer large enough for the task. To allow sufficient computation time in a computer physically small enough to place on the aircraft may require observation during windows spaced several seconds apart. In the second stage of the data analysis, we envision a cross correlation of the data in different channels in an attempt to decide from that information how the head is oriented and thus how to value the signals. The ultimate step is to decide whether the entire pattern is "O.K. or not O.K." and this seems like a problem of fantastic order, perhaps beyond the capabilities of current hardware and software.

In addition to these computing extravagances our scheme also presumes the existence of a body of brain research which would determine which MEG

patterns are "O.K." and which are not. This is certainly not the case and at the pace with which advances have been customary in such difficult areas of science it may be decades rather than years before enough is known about brain function to allow such sophisticated information.

It seems that any grand scheme for using magnetic field information to make a sophisticated judgment of pilot capability is far in the future -- if at all possible. However, perhaps a far more modest but useful device may be practical in the near future -- providing the technical limitations of noise, and vibration could be dealt with. A monitor sufficient to determine whether the pilot was in a sleeping or wakeful state based on the large difference in alpha activity in these two states may be possible for, as discussed in the above review of the literature, the MEG is especially useful as an alpha rhythm monitor. If one were to accept such a limited device and felt that the information to be derived is sufficiently valuable then there may be merit in pursuing this goal farther. An obvious problem is that the alpha rhythms vary widely among different (normal) persons and it is doubtful that a universal standard of activity could be established. This simplified monitor would require at least one SQUID probe highly isolated from vibration operating in a ferromagnetically quiet and current-quiet environment and a modest large onboard computer capable of making a frequency analysis of the data in real time. Such a system would be out of service whenever the pilot moved his head or if the aircraft were subject to vibrations or acoustic noise beyond the capabilities of the vibrational isolation scheme.

Possibly the (much larger) signals of the heart field or of skeletal muscles may be suitable for monitoring. Remote recording of the heart field seems feasible, again with considerable effort towards reduction of magnetic noise in the cockpit and vibration isolation of the probe. The advantages of

magnetic field recording of heart activity are primarily in the non-invasive character of the probe. However, this factor is purchased at the price that any motion by the pilot will change the character of the signal making simple analysis by machine (computer) very difficult. This difficulty is compounded by the fact that the heart's magntic field pattern varies quite rapidly with centimeter distances along the torso.

It is not clear how evidence from skeletal muscle activity could be made useful in a monitor.

In summary, it is our opinion that the limitations imposed by the magnetic probe's bulk, the need for acoustic, vibrational and magnetic isolation and the requirement of the pilot's relative immobility leave little prospect for near term development of a practical device which could reliably determine even the most fundamental parmeters of the pilot's competence to carry out his duties. Unfortunately the attractions of a non-invasive magnetic monitor are available only at gh price in terms of technical limitations. Further, the necessary information on brain function is lacking. Looking into the future one's imagination is fired by the prospect of an advanced monitor which truly evaluates many aspects of the pilot's mental functions. However, such a scheme suffers from the same limitation and is rescued in the imagination only by dependence on a very advanced application of computer technology to deal with the complex data in a subtle, intelligent manner. Neither the computer ability, programmer ability or knowledge of the brain are in the immediate future so that this remains a highly speculative idea.

Our final comment is that this question should be reexamined at some point in the future when the research which is likely to occur in this field is more fully developed. It then may be possible to see a middle ground in the problems attending the determination of a human being's state of consciousness and physical well being.

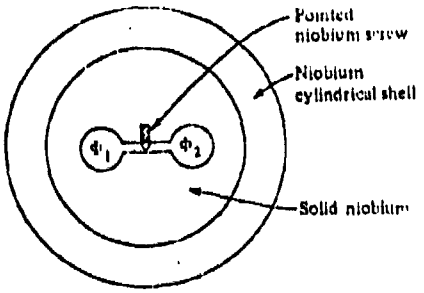

Figure 1. Point contact superconducting magnetometer ring. Two wire loops pass through the region containing flux Φ_1 . One loop is connected to the RC tank circuit and is labelled L_1 in Figure 2, below.

Source: Tinkham, 1975

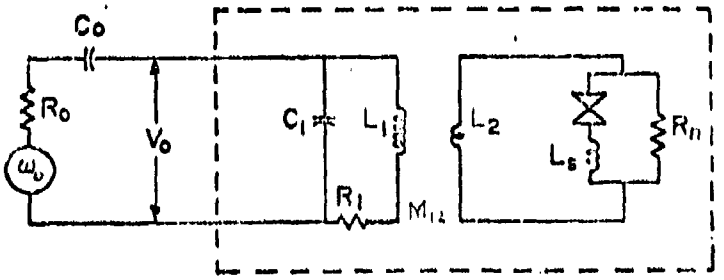

Figure 2. Effective circuit of RF SQUID Magnetometer. L_1, C_1 and R_1 form a tank circuit driven by a radio frequency oscillator at ω_o . L_1 is coupled to L_2 by mutual inductance M_{12} . L_2 represents the inductance of the superconducting ring while L_s represents the self inductance of the supercurrentwhich is "gated" by the superconducting weak link (SWL). R_n is the resistance to the normal current which shunts the supercurrent.

L_1 and L_2 are each of the order of 10^{-9} henry; R_n is about 1 ohm; ω_o is of the order of 10^8 /sec.

Source: Webb, 1973

Three Alternative Non-Invasive Physiological Probes

The questionable utility of the magneteencephalographic monitor led us to consider alternative physiological information without invasion of the body. The three methods considered are: 1) remote sensing of eye movements for analysis of saccadic motions 2) remote thermometry to detect the pulse as blood fills superficial capillaries and 3) remote calorimetry to detect the pulse from capillary flushing.

1) Monitoring saccadic eye movements

The synchronized jumps which each eye makes in moving from one visual target to the next, known as saccades, represent a complex interaction of the brain and the neuromusclula-system of the eye. The saccades have been studied for some time but until now clinical usefulness was limited by high degree of variability in the characteristic variables: amplitudes of motion, velocities and dynamic characteristics (overshoot, undershoot, velocity profile, etc.) Recent evidence (Baloh, et al., 1976; Baloh, et al., 1975) suggests that the maximum velocity achieved during the saccade is a reliable parameter to characterize the system. This maximum velocity depends upon the amplitude of the saccade and it is also known that it can be affected by fatigue, alcohol, tranquilizers and several diseases of the central nervous system. The high velocity with which the globe of the eye is moved (up to 700 degrees per second) requires a fast recorder.

In the usual laboratory procedure the saccadic motion is measured by the techniques of nystygmography involving external electrodes or in more specialized research situations, by use of magnetic coils attached to the eye, or by high speed photography. We propose a device which could be incorporated into the visor

of pilot's helmet utilizing infrared illuminators and detectors. The illuminators (using the technology of the light emitting diode) would be of microscopic proportions and so arranged as to provide an even illumination over the area of the eye. The radiation reflected from the eye would be sensed by a matrix of infrared sensitive, microscopically sized chips also incorporated into the visor. Since the system operates in the infrared it would not interfere with the pilot's vision and being miniaturized it would not be noticeably opaque. Also, being located at the visor, within the minimum distance of accommodation the device would not be optically distracting. The differential reflectance from pupil or iris and the sclera provides the data which can be reduced by electronic (located elsewhere) to determine the angular position of the eye with respect to an axis, such as the perpendicular to the visor. This angular position is the primary datum which is then further analyzed to determine the amplitude of each saccade and its velocity profile. The parameters of the velocity profile, especially the peak velocity can, we propose, be used to gauge the overall condition of the central nervous system.

At present, the research has established that the maximum velocity is non-linearly related to the amplitude of the saccade, with maximum velocity increasing faster with amplitude for the small saccades (less than 15 degrees) and tending toward an asymptotic maximum velocity as the amplitude approaches maximum (about 700 degrees per second at amplitudes above 30 degrees). Thus, the low amplitude saccades may be most useful in detecting any alteration in the performance of the saccadic system. Alternatively, other features (the asymptotic value of the velocity) may be preferred. Additional research required could be quite clearly defined to determine the necessary physiological boundaries and correlations in a reasonable short time.

Other characteristics of the saccadic system may be chosen in place of maximum velocity. These include the duration of the saccade as a function of amplitude (a linear relation) or the slope of the velocity versus amplitude plot or the time lag until the maximum velocity is achieved. Although we cannot state the degree of precision with which such parameters could be correlated to other data of central nervous system operation, this scheme, should, at the least, be an indicator of gross dysfunctions of the central nervous system. At the level of our outline, we have omitted discussion of such technical problems as design of a program to discriminate artifacts caused by blinking or other cases, the details of the data analysis and storage in order achieve usable criteria for making decisions on when impairment had occurred. An onboard computer of reasonable proportion could be designed to perform the necessary data acquisition and analysis. We have also not made a detailed description of the sensor or infrared light source. It is our intuition that, if further discussion suggests this monitor for possible development such questions could be answered in a rigorous fashion with relatively little difficulty.

2) Infrared sensing of surface vascular pulsations.

We have also considered remote sensing of the pulse rate by thermometry of the cheek, ear lobe or eye. As the blood flows into the superficial capillaries there is a significant change in temperature. This temperature pulse, of the order of 1 to 2 degrees (celsias) could be easily detected by an infrared sensor located near or at the surface of the skin. For example, the probe could be incorporated into an earring or as a part of the helmet. Another possibility is the use of a bracelet with an integral temperature sensor. (The bracelet loses some of the advantages of a more remote device but may be the simplest means of detecting the pulse).

Information about pulse rate is, of course, of great diagnostic and descriptive value. Short term fluctuations, even from beat to beat, have been correlated with brief alerting reactions and stressful situations (Lacy, 1958). More elaborate analyses of long term patterns, including cyclic variations associated with altered states of consciousness in the aerospace environment, have been estensively described in the Soviet literature (Moskalenko, 1970).

Recent reports of noninvasive temperature measurement by natural microwave emission at 3.3 GHz from subcutaneous tissues (Barrett and Myers, 1975) also raise the possibility of using this technique for pulse detection, based on vascular flow in deep tissues

3) Optical sensing of vascular flow

The third device we considered also measure the pulse and offers the same information as described above. In this case the pulse would be detected by the flushing of the skin in response to the filling of the small vessels with each arterial pulse. Suitable tissues for observation might be in the eye or on the cheek or at the ear. The means of detection could be a simple phototransister with appropriate spectral specificity in the red or infrared. Illumination would be provided by the ambient cockpit lighting, or more desirably by a small light bulb located away from the pilot's line of sight. The scheme depends on a difference in color and so could, in principle, operate at very low ambient light levels.

1. Baloh, R.W., H.R. Konrad, A.W. Sills, and V. Honrubia. The saccade velocity test. Neurology 25: 1071-1076, 1975.

2. Baloh, R.W., W.E. Kumley, and V. Honrubia. Algorithm for analyses of saccadic eye movements using a digital computer. Aviat. Space Environ. Med. 47: 523-527, 1976.

3. Baloh, R.W., A.W. Sills, W.E. Kumley, and V. Honrubia. Quantitative measurement of saccade amplitude, duration, and velocity. Neurology 25: 1065-1070, 1975.

4. Baule, G. and R. McFee. Detection of the magnetic field of the heart. Am. Heart J. 66: 95-96, 1963.

5. Baule, G. and R. McFee. The magnetic heart vector. Am. Heart J. 79: 223-236, 1970.

6. Bloch, F. Josephson effect in a superconducting ring. Physical Rev. B 2: 109-121, 1970.

7. Brenner, D., S.J. Williamson, and L. Kaufman. Visually evoked magnetic fields of the human brain. Science 190: 480-481, 1975.

8. Cohen, D. Magnetoencephalography: evidence of magnetic fields produced by alpha-rhythm currents. Science 161: 784-786, 1968.

9. Cohen, D. Magnetoencephalography: detection of the brain's electrical activity with a superconducting magnetometer. Science 175: 664-666, 1972.

10. Cohen, D. Magnetic fields of the human body. Physics Today 28: 34-43, 1975.

11. Cohen, D. Measurements of the magnetic fields produced by the human heart, brain and lungs. IEEE Trans. Mag. 11: 694-700, 1975.

12. Cohen, D., and B.N. Cuffin. Magnetic fields of a dipole in special volume conductor shapes. IEEE Trans. Biomed. Eng. (in press).

13. Cohen, D., and E. Givler. Magnetomyography: magnetic fields around the human body produced by skeletal muscles. Appl. Phys. Lett. 21: 114-116, 1972.

14. Cohen, D., and H. Hosaka. Magnetic field produced by a current dipole. J. Electrocardiol. (in press).

15. Cohen, D., and L.A. Kaufman. Magnetic determination of the relationship between the S-T segment shift and the injury current produced by coronary artery occlusion. Circ. Res. 36: 414-424, 1974.

16. Cohen, D., and D. McCaughan. Magnetocardiograms and their variation over the chest in normal subjects. Am. J. Cardiol. 29: 678-685, 1972.

17. Cuffin, B.N., and Cohen, D. Magnetic fields produced by special biological sources. Preprint, Francis Bitter Magnet Laboratory, Cambridge, MA.

18. Deaver, B.S., Jr. Physics of superconductive devices. In: The Science and Technology of Superconductivity, vol. 2, ed. by W.D. Gregory, W.N. Mathews, Jr., and E.A. Edelsack. Plenum Press, New York, 1973, pp. 539-564.

19. Hughes, J.R., D.E. Hendrix, J. Cohen, F.H. Duffy, C.I. Mayman, M.L. Scholl, and B.N. Cuffin. Relationship of the magnetoencephalogram to the electroencephalogram. Normal wake and sleep activity. Electroencephalogr. Clin. Neurophysiol. 40: 261-278, 1976.

20. Kolin, A. Magnetic fields in biology. Physics Today 21: 39-50, 1968.

21. Konig, H.L. ELF and VLF signal properties: Physical characteristics. In: ELF and VLF Electromagnetic Field Effects, ed. by M.A. Persinger. Plenum Press, New York, 1974, p. 14.

22. Krogh, E. Normal values in clinical electrooculography. Acta Ophthalmol. 53: 563-575, 1975.

23. Reite, M., J.E. Zimmerman, J. Edrich, and J. Zimmerman. The human magnetoencephalogram: some EEG and related correlations. Electroencephalogr. Clin. Neurophysiol. 40: 59-66, 1976.

24. Teyler, T.J., B.N. Cuffin, and D. Cohen. The visual evoked magnetoencephalogram. Life Sci. 17: 683-692, 1975.

25. Tinkham, M. Introduction to Superconductivity. McGraw-Hill, New York, 1975, Chapter 6.

26. Webb, W.W. Magnetometers and interference devices. In: The Science and Technology of Superconductivity, vol. 2, ed. by W.D. Gregory, W.N. Mathews, Jr., and E.A. Edelsack. Plenum Press, New York, 1973, pp. 653-677.

27. Zimmerman, J.E., and N.V. Frederick. Miniature ultra-sensitive magnetic gradiometer and its use in cardiography and other applications. Appl. Phys. Lett. 19: 16-19. 1971.

28. Zimmerman, J.E., P. Thiene, and J.T. Harding. Design and operation of stable R-F biased superconducting point-contact quantum devices, and a note on properties of perfectly clean metal contacts. J. Appl. Phys. 41: 1572-1580, 1970.

SECTION VII

BIBLIOGRAPHY

7. Bibliography

Please note: Certain earlier publications from the Laboratory that were included in the previous Final Report are included here, because they are cited specifically in the text.

Adey, W.R. 1975. Evidence for cooperative mechanisms in the susceptibility of cerebral tissues to environmental and intrinsic electric fields. In: "Functional Linkage in Biomolecular Systems," ed. F.O. Schmitt, D.M. Schneider and D.M. Crothers, Raven Press, New York, pp.325-342.

Adey, W.R. 1975. On-line analysis and pattern-recognition techniques for the electroencephalogram. In: "Signal Analysis and Pattern Recognition in Biomedical Engineering," ed. G.F. Inbar, Wiley, New York, pp. 93-120.

Adey, W.R. 1975. Introduction: effects of electromagnetic radiation on the nervous system. Ann. New York Acad. Sci. 247:15-20.

Adey, W.R. 1976. The influences of impressed electrical fields at FEG frequencies on brain and behavior. In: "Behavior and Brain Electrical Activity," N. Burch and H. Altshuler, eds. Plenum Press, New York, pp. 363-390.

Adey, W.R. 1976. The sensorium and the modulation of cerebral states: tonic environmental influences on limbic and related systems. Ann. New York Acad. Sci., in press.

Adey, W.R. 1976. Models of membranes of cerebral cells as substrates for information storage. BioSystems, in press.

Bawin, S.M., and Adey, W.R. 1976. Sensitivity of calcium binding in cerebral tissues to weak environmental electric fields oscillating at low frequency. Proc. Nat. Acad. Sci., USA 73:1999-2003.

Bawin, S.M., and Adey, W.R. eds. 1977. Brain Interactions with Weak Electric and Magnetic Fields. MIT Neuroscience Research Program Bull. 15: Part 1.

Bawin, S.M., Kaczmarek, L.K., and Adey, W.R. 1975. Effects of modulated VHF fields on specific brain rhythms in cats. Brain Research 58:365-384.

Costin, A., Bystrom, B., Rovner, E., and Sabbot, I. 1974. Effect of a chelating ion exchange resin (Chelex 100) on impedance and evoked potentials. Experientia 30:159-161.

Costin, A., and Sabbot, I. 1974. Uptake and distribution of radio labeled calcium and magnesium in the brain and the pituitary gland. Proc. XXVI Internat. Congr. Physiol. Sci., p. 310 (abstract).

Costin, A., and Sabbot, I. 1976. Magnesium uptake and distribution in the brain and pituitary gland of the rat. Proc. 2nd. Internat. Symp. on Magnesium, Montreal, p. 36. (abstract)

Gavalas, R.J., Walter, D.O., Hamer, J., and Adey, W.R. 1970. Effect of low-level, low frequency electric fields on EEG and behavior in Macaca nemestrina. Brain Research 18:491-501.

Gavalas-Medici, R.J., and Day-Magdaleno, S.R. 1976. Extremely low frequency, weak electric fields affect schedule-controlled behavior of monkeys. Nature, London 261:256-258.

Hanley, J. 1975. Electroencephalographic correlates of verbally induced stress in man. Int'l. J. Psychiat. in Med. 6:3-13.

Kaczmarek, L.K., and Adey, W.R. 1973. The efflux of $^{45}Ca^{2+}$ and ^{3}H-gamma-aminobutyric acid from cat cerebral cortex. Brain Research 63:331-342.

Kaczmarek, L.K. and Adey, W.R. 1974. Some chemical and electrophysiological effects of glutamate in cerebral cortex. J. Neurobiol. 5:231-241.

Kaczmarek, L.K., and Adey, W.R. 1974. Factors affecting the release of ^{14}C-taurine from cat brain; the electrical effects of taurine on normal and seizure prone cortex. Brain Research 76:83-94.

Kaczmarek, L.K., and Adey, W.R. 1975. Cortical release of labeled compounds during arousal in the cat: correlations with carbon dioxide, brain temperature and EEG. Exper. Neurol. 46:57-68.

Kaczmarek, L.K., and Adey, W.R. 1975. Extracellular release of cerebral macromolecules during potassium - and low calcium-induced seizures. Epilepsia 16: 91-97.

Moise, S.L., Olsen, D.E., and Huston, S.W. 1974. Computer technology: an automated system for primate instruction for behavioral neurophysiology. Behavior Research Methods and Instrumentation 6:557-564.

Olsen, D.E., Moise, S.L. and Huston, S.W. 1974. An eight channel semi-implantable telemetry system for animal research. Proc. Sec. Internat. Biotelemetry Symp. pp. 173-175, Kargla, Basel.

Sabbot, I., and Costin, A. 1974. Effect of stress on the uptake of radiolabeled calcium in the pituitary gland and the brain of the rat. J. Neurochem. 22: 731-734.

Sabbot, I., and Costin, A. 1974. Cold stress induced changes in the uptake and distribution of radiolabeled magnesium in the brain and pituitary of the rat. Experientia 30:905-906.